

CERN-TH/98-383  
NYU/98-12-02  
RU-98-46  
SU-ITP 98-69  
hep-ph/9902443

## Soft Yukawa couplings in supersymmetric theories

Francesca Borzumati<sup>a</sup>, Glennys R. Farrar<sup>b</sup>, Nir Polonsky<sup>c</sup>, and Scott Thomas<sup>d</sup>

<sup>a</sup> *Theory Division, CERN, CH-1211 Geneva 23, Switzerland*

<sup>b</sup> *Department of Physics, New York University, New York, NY 10003, USA*

<sup>c</sup> *Department of Physics and Astronomy, Rutgers University, Piscataway, NJ 08854-8019, USA*

<sup>d</sup> *Department of Physics, Stanford University, Stanford, CA 94305, USA*

### Abstract

The possibility of radiatively generated fermion masses arising from chiral flavor violation in soft supersymmetry-breaking terms is explored. Vacuum stability constraints are considered in various classes of models, and allow in principle all of the first- and second-generation quarks and leptons and the  $b$ -quark to obtain masses radiatively. Radiatively induced Higgs-fermion couplings have non-trivial momentum-dependent form factors, which at low momentum are enhanced with respect to the case of tree-level Yukawa couplings. These form factors may be probed by various sum rules and relations among Higgs boson decay widths and branching ratios to fermion final states. An apparent, large, hard violation of supersymmetry also results for Higgsino couplings. Mixing between left- and right-handed scalar superpartners is enhanced. A radiative muon mass is shown to lead to a relatively large and potentially measurable contribution to the muon anomalous magnetic moment. If the light-quark masses arise radiatively, the neutron electric dipole moment is suppressed by a natural phase alignment between the masses and dipole moment, and is below the current experimental bound. The possibility of neutrino masses arising from softly broken lepton number, and concomitant enhanced sneutrino-antisneutrino oscillations, is briefly discussed.

## I. INTRODUCTION

Fermion masses are signals of broken chiral flavor symmetries. In the standard model of electroweak and strong interactions, this flavor violation arises from tree-level Yukawa interactions between the Higgs boson and fermions of opposite chirality. With these interactions, the Higgs boson vacuum expectation value, which breaks electroweak symmetry, then gives rise to the fermion masses. However, the Yukawa couplings are arbitrary parameters, and it is widely accepted that they represent an effective low-energy description of a full theory of flavor. In this paper we explore the possibility, which presents itself in supersymmetric theories, that chiral flavor symmetries are broken predominantly by soft, dimension-three supersymmetry-breaking terms rather than hard dimension-four superpotential Yukawa couplings. This scenario has a number of interesting phenomenological consequences, including enhanced Higgs couplings; apparent, large, hard violations of supersymmetry in Higgsino couplings; relatively large contributions to anomalous magnetic moments; suppression of electric dipole moments; and enhanced mixing between left- and right-handed scalar partners.

In many extended frameworks for flavor, the standard model Yukawa couplings are understood as spurious degrees of freedom in the low energy theory, which parametrize flavor symmetry breaking. In the Froggatt–Nielsen mechanism these spurions are related to powers of scalar expectation values which spontaneously break the flavor symmetries in the underlying fundamental theory [1]. In this case the texture of hierarchies that appear in the Yukawa coupling matrices can then be related to “horizontal” flavor symmetries, which restrict the powers of the flavor-breaking expectation values. In supersymmetric theories, such flavor-breaking scalar expectation values preserve supersymmetry and therefore induce superpotential couplings, which give tree-level fermion Yukawa couplings directly. Enforcing particular flavor textures in the Yukawa matrix via continuous or discrete horizontal symmetries [2,3] is natural because of the holomorphy of the superpotential.

Supersymmetric theories also allow the interesting possibility that chiral flavor symmetries are broken by auxiliary rather than scalar expectation values. Such expectation values break supersymmetry and cannot induce superpotential couplings directly. In the low-energy theory these breakings appear as either holomorphic or non-holomorphic scalar tri-linear terms involving a Higgs field and the scalar partners of the left- and right-handed fermions. These soft tri-linear terms differ in  $U(1)_R$  charge from fermion Yukawa couplings. Contributions to Yukawa couplings from these terms therefore also require breaking of  $U(1)_R$  symmetry. With a non-vanishing gaugino mass providing the  $U(1)_R$  breaking, soft chiral flavor breaking leads to radiative fermion masses at one loop. In this mechanism the violation of fermionic chirality required for a fermion mass is provided by the massive gaugino, while the violation of chiral flavor symmetry originates in the scalar tri-linear terms. These quantum contributions to the fermion masses are finite and in principle calculable in terms of the parameters of the low-energy theory. The necessity of both  $U(1)_R$  and chiral flavor breaking, along with non-renormalization of the superpotential, give a natural context in which a fermion mass can be purely radiative. The tree-level Yukawa coupling can vanish, and yet receive a *finite* radiative contribution. This may be enforced by continuous or discrete horizontal flavor  $R$ -symmetries. In this scenario some of the flavor symmetries

are broken in the supersymmetry-breaking sector, either spontaneously or explicitly by interactions with a messenger sector. Since supersymmetry breaking requires non-vanishing auxiliary expectation values, this mechanism for fermion masses amounts to an auxiliary field version of the Froggatt–Nielsen mechanism.

It is well known that in supersymmetric theories there can be significant quantum contributions to fermion masses in certain regions of parameter space [4,5]. However, these contributions are usually assumed to be proportional to the tree-level Yukawa coupling. Various versions of radiative fermion masses arising predominantly from soft terms have been considered in the following scenarios: softly broken  $N = 2$  theories as a solution of the fermion mass problem in these models [6], for the first two generations of quarks and leptons in the softly broken supersymmetric standard model [7], including radiative contributions from an exotic sector near the electroweak scale [8], and for the first generation of quarks and leptons within the context of a grand unified theory [9]. The relatively large soft tri-linear scalar terms required, in particular to obtain radiative second-generation fermion masses, can lead to charge or color breaking vacua along certain directions in field space [10]. However, as discussed below, metastability of the charge and color preserving vacuum on cosmological time scales is in general possible. In addition, we identify several classes of theories in which the global minimum preserves color and charge.

The magnitude of masses and mixings that emerges in such models depend on the specific textures for both soft and hard chiral flavor breaking, and on details of the supersymmetric particle spectrum. While these are model-dependent, some general features are characteristic. Since radiative masses are intrinsically suppressed by a loop factor, purely radiative generation of masses for the first and second generations leads to quarks and leptons in general much lighter than the third-generation fermions, and with suppressed mixings. In addition, since flavor and supersymmetry breaking are intimately linked in this scenario for radiative masses, interesting levels of supersymmetric contributions to low-energy flavor-changing processes can occur. These however depend on specific model-dependent textures and the over-all scale of the superpartner masses, and may be avoided in some models. In this paper we concentrate on model-independent consequences and signatures of radiative fermion masses from soft chiral flavor violation, and leave the study of specific textures and flavor violating processes to future work.

Radiative fermion masses have a number of striking phenomenological consequences, many related either directly or indirectly to the softness of the fermion mass. Chief among these is that the chirality violating fermion mass and Yukawa couplings are momentum-dependent, with non-trivial form factors. The Higgs–fermion coupling turns out to be enhanced at low momentum with respect to a tree-level Yukawa coupling. In addition, if the soft chirality violation arises in non-holomorphic scalar tri-linear terms, the corresponding fermions receive mass from the “wrong Higgs” field. The dependence of the physical Higgs boson couplings on the Higgs vacuum expectation values then differs drastically from the minimal case. For fermions with radiative masses, the corresponding Higgsino couplings also arise radiatively with non-trivial form factors, but with different parametric dependences on gauge couplings. This leads to an apparent, large, hard violation of supersymmetry in the low-energy theory. The leading low-energy momentum dependence of these radiatively generated couplings can be represented as effective radii for the appropriate couplings. All these

deviations from the minimal expectations for these couplings are potentially measurable with high-precision collider measurements of Higgs couplings, as well as from Higgsino branching ratios. Another important feature of this scenario for soft Yukawa couplings is that both the mass and anomalous magnetic moments arise at one loop. This has the consequence that supersymmetric contributions to magnetic moments are effectively a loop factor larger than with tree-level Yukawa couplings. The current experimental bound on the muon anomalous magnetic moment represents the best probe for a radiative muon mass, and already constrains part of the parameter space. CP-violating electric dipole moments (EDMs) are suppressed by a natural phase alignment between the masses and dipole moment in interesting regions of parameter space. With radiative light-quark masses, the neutron EDM is easily below the current experimental bound, but could be measurable in future experiments. For a radiative electron mass, the electron EDM is more model-dependent. The current experimental bound may already be used to infer preferred regions of neutralino/selectron parameter space if the electron mass is radiative. Finally, radiative fermion masses imply enhanced mixing between the associated left- and right-handed scalar partners, respect to a tree-level Yukawa. These mixings can significantly modify the production cross sections and branching ratios of scalar superpartners.

In the next section, the radiative contributions to fermion masses in softly-broken supersymmetric models are discussed. Non-trivial momentum dependence of the Higgs coupling, the Higgs Yukawa radius, and enhancement of the Higgs coupling at zero momentum transfer are introduced and calculated. The apparent violation of supersymmetry in the relatively large difference between Higgs and Higgsino couplings is introduced. In section III the magnitude of the soft tri-linear terms required to obtain particular fermion masses are presented. Enhanced left–right mixing of scalar superpartners, the origin of the Cabibbo–Kobayashi–Maskawa (CKM) quark mixing terms, and various scenarios for supersymmetric contributions to flavor-changing processes are also discussed. A stability analysis of the scalar potential is presented in section IV. A number of classes of models for introducing stabilizing quartic scalar couplings are discussed. These can lead to either a globally stable charge- and color-preserving vacuum, or metastability on cosmological time scales. The (meta)stability bounds allow in principle all of the first-two-generation quarks and leptons, as well as the  $b$ -quark, to obtain masses radiatively. A classification of the effective operators that give rise to the auxiliary spurion version of the Froggatt–Nielson mechanism for either holomorphic or non-holomorphic scalar tri-linear terms is presented in section V. It is pointed out that non-holomorphic soft tri-linear terms require a low scale of supersymmetry breaking. In section VI the relatively large contribution to the muon anomalous magnetic moment in this scenario is compared with current experimental bounds. This already constrains some of the parameter space in this scenario, and is shown to place an upper limit on the enhancement of the Higgs–muon coupling compared to the tree-level case. If both muon and  $b$ -quark masses are radiative, an analogous upper limit on the Higgs– $b$ -quark coupling can be extracted from the muon anomalous magnetic moment bound, assuming gaugino universality. CP-violating Higgs–fermion couplings and fermion EDMs are investigated in section VII. With radiative masses for the light quarks, the neutron EDM is shown to be comfortably below the current experimental bound due to a natural high degree of phase alignment between the quark masses and dipole moment. The electron EDM is shown to be more model-dependent, but sufficiently suppressed in certain regions of the neu-

tralino/selectron parameter space. In section VIII a number of sum rules, relations among Higgs-boson decay widths and branching ratios to fermion final states are presented. These hold in large classes of supersymmetric theories including the minimal supersymmetric standard model. For radiative masses, deviations from minimal expectations for these sum rules and relations due to non-trivial form factors and possible non-holomorphic Higgs couplings may be measurable at future colliders. The possibility of softly broken lepton number as a source of neutrino mass and concomitant enhanced sneutrino–antisneutrino oscillation is discussed in section IX. Conventions and one-loop integrals for fermion masses, Higgs and Higgsino couplings, and anomalous moments are given in the appendices. Preliminary results were presented previously in ref. [11].

## II. SOFT YUKAWA COUPLINGS

In a supersymmetric theory the scalar superpartners of the quarks and leptons carry the same flavor symmetries as the associated quarks and leptons. Flavor symmetries may therefore be broken by terms that involve only scalar fields. Quark and lepton masses require terms that break flavor symmetries for both left- and right-handed fields. The most general softly broken supersymmetric Lagrangian contains holomorphic scalar tri-linear operators of the form

$$\mathcal{L} \supset AH_\alpha\phi_L\phi_R + \text{h.c.} \quad (1)$$

as well as non-holomorphic operators [12] of the form

$$\mathcal{L} \supset A'H_\alpha^*\phi_L\phi_R + \text{h.c.}, \quad (2)$$

where flavor indices on the scalar fields and the complex  $A$ - and  $A'$ -parameters are suppressed. For leptons and down-type quarks, the holomorphic (non-holomorphic) operator contains the Higgs doublet  $H_\alpha = H_1$  ( $H_2$ ) with  $U(1)_Y$  hypercharge  $Y = -1$  (1). For up-type quarks the holomorphic(non-holomorphic) operators contain  $H_\alpha = H_2$  ( $H_1$ ). The  $A$ - and  $A'$ -parameters break the chiral flavor symmetries carried by the scalars. Even though the scalar superpartners carry the same flavor symmetries as the associated fermion, they differ by one unit of  $R$ -charge under  $U(1)_R$  symmetry. Inducing a fermion mass at the quantum level from the flavor-violating  $A$ - or  $A'$ -parameters therefore requires additional terms that violate  $U(1)_R$  symmetry. At lowest order this  $U(1)_R$  breaking can be provided by a gaugino mass, which along with the flavor-violating  $A$ -parameters give rise to fermion masses at one loop, as given explicitly below. The insertion of a gaugino mass can also be understood in terms of the necessity of fermionic chirality violation for a quark or lepton mass. Since the dimensionless fermion Yukawa coupling arises quantum mechanically from dimensionful parameters, the radiative contributions are finite and calculable. The fermion mass and the Higgs and Higgsino Yukawa couplings discussed below are therefore soft in the technical sense that no counter-terms are required in the high energy theory. The couplings are also soft in the more colloquial sense that the quantum contributions arise at the superpartner scale from soft supersymmetry-breaking terms (which do require counter-terms but do not introduce quadratic divergences into the low-energy theory).

For a quark or lepton that receives a radiative mass, Higgs and Higgsino couplings also arise radiatively. However, since the chiral flavor breaking arises in supersymmetry-breaking terms, there is no symmetry that enforces the equality of the effective Higgs and Higgsino couplings. This is unlike the case of a tree-level superpotential Yukawa coupling, where equality of these couplings is enforced by supersymmetry. In fact, as discussed below, even the parametric dependence on gauge coupling constants of the effective Higgsino coupling differs from that of the fermion mass and effective Higgs coupling. This leading order difference between Higgs and Higgsino Yukawa couplings amounts to a large violation of supersymmetry in a dimensionless coupling at low energy, i.e. an apparent hard violation of supersymmetry.

The over-all magnitude and parametric dependence of radiative fermion masses and Higgs and Higgsino couplings are discussed in the following subsections. In this section flavor-changing effects are suppressed and scalar masses generally taken to be flavor-independent for simplicity.

### A. The fermion mass

The one-loop scalar partner–gaugino diagram that dresses the fermion propagator generates a finite contribution to the fermion mass, as shown in fig. 1. The  $A$ - or  $A'$ -

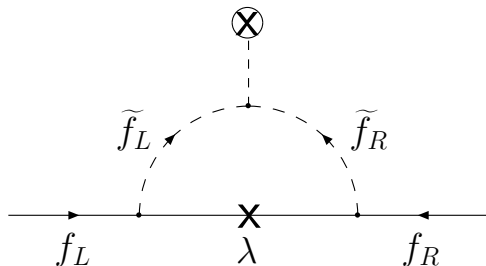


FIG. 1. One-loop contribution to fermion mass from soft chiral flavor breaking and gaugino mass.

parameter breaks both left and right flavor symmetries, while the gaugino mass insertion connects left and right chiral fermions. For  $m_f^2 \ll m_{\tilde{f}}^2, m_\lambda^2$ , with  $m_f$  the physical scalar mass eigenvalues, the one-loop radiative fermion mass may be evaluated at  $p^2 = 0$ , and is given by

$$m_f = -m_{LR}^2 \left\{ \frac{\alpha_s}{2\pi} C_f m_{\tilde{g}} I(m_{\tilde{f}_1}^2, m_{\tilde{f}_2}^2, m_{\tilde{g}}^2) + \frac{\alpha'}{2\pi} \sum_j K_f^j m_{\tilde{\chi}_j^0} I(m_{\tilde{f}_1}^2, m_{\tilde{f}_2}^2, m_{\tilde{\chi}_j^0}^2) \right\}, \quad (3)$$

where  $C_f = 4/3, 0$  for quarks and leptons, respectively. The sum is over neutralino eigenstates with coupling coefficients  $K_f^j$  to the fermions, and  $I(m_{\tilde{f}_1}^2, m_{\tilde{f}_2}^2, m^2)$  is a loop function discussed below. The dependence on the left–right squark or slepton mixing,  $m_{LR}^2 = A\langle H_\alpha \rangle$  or  $A'\langle H_\alpha \rangle$ , and on the chiral violation arising from the gaugino masses,  $m_{\tilde{g}}$ , and/or  $m_{\tilde{\chi}_j^0}$ ,

is displayed explicitly in (3). Note that without hard tree-level Yukawa couplings in the superpotential, there are no left–right mixing terms arising from interference with the superpotential Higgsino mass,  $W \supset \mu H_1 H_2$ . The first and second terms in (3) correspond to the strong (gluino) and hypercharge/weak (neutralino) contributions, respectively. The neutralino contributions include both a pure  $\tilde{B}$ – $\tilde{B}$  and mixed  $\tilde{B}$ – $\tilde{W}_3$  propagators. The coupling coefficients  $K_f^j$  are

$$K_f^j = \frac{Y_{fL}}{2} N_{jB} \left[ \frac{Y_{fR}}{2} N_{jB} + \cot \theta_W N_{jW} \right], \quad (4)$$

where  $N_{ij}$  is the neutralino eigenvector mixing matrix, and the hypercharge is normalized as  $Q = T_3 + \frac{1}{2}Y$ . In the mostly gaugino or mostly Higgsino region of parameter space, the neutralino propagator is well approximated by pure  $\tilde{B}$ – $\tilde{B}$  exchange, since the  $\tilde{B}$ – $\tilde{W}_3$  contributions are suppressed by gaugino–Higgsino mixing;  $N_{jB}N_{jW} \sim \mathcal{O}(m_Z^2\mu/(\mu^2-m_{\tilde{W}}^2)(m_{\tilde{W}}-m_{\tilde{B}}))$  for a given mass eigenstate. Chargino contributions to the mass are forbidden by gauge invariance in the absence of hard tree-level Yukawa couplings. Hereafter only the strong contribution to the quark masses will be retained, except in the discussion of CP-violating effects given in section VII. In general the parameters  $m_{LR}^2$ ,  $m_{\tilde{g}}$ ,  $m_{\tilde{\chi}_j^0}$ , and the coupling coefficients  $K_f^j$  appearing in (3) may be complex, but the masses appearing in the loop functions are understood to be the real positive mass eigenvalues. In the absence of a tree-level Yukawa coupling, it is always possible to work in a basis in which the radiative fermion mass is real. Note that throughout, all calculations are performed using mass eigenstates. Insertion approximation is not employed; the over-all factors of  $m_{LR}^2 m_{\tilde{g}}$  and  $m_{LR}^2 K_f^j m_{\tilde{B}}$  in (3) appear as a consequence of algebraic relationships between the factors in mixing coefficients.

The loop function  $I(m_{\tilde{f}_1}^2, m_{\tilde{f}_2}^2, m_\lambda^2)$ , with  $\lambda$  denoting generically a gaugino, is given explicitly in appendix A 2, along with definitions of the scalar mass eigenstates and mixing matrices. The dominant momentum in the loop is controlled by the largest mass scale. The loop function is then typically bounded by  $\tilde{m}^2 I(m_{\tilde{f}_1}^2, m_{\tilde{f}_2}^2, m_\lambda^2) \lesssim \mathcal{O}(1)$ , where  $\tilde{m} = \max(m_{\tilde{f}_1}, m_{\tilde{f}_2}, m_\lambda)$  (see, e.g., ref. [13]). This bound is typically saturated for  $m_{\tilde{f}} \simeq m_\lambda$  (but is evaded in certain limits – see appendix A 2). The radiative fermion masses then scale as  $m_f \sim (\alpha/2\pi) m_{LR}^2 m_\lambda / \tilde{m}^2$ , where  $\alpha = (4/3)\alpha_s$  or  $\alpha'$ , for quarks or leptons respectively. With this scaling and the form of the left–right mixing given above, it is apparent that, if the superpartners are decoupled, by taking all soft supersymmetry-breaking parameters simultaneously large, including the flavor-breaking  $A$ -parameters, the resulting radiative fermion mass becomes independent of the supersymmetry-breaking scale. This can be seen directly by considering the effective mass Yukawa coupling,  $m_f/|\langle H_\alpha \rangle|$ . This dimensionless one-loop finite coupling must approach a constant as the superpartners are decoupled, since the fermion mass must be proportional to the electroweak symmetry-breaking scale in this limit.

In order to present the numerical results for the one-loop radiative mass and associated couplings, it is convenient to trade the three parameters that describe the scalar partner sector,  $m_{LL}^2$ ,  $m_{RR}^2$ , and  $m_{LR}^2$  used in appendix A 1, for

$$\phi_f \equiv \frac{m_{f_2}^2 - m_{f_1}^2}{m_{f_2}^2 + m_{f_1}^2}; \quad \rho_f^\lambda \equiv \frac{m_{f_1}^2 + m_{f_2}^2}{2m_\lambda^2}; \quad \sin 2\theta_f = -\frac{2m_{LR}^2}{m_{f_2}^2 - m_{f_1}^2}, \quad (5)$$

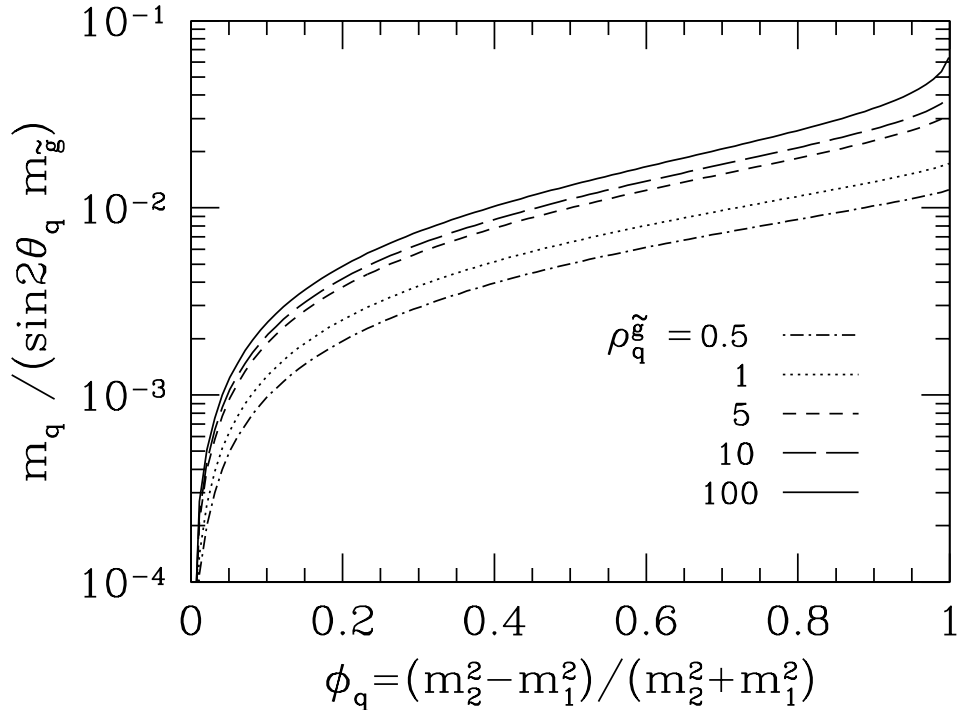


FIG. 2. Radiative quark mass,  $m_q$ , in units of the squark mixing angle times the gluino mass,  $\sin 2\theta_q m_{\tilde{g}}$ , as a function of the fractional squark mass splitting  $\phi_q$ , where  $m_i^2$  here indicates  $m_{q_i}^2$ . The mass is shown for various values of the ratio  $\rho_q^{\tilde{g}}$ . For a radiative lepton mass, the squark parameters are replaced by slepton parameters, the gluino mass by the Bino mass, and the over-all result is scaled by a factor of  $(3/8)(\alpha'/\alpha_s) \simeq 0.03$  for the hypercharge coupling and charges.

which are respectively the fractional scalar partner mass-squared splitting, the average scalar partner mass squared, normalized to the relevant gaugino mass squared,  $m_{\tilde{g}}^2$ ,  $m_{\tilde{B}}^2$ , or  $m_{\tilde{\chi}_j^0}^2$  generically indicated as  $m_{\tilde{\lambda}}^2$ , and the scalar partner mixing angle. In terms of these parameters, and in the pure gaugino limit for which  $\tilde{B}-\tilde{W}_3$  vanishes, the radiative mass (3) is

$$m_f = -\sin 2\theta_f \phi_f \left\{ \frac{\alpha_s}{2\pi} C_f \rho_f^{\tilde{g}} m_{\tilde{g}}^3 I(m_{\tilde{f}_1}^2, m_{\tilde{f}_2}^2, m_{\tilde{g}}^2) + \frac{\alpha'}{2\pi} \rho_f^{\tilde{B}} m_{\tilde{B}}^3 I(m_{\tilde{f}_1}^2, m_{\tilde{f}_2}^2, m_{\tilde{B}}^2) \right\}. \quad (6)$$

The on-shell quark mass radiatively generated at one loop through gluino exchange, is plotted in fig. 2 as a function of  $\phi_q$ . The mass is displayed in units of the squark mixing angle times the gluino mass,  $\sin 2\theta_q m_{\tilde{g}}$ , for various values of  $\rho_q^{\tilde{g}}$ . The lepton mass, radiatively generated in the pure gaugino limit, can be obtained from the same figure, by replacing the squark parameters by slepton parameters, the gluino mass by the Bino mass, and by rescaling the over-all result by a factor of  $\frac{3}{8}(\alpha'/\alpha_s) \simeq 0.03$  for the hypercharge coupling.



## B. The Higgs coupling

The momentum-dependent coupling of the physical Higgs bosons to fermions arises radiatively in a manner similar to the fermion masses, as shown in fig. 3. For simplicity, the discussion here is restricted to the neutral Higgs bosons,  $h^0$ ,  $H^0$ , and  $A^0$ , which accompany a single pair of Higgs doublets.

The generic neutral Higgs–fermion–fermion operator obtained at the one-loop level, has the form  $H_\alpha(q)\bar{f}_L(q_1)f_R(q_2)$ , where  $q = q_1 - q_2$  and  $\alpha = 1, 2$ . Consider first the couplings

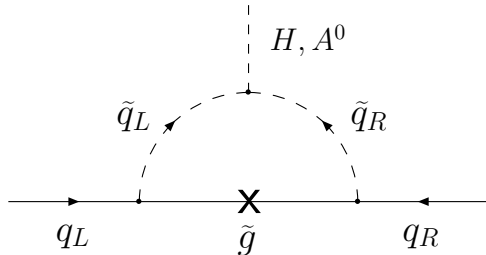


FIG. 3. One-loop radiative couplings of quarks to neutral scalar Higgs bosons  $H$  ( $= h^0, H^0$ ) or the neutral pseudoscalar  $A^0$  from chiral flavor violation and gaugino mass.

of the physical scalar Higgs bosons,  $h^0$  and  $H^0$ , which differ somewhat from that of the pseudoscalar Higgs  $A^0$ . The physical mass eigenstates couple to the fermions with amplitude  $\lambda_{h^0, H^0} = \Theta\{\cos\beta, \sin\beta\}\bar{h}_{f,H}/\sqrt{2}$ , where  $\Theta$  is the Higgs mixing matrix between physical and interaction eigenstates. The mixing matrix  $\Theta$  is non-trivial and differs in the holomorphic and non-holomorphic cases as discussed in section VIII. The first (second) term in the curly brackets corresponds to  $\alpha = 1(2)$ , and  $\sqrt{2}$  is the standard normalization factor for a real scalar field. With all external particles on-shell, relevant to, for instance, the decay  $H(q) \rightarrow f_L(q_1)\bar{f}_R(-q_2)$  or the resonant production  $f_L(q_1)\bar{f}_R(-q_2) \rightarrow H(q)$  with  $H = h^0, H^0$ , then in the approximation  $q_1^2 = q_2^2 = 0$ , as is appropriate for  $m_f^2 \ll m_H^2$ , the radiative Higgs Yukawa coupling to  $h^0$  or  $H^0$  through an  $A$ - or  $A'$ -term may be related to the corresponding fermion mass Yukawa coupling,  $m_f/|\langle H_\alpha \rangle|$ . Summing over the scalar partner mass eigenstates and retaining only the gluino contribution for quarks and the Bino contribution for leptons:

$$\bar{h}_{f,H}(m_H^2) = \frac{m_f}{|\langle H_\alpha \rangle|} \left( \sin^2 2\theta_f J_1(m_H^2; m_{\tilde{f}_1}^2, m_\lambda^2, m_{\tilde{f}_2}^2) + \cos^2 2\theta_f J_2(m_H^2; m_{\tilde{f}_1}^2, m_\lambda^2, m_{\tilde{f}_2}^2) \right), \quad (7)$$

where  $\alpha = 1$  or  $2$ . With this definition,  $\bar{h}_{f,H}$  is the effective Yukawa coupling for  $h^0$  or  $H^0$  with Higgs mixing effects factored out. The loop functions with  $q^2 = m_H^2$  are defined as

$$J_1(m_H^2; m_{\tilde{f}_1}^2, m_\lambda^2, m_{\tilde{f}_2}^2) = \frac{1}{2} \frac{\sum_{i=1,2} C_0(0, 0, m_H^2; m_{\tilde{f}_i}^2, m_\lambda^2, m_{\tilde{f}_i}^2)}{I(m_{\tilde{f}_1}^2, m_{\tilde{f}_2}^2, m_\lambda^2)},$$

$$J_2(m_H^2; m_{\tilde{f}_1}^2, m_\lambda^2, m_{\tilde{f}_2}^2) = \frac{C_0(0, 0, m_H^2; m_{\tilde{f}_1}^2, m_\lambda^2, m_{\tilde{f}_2}^2)}{I(m_{\tilde{f}_1}^2, m_{\tilde{f}_2}^2, m_\lambda^2)}, \quad (8)$$

where the conventions for the three-point functions  $C_0(0, 0, m_H^2; m_a^2, m_b^2, m_c^2)$  are defined in appendix A 3.

The expression (7) is significantly simplified in the heavy superpartner limit  $m_{\tilde{f}}, m_\lambda^2 \gg m_H^2$ , which is particularly relevant to the case of the light Higgs boson,  $h^0$ , for which  $m_{h^0} \leq m_Z$  at tree level. In this limit the vertex loop functions may be evaluated at  $q^2 = 0$ , and reduce to the mass loop function  $C_0(0, 0, 0; m_a^2, m_b^2, m_c^2) = I(m_a^2, m_b^2, m_c^2)$  (see appendix A 3). Making this approximation also isolates intrinsic coupling effects from momentum-dependent effects at finite  $q^2$  discussed below. The coupling (7) in this limit becomes

$$\bar{h}_{f,H}(0) = \frac{m_f}{|\langle H_\alpha \rangle|} \left\{ \sin^2 2\theta_f \left[ \frac{1}{2} \frac{\sum_i I(m_{\tilde{f}_i}^2, m_{\tilde{f}_i}^2, m_\lambda^2)}{I(m_{\tilde{f}_1}^2, m_{\tilde{f}_2}^2, m_\lambda^2)} - 1 \right] + 1 \right\}. \quad (9)$$

In order to characterize the magnitude of the intrinsic coupling of the Higgs bosons to fermions it is useful to define the ratio of the effective Higgs Yukawa coupling to the effective mass Yukawa coupling with the Higgs mixing effects factored out:

$$r_{f,H}(m_H^2) \equiv \frac{\bar{h}_{f,H}(m_H^2)}{(m_f/|\langle H_\alpha \rangle|)} \equiv \frac{\bar{h}_{f,H}(m_H^2)}{\bar{h}_{f,m}(0)}. \quad (10)$$

From eqs. (7) and (8) it can be shown that  $r_{f,H} \geq 1$ . This compares with  $r_{f,H} = 1$  at lowest order for a fermion mass arising from a hard tree-level Yukawa coupling. The ratio  $r_{f,H}$  for a soft radiative mass is plotted in fig. 4 as a function of the fractional scalar mass splitting  $\phi_f$  for  $q^2 = 0$ . For  $m_{LR}^2 \sim m_{\tilde{f}}, m_\lambda^2$  the enhancement  $r_{f,H}(0) \geq 1$  can be sizeable, and increases with the scalar mass splitting. The divergence in  $r_{f,H}(0)$  for  $\phi_f \rightarrow 1$  is due to a vanishing eigenvalue in the scalar partner mass squared matrix in this limit. The physical Higgs coupling is infrared-singular in this limit from diagrams in fig. 3 with two massless scalar propagators. The fermion mass however remains finite in this limit, with a single massless scalar propagator in the diagrams of fig. 1.

The disparity between the effective Higgs and mass Yukawa coupling is due to the difference in the loop momentum integrations. For  $m_{\tilde{f}}, m_\lambda^2 \gg m_H^2$ , the difference may be understood as arising from the differing combinatorics for chiral insertions, proportional to  $m_{LR}^2$ , between figs. 1 and 3 (the scalar mass eigenstate propagators implicitly contain a resummation of an arbitrary number of chiral insertions). For  $q^2 = 0$  and at first order in  $m_{LR}^2/\tilde{m}^2$ , where  $\tilde{m} = \max(m_{\tilde{f}}, m_\lambda)$ , the diagrams in figs. 1 and 3 are identical, with a single chiral insertion, yielding  $r_{f,H}(0) = 1$  at this order. Since an odd number of  $m_{LR}^2$  left-right mixing insertions are required by chirality, the mass and Higgs Yukawa diagrams only differ through diagrams with three or more such insertions. The  $q^2 = 0$  ratio in the heavy superpartner limit is thus parametrically  $r_{f,H}(0) = 1 + \mathcal{O}(m_{LR}^4/\tilde{m}^4)$ . This behavior may also be obtained directly from (9), with the limiting values of the mixing angle and loop functions given in appendix A 3. In the strict superpartner decoupling limit,  $r_{f,H}(0) \rightarrow 1$ , so that the effective Higgs and mass Yukawa coupling coincide.

The parametric dependence of the Higgs coupling ratio (10) at  $q^2 = 0$  can also be understood from the general form of the effective Higgs Yukawa coupling. Promoting all

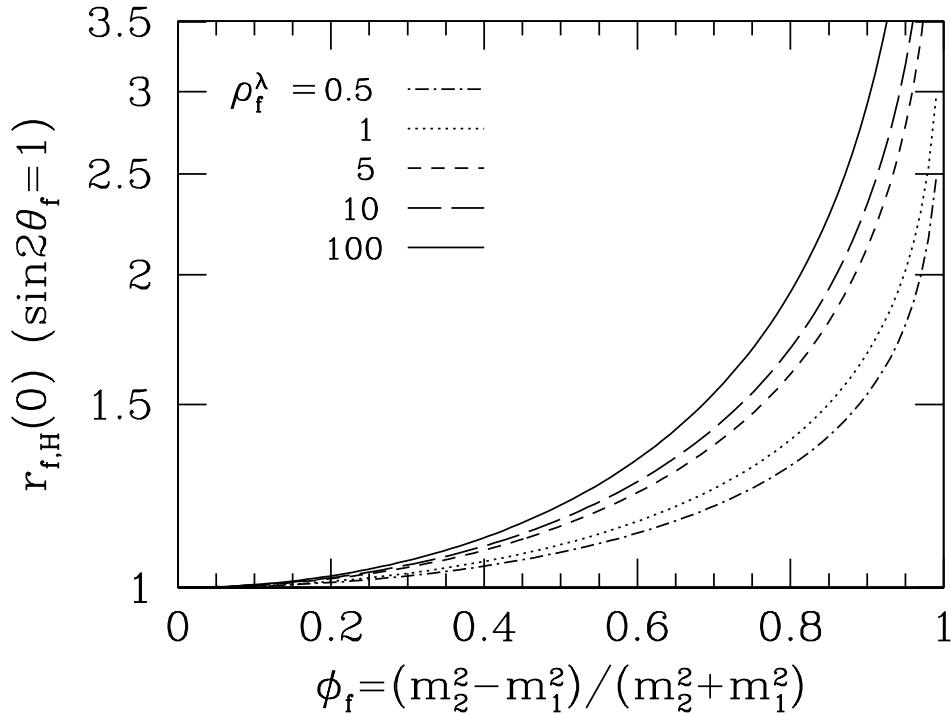


FIG. 4. The ratio of  $h^0$  and  $H^0$  Higgs–fermion Yukawa couplings to the mass Yukawa coupling,  $r_{f,H} = \bar{h}_{f,H} / \bar{h}_{f,m}$ , as a function of the fractional scalar mass splitting  $\phi_f$  for different values of  $\rho_f^\lambda$ . The ratio is shown for  $q^2 = 0$  and for maximal scalar mixing,  $\sin 2\theta_f = 1$ .

parameters to background fields, and requiring invariance with respect to all background and gauge symmetries, the functional dependence of the radiative fermion masses at one loop may be written

$$m_f = \bar{h}_{f,m}(0)H_\alpha = \mathcal{F} \left( m_{\tilde{f}}^2 (A^* A H_\alpha^* H_\alpha, H_\beta^* H_\beta), m_\lambda^* m_\lambda, \frac{\mu H_1 H_2}{m_\lambda^*} \right) \frac{m_\lambda^* A}{m_{\tilde{f}}^2} H_\alpha, \quad (11)$$

where  $\bar{h}_{f,m}(0)$  is the radiative mass Yukawa coupling defined by (10),  $A^* A H_\alpha^* H_\alpha = m_{LR}^4$ ,  $m_{\tilde{f}}$  are the physical mass eigenvalues, the Higgs doublets  $H_{\alpha,\beta}$  are understood as expectation values, and here  $\beta = 1, 2$  is summed while  $\alpha = 1$  or  $2$  is determined by the scalar tri-linear coupling and is not summed.  $\mathcal{F}$  is a dimensionless function that depends only on the particular combinations of parameters indicated in (11). These combinations of parameters are invariant under the gauge and background symmetries. In the heavy superpartner limit,  $\mathcal{F}$  is an analytic function with power series expansion and non-vanishing first derivatives with respect to any of the invariant combinations of dependent variables. The non-trivial dependence on  $H_{\alpha,\beta}$  represents, in the heavy superpartner limit, non-renormalizable operators with multiple Higgs expectation values, which contribute to the fermion mass. All such one-loop operators, coupling through the  $A$ - or  $A'$ -terms, are implicitly included in the effective Yukawa coupling (7). Additional non-trivial dependence on  $H_\beta^* H_\beta$  arises implicitly through  $\mathcal{O}(g^2 H_\beta^* H_\beta)$   $D$ -term contributions to the scalar partner mass-squared eigenvalues  $m_{\tilde{f}}^2$ . The dependence on  $H_1 H_2$  arises from  $\mathcal{O}(gg' H_1 H_2 \mu / (m_{\tilde{B}}(\mu^2 - m_{\tilde{W}}^2)))$  neutralino mixing

effects between gaugino and Higgsino eigenstates through Higgs expectation values. This functional dependence vanishes in the pure gaugino limit.

The effective Yukawa coupling at  $q^2 = 0$  of a Higgs boson to a fermion, again with mixing effects factored out, is very generally related to the mass by

$$\bar{h}_{f,H}(0) \equiv \frac{\partial m_f}{\partial |H_\alpha|}. \quad (12)$$

With this definition and the general form of the radiative fermion mass (11), the ratio of physical Higgs to mass Yukawa couplings (10) at  $q^2 = 0$  is given by

$$r_{f,H}(0) = 1 + 2m_{LR}^4 \frac{\partial \bar{h}_{f,m}(0)}{\partial m_{LR}^4} + 2m_Z^2 \{ \cos^2 \beta, \sin^2 \beta \} \left( \frac{\partial m_f^2}{\partial m_Z^2} \frac{\partial \bar{h}_{f,m}(0)}{\partial m_f^2} + \frac{\partial \bar{h}_{f,m}(0)}{\partial m_Z^2} \right). \quad (13)$$

The first term on the right-hand side arises from differentiating (11) with respect to the Higgs doublet  $H_\alpha$  multiplying  $\bar{h}_{f,m}(0)$ . The second term comes from  $A$ - or  $A'$ -term contributions to  $\bar{h}_{f,m}(0)$  through the  $m_{LR}^4$  dependence. The third term comes from  $D$ -term contributions through  $m_f^2$  where the first (second) term in the brackets is for  $\alpha = 1$  (2). The fourth term represents contributions through neutralino mixing effects. In the heavy superpartner limit, the mass scale for variations of  $\bar{h}_{f,m}$  are controlled by the largest superpartner mass,  $\partial \bar{h}_{f,m}(0)/\partial m_{LR}^4$  is of  $\mathcal{O}(1/\tilde{m}^4)$ , which agrees with the scaling given above based on chiral insertions in the one-loop radiative mass diagram. Likewise, for the  $D$ -term effects  $\partial \bar{h}_{f,m}(0)/\partial m_f^2$  is of  $\mathcal{O}(1/\tilde{m}^2)$ ,  $\partial m_f^2/\partial m_Z^2$  of  $\mathcal{O}(1)$ , and for the neutralino mixing effects  $\partial \bar{h}_{f,m}(0)/\partial m_Z^2$  is of  $\mathcal{O}(1/\tilde{m}^2)$ . In the heavy superpartner limit the full parametric dependence of the Higgs coupling ratio is then  $r_{f,H}(0) = 1 + \mathcal{O}(m_{LR}^4/\tilde{m}^4) + \mathcal{O}(m_Z^2/\tilde{m}^2) + \mathcal{O}(\mu m_Z^2/(m_{\tilde{B},\tilde{g}} \tilde{m}^2))$ . The  $D$ -term and neutralino mixing contributions to the effective Higgs Yukawa couplings are not explicitly included in (7), and are only important respect to the non-linear dependence on the  $A$ - or  $A'$ -terms if  $A \lesssim m_Z$  (and are therefore not dominant for second or third generation radiative masses, which require  $A$  or  $A' \sim \tilde{m}$  as discussed in section III). An effect of the  $D$ -terms and neutralino mixings is to introduce additional “wrong Higgs” couplings to fermions through the functional dependence of (11). Such couplings, however, are suppressed in the heavy superpartner limit respect to the dominant coupling through the over-all Higgs doublet  $H_\alpha$  multiplying  $\bar{h}_{f,m}$  in (11) by  $\mathcal{O}(m_Z^2/\tilde{m}^2)$  and  $\mathcal{O}(\mu m_Z^2/(m_{\tilde{B},\tilde{g}} \tilde{m}^2))$  respectively. In the strict superpartner decoupling limit the only operator that couples Higgs doublets to fermions is the renormalizable effective Yukawa coupling. All other operators are non-renormalizable, and vanish in this limit. So  $\bar{h}_{f,m}(0)$  necessarily approaches an  $H_\alpha$ -independent function with  $r_{f,H}(0) \rightarrow 1$  in this limit.

It is apparent from fig. 4 that the scalar Higgs couplings generated radiatively through the  $A$ - or  $A'$ -terms enhances the ratio  $r_{f,H}(0)$  in the heavy superpartner limit. The enhancement  $r_{f,H} \geq 1$  persists for finite superpartner masses,  $m_f^2, m_\lambda^2 \sim m_H^2$ . In this case the Higgs-fermion Yukawa couplings have non-trivial form factors,  $\bar{h}_{f,H} = \bar{h}_{f,H}(q^2)$ , in addition to the usual renormalization group evolution of a Yukawa coupling. For  $m_f^2, m_\lambda^2 \sim m_H^2$  the fractional change in the loop functions between  $q^2 = 0$  and  $q^2 = m_H^2$ , relevant to the coupling to a physical Higgs boson, can lead to significant variation in the radiative Yukawa

couplings. Neglecting Higgs couplings through  $D$ -terms and neutralino mixing effects (which are subdominant for second and third generation radiative masses as mentioned above), the general expression for the  $q^2 = m_H^2$  momentum dependence of the radiative Higgs Yukawa couplings can be obtained from (7) and (8). These expressions are considerably simplified in the limit of degenerate superpartners  $m_{\tilde{f}_1} = m_{\tilde{f}_2} = m_\lambda \equiv \tilde{m}$  for which  $J_1(m_H^2; \tilde{m}^2, \tilde{m}^2, \tilde{m}^2) = J_2(m_H^2; \tilde{m}^2, \tilde{m}^2, \tilde{m}^2)$ . The leading  $q^2 = m_H^2$  dependence of the ratio of physical Higgs to mass Yukawa couplings (10) in the heavy degenerate superpartner limit,  $\tilde{m}^2 \gg m_H^2$ , can then be obtained from the limiting forms of the loop integrals given in appendix A 3. For  $\tilde{m}^2 \gg m_H^2$

$$r_{f,H}(m_H^2) = 1 + \frac{1}{12} \frac{m_H^2}{\tilde{m}^2} + \dots \quad (14)$$

where  $+\dots$  represents higher-order dependence. (The full functional momentum dependence, is given below in the context of the pseudoscalar Higgs radiative Yukawa coupling.) For finite superpartner masses it is possible to characterize the leading low-energy momentum dependence in terms of a finite Higgs Yukawa radius,

$$\bar{R}_{f,H}^2 \equiv \frac{6}{\bar{h}_{f,H}(0)} \frac{\partial \bar{h}_{f,H}(0)}{\partial q^2} \quad (15)$$

analogous to the charge radius of an electromagnetic coupling. From (14) the Higgs Yukawa radius for a radiative fermion mass in the heavy degenerate superpartner limit is  $\bar{R}_{f,H}^2(m_H^2) \simeq 1/(2\tilde{m}^2)$ . In real space this radius is determined by the Compton wavelength of the virtual superpartners, and vanishes in the superpartner decoupling limit. Note that since both the Higgs Yukawa radius and the radiative fermion mass arise from the same diagrams, the Higgs Yukawa radius is effectively not suppressed by a loop factor. This is unlike the case of a tree-level Yukawa coupling, for which the Higgs Yukawa radius is smaller by a loop factor than the Compton wavelength of the contributing virtual particles. Analogous radii can also be defined from the form factors for the Higgsino couplings discussed in the next subsection, and, in the case of an off-shell fermion, for the fermion mass itself.

The effective radiative Yukawa couplings for the pseudoscalar Higgs,  $A^0$ , differ somewhat from those of the scalar Higgs bosons. The pseudoscalar Higgs couplings in fig. 3 only connect one scalar partner mass eigenstate with the other mass eigenstate, unlike the scalar Higgs couplings, which connect all possible combinations of mass eigenstates. Summing over scalar partner mass eigenstates, the one-loop  $A^0$  effective Yukawa coupling in the pure gaugino limit can then be related to the fermion mass Yukawa by

$$\bar{h}_{f,A}(m_{A^0}^2) = \frac{m_f}{|\langle H_\alpha \rangle|} J_2(m_{A^0}^2; m_{\tilde{f}_1}^2, m_\lambda^2, m_{\tilde{f}_2}^2), \quad (16)$$

where  $\lambda_{A^0} = \Theta\{\cos\beta, \sin\beta\} \bar{h}_{f,A}/\sqrt{2}$  for  $\alpha = 1, 2$  is the amplitude for coupling of the physical  $A^0$  eigenstate to fermions (all considered on-shell), and  $\Theta$  represents the projection of  $A^0$  onto the Higgs doublets. A definition of the ratio of the effective  $A^0$  Yukawa coupling to the effective mass coupling may be introduced

$$r_{f,A}(m_{A^0}^2) \equiv \frac{\bar{h}_{f,A}(m_{A^0}^2)}{\bar{h}_{f,m}(0)}, \quad (17)$$

analogous to that for the scalar Higgs coupling (10).

The one-loop result for the effective pseudoscalar Higgs Yukawa coupling (16) has a number of interesting properties. It is independent of the scalar partner mixing angles and only depends on the superpartner spectrum and momentum transfer  $q^2 = m_{A^0}^2$ . In addition, in the heavy superpartner decoupling limit,  $m_{\tilde{f}}^2, m_{\tilde{\lambda}}^2 \gg m_{A^0}^2$ , the loop function may be evaluated at  $q^2 = 0$ , for which the vertex loop function reduces to the mass loop function, as discussed above, yielding  $J_2(0; m_{\tilde{f}_1}^2, m_{\tilde{\lambda}}^2, m_{\tilde{f}_2}^2) = 1$ . The intrinsic one-loop pseudoscalar radiative couplings evaluated at  $q^2 = 0$  therefore do not differ from the effective Yukawa coupling, unlike the scalar Higgs–fermion couplings. This result may also be obtained from the general form of the radiative fermion mass (11). The effective Yukawa coupling at  $q^2 = 0$  of the physical  $A^0$  Higgs boson to a fermion, again with mixing effects factored out, is very generally related to the mass by

$$\bar{h}_{f,A}(0) = \frac{1}{|H_\alpha|} \frac{\partial m_f}{\partial \theta_\alpha}, \quad (18)$$

where  $H_\alpha = |H_\alpha|e^{i\theta_\alpha}$ . Since in the pure gaugino limit,  $\bar{h}_{f,A}$  is a function of the Higgs doublets at one loop only through the combination  $H_\beta^* H_\beta$ , which is independent of  $\theta_\beta$ , the pseudoscalar coupling arises only through the over-all Higgs doublet,  $H_\alpha$ , multiplying  $\bar{h}_{f,m}$  in (11). The ratio of pseudoscalar Higgs to mass Yukawa couplings at  $q^2 = 0$  neglecting neutralino mixing is therefore

$$r_{f,A}(0) = 1, \quad (19)$$

in agreement with the explicit calculation (16) in the  $q^2 = 0$  limit. This result amounts to a very general low-energy theorem for the  $q^2 = 0$  coupling of  $A^0$  to fermions in any theory with a single pair of Higgs doublets, and with only one doublet coupling to the given fermion. It can only be spoiled by effects that allow an  $H_1 H_2$  dependence of the effective Yukawa coupling. In the present context if radiative masses arise from either  $A$ - or  $A'$ -terms, but not both, such a dependence arises in the one-loop diagram only the from gaugino–Higgsino mixing effects discussed above. Inclusion of these effects does give  $\mathcal{O}(\mu m_Z^2 / (m_{\tilde{B},\tilde{g}} \tilde{m}^2))$  corrections to (19). In contrast, inclusion of  $D$ -term contributions to the scalar masses does not modify the ratio.

Since the  $A^0$ –fermion couplings are independent of scalar partner mixing effects and  $D$ -term Higgs couplings, and are only modified by finite-momentum effects in the pure gaugino limit, it is instructive to consider the  $q^2 = m_{A^0}^2$  dependence explicitly. From the expressions for the loop functions given in appendix A 3, in the pure gaugino limit with degenerate scalar partners and gaugino of mass  $\tilde{m} = m_{\tilde{f}_1} = m_{\tilde{f}_2} = \tilde{m}_\lambda$ , the ratio of pseudoscalar Higgs Yukawa coupling to mass Yukawa coupling is given by

$$r_{f,A}(m_{A^0}^2) = \begin{cases} -\frac{\tilde{m}^2}{m_{A^0}^2} \left[ \log \left( \frac{1 + \sqrt{1 - 4\tilde{m}^2/m_{A^0}^2}}{1 - \sqrt{1 - 4\tilde{m}^2/m_{A^0}^2}} \right) - i\pi \right]^2 & \tilde{m} < \frac{1}{2}m_{A^0} \\ +\frac{4\tilde{m}^2}{m_{A^0}^2} \arcsin^2 \left( \frac{m_{A^0}}{2\tilde{m}} \right) & \tilde{m} \geq \frac{1}{2}m_{A^0} \end{cases}. \quad (20)$$

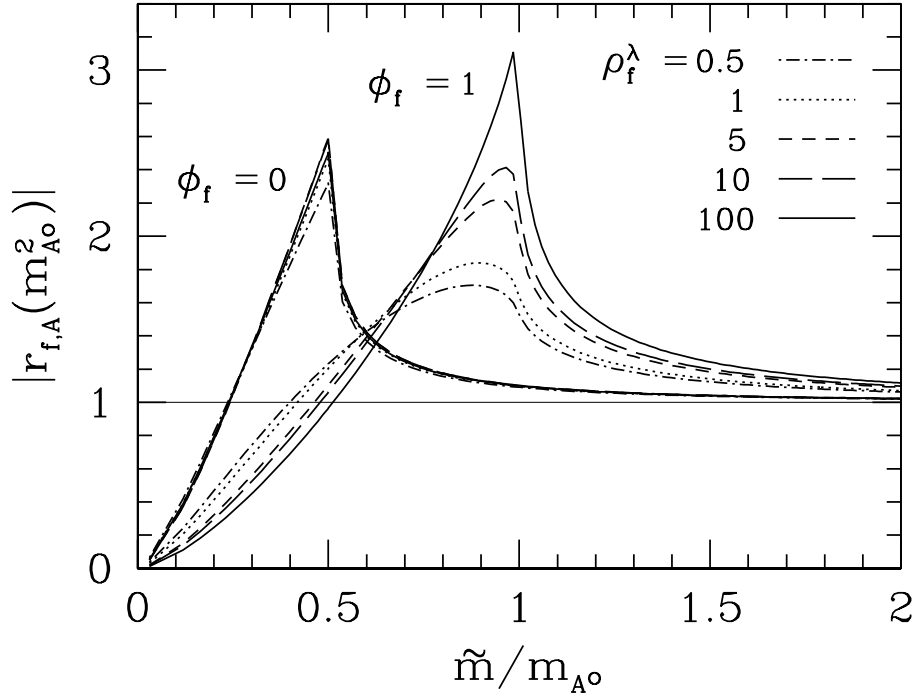


FIG. 5. Magnitude of the ratio  $r_{f,A}(m_{A^0}^2)$  in the limit of degenerate scalar partners  $m_{\tilde{f}_1} = m_{\tilde{f}_2} = \tilde{m}$  ( $\phi_f = 0$ ), and of maximal splitting among superpartner masses  $m_{\tilde{f}_1} = 0$ ,  $m_{\tilde{f}_2} = \tilde{m}$  ( $\phi_f = 1$ ), for different values of  $\rho_f^\lambda$ . In both cases, the ratio is shown as a function of  $\tilde{m}$  divided by the pseudoscalar Higgs mass  $m_{A^0}$ . The horizontal line indicates the value  $r_{f,A}(m_{A^0}^2) = 1$ .

For  $\tilde{m} < \frac{1}{2}m_{A^0}$  the imaginary piece arises from the branch cut for physical intermediate states in the loop. The ratio  $r_{f,A}(m_{A^0}^2) \geq 1$  for all  $\tilde{m} > \frac{1}{2}m_{A^0}$ , and  $r_{f,A}(m_{A^0}^2) \rightarrow 0$  as  $\tilde{m} \rightarrow 0$ . The finite momentum enhancement can be sizeable for  $\tilde{m} \sim m_{A^0}$ , and persists away from the degenerate superpartner limit. The  $\tilde{m} \gg m_{A^0}$  behavior is identical to the scalar Higgs ratio (14), with Higgs Yukawa radius vanishing in the strict superpartner decoupling limit. Figure 5 shows the ratio  $r_{f,A}(m_{A^0}^2)$  as a function of  $\tilde{m}/m_{A^0}$  for two extreme choices of the scalar partner mass spectrum. In the first case,  $\phi_f = 0$ , corresponding to a degenerate scalar spectrum  $m_{\tilde{f}_1} = m_{\tilde{f}_2} = \tilde{m}$ , for different values of  $\rho_f^\lambda$ , with  $\rho_f^\lambda = \tilde{m}^2/m_\lambda^2$  in this case. The analytic expression given in eq. (20) corresponds to this case, with  $\rho_f^\lambda = 1$ . In the second case  $\phi_f = 1$ , corresponding to maximal splittings among superpartner masses,  $m_{\tilde{f}_1} = 0$ ,  $m_{\tilde{f}_2} = \tilde{m}$ . Again,  $r_{f,A}(m_{A^0}^2)$  is shown for different values of  $\rho_f^\lambda$ , which for this case  $\rho_f^\lambda = \tilde{m}^2/(2m_\lambda^2)$ . A simple, analytic expression can be obtained also in this case with  $\tilde{m} = m_\lambda$ , i.e.  $\rho_f^\lambda = \frac{1}{2}$ , by using results listed in appendices A 2 and A 3. For a numerical evaluation of the loop function that appears in  $r_{f,A}(m_{A^0}^2)$ , shown in fig. 5, see ref. [14].

As discussed in section VIII below, measurements of  $h^{0-}$ ,  $H^{0-}$ , and  $A^0$ -fermion couplings offer the possibility of isolating intrinsic coupling effects from momentum-dependent form factors.

### C. The Higgsino coupling

The couplings of neutral Higgsinos  $\widetilde{H}_1^0, \widetilde{H}_2^0$  to fermions  $f$  and associated scalar partners  $\widetilde{f}$ , arise radiatively in a manner similar to the fermion masses and Higgs couplings, as shown in fig. 6. The one-loop radiative couplings have to be calculated separately for the two cases in which the coupled fermions are both left- or right-handed.

The momentum-dependent coupling  $\widetilde{h}_{f_R}$  of right-handed fermions to left-handed scalars,  $\widetilde{h}_{f_R} \overline{f}_R(q_1) \widetilde{H}_\alpha^0(q) \widetilde{f}_L(q_2)$ , arises, for example, at one loop from pure  $\widetilde{B}$ – $\widetilde{B}$  and mixed  $\widetilde{B}$ – $\widetilde{W}$  propagators. With all external particles on-shell, relevant to the decay  $\widetilde{f}_h(q_2) \rightarrow f_R(q_1) \widetilde{\chi}_i^0(q)$ , where  $\widetilde{f}_h$  is the scalar partner eigenstate labelled by  $h$  ( $h = 1, 2$ ), the neutralino–neutral Higgs contribution to the effective Yukawa coupling is

$$\widetilde{h}_{f_R} = -\frac{\alpha'}{8\sqrt{2}\pi} A \widetilde{K}_{f_R}^{ijklkh} V_{ijklkh} \quad (21)$$

with only the indices  $jlkh$  summed. The coupling  $\widetilde{K}_{f_R}^{ijklkh}$  is given by

$$\begin{aligned} \widetilde{K}_{f_R}^{ijklkh} = & \frac{Y_{f_R}}{2} N_{jB} [N_{jB} - \cot \theta_W N_{jW}] \times \\ & [\delta_{l2} (N_{iH_1} \sin \alpha + N_{iH_2} \cos \alpha) - \delta_{l1} (N_{iH_1} \cos \alpha - N_{iH_2} \sin \alpha)] \times \\ & (U_{k1} U_{h2} + U_{k2} U_{h1}) U_{k1}. \end{aligned} \quad (22)$$

where  $N_{iH_1}, N_{iH_2}$  are the projection factors for the external neutralino  $\widetilde{\chi}_i^0$  onto the Higgsino states  $\widetilde{H}_1^0$  and  $\widetilde{H}_2^0$  respectively. Note that both  $N_{iH_1}$  and  $N_{iH_2}$  are, in general, non-vanishing, regardless of which of the two Higgs expectation values induces the corresponding fermion mass. The index  $j = 1, \dots, 4$  refers to the external neutralino mass eigenstate;  $l$  to the type of CP-even neutral Higgs exchanged in the loop,  $h^0, H^0$ . The matrix  $U$ , which diagonalizes the scalar mass matrix (A1), is defined in appendix A 1 and the loop function  $V_{ijhkl}$  is given explicitly in appendix A 3 in terms of  $C_0$  and  $B_0$  functions.

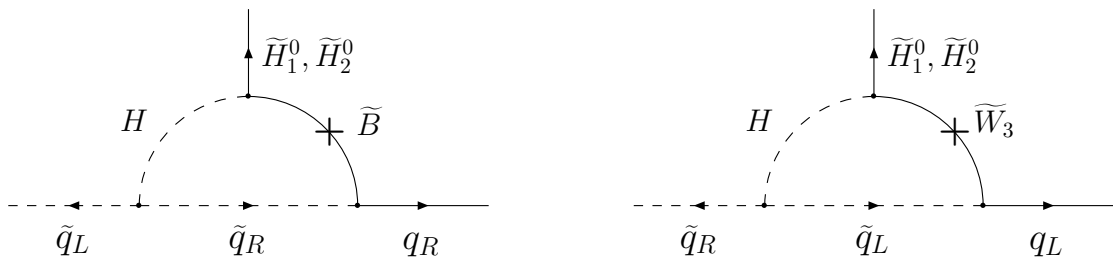


FIG. 6. One-loop radiative Wino and Bino contributions to the Higgsino–scalar–fermion couplings from soft flavor violation. The neutral Higgs  $H$  exchanged virtually in the loop, can be  $h^0$  or  $H^0$ .

In the case of left-handed fermions, the momentum-dependent coupling  $\widetilde{h}_{f_L}$  relative to the vertex  $\widetilde{h}_{f_L} \overline{f}_L(q_1) \widetilde{H}_\alpha^0(q) \widetilde{f}_R(q_2)$  can be mediated by pure  $\widetilde{W}$ – $\widetilde{W}$  and  $\widetilde{B}$ – $\widetilde{B}$  as well as by



mixed  $\widetilde{W}$ – $\widetilde{B}$  propagators. For on-shell external particles, as in the case of the decay  $\widetilde{f}_h(q_2) \rightarrow f_L(q_1) \widetilde{\chi}_i^0(q)$ , the neutralino–neutral Higgs contribution to the effective Yukawa coupling is

$$\widetilde{h}_{f_L} = \frac{\alpha_2}{8\sqrt{2}\pi} A \widetilde{K}_{f_L}^{ijklkh} V_{ijklkh} \quad (23)$$

where  $\widetilde{K}_{f_L}^{ijklkh}$  has the expression

$$\begin{aligned} \widetilde{K}_{f_L}^{ijklkh} = & \left[ T_f N_{jW} + \tan \theta_W \frac{Y_{f_L}}{2} N_{jB} \right] [N_{jW} - \tan \theta_W N_{jB}] \times \\ & [\delta_{l1}(N_{iH_1} \cos \alpha - N_{iH_2} \sin \alpha) - \delta_{l2}(N_{iH_1} \sin \alpha + N_{iH_2} \cos \alpha)] \times \\ & (U_{k1} U_{h2} + U_{k2} U_{h1}) U_{k2}. \end{aligned} \quad (24)$$

Also in this case, both projection factors  $N_{iH_1}$  and  $N_{iH_2}$  for the external neutralino  $\widetilde{\chi}_i^0$  onto the two Higgsino states  $\widetilde{H}_1^0$  and  $\widetilde{H}_2^0$  are present.

For both decays,  $\widetilde{f}_h(q_2) \rightarrow f_R(q_1) \widetilde{\chi}_i^0(q)$  and  $\widetilde{f}_h(q_2) \rightarrow f_L(q_1) \widetilde{\chi}_i^0(q)$ , there exist also chargino–charged Higgs loop contributions, which are not explicitly given here. Their dependence on gauge couplings is the same as that of neutralino–neutral Higgs contributions.

The radiatively generated effective Higgsino Yukawa coupling differs from the effective mass and Higgs Yukawa couplings in a number of ways. Most importantly, radiatively induced quark masses get contributions from both gluino and neutralino exchange, whereas the Higgsino couplings only receive contributions from neutralino exchange in the loop. This profound difference is due to the absence of a Higgsino analogue of the flavor-violating scalar tri-linear coupling, combined with the requirement of gauge invariance. Thus, radiative Higgsino couplings differ significantly in magnitude from the associated radiative mass or Higgs Yukawa couplings. Furthermore, the fact that the right-handed fermion states couple only through  $U(1)_Y$  interactions, while the left-handed ones couple through both  $U(1)_Y$  and  $SU(2)_L$  interactions, yields distinct Higgsino couplings to the right- and left-handed fermions,  $\widetilde{h}_{f_R}$  and  $\widetilde{h}_{f_L}$ , with  $\widetilde{h}_{f_R}/\widetilde{h}_{f_L} \sim \mathcal{O}(\alpha'/\alpha_2)$ . This compares with  $\widetilde{h}_{f_R}/\widetilde{h}_{f_L} = 1$  at lowest order for a fermion mass arising from a hard tree-level Yukawa coupling. Finally, the type of Higgsino appearing in the coupling,  $\widetilde{H}_1^0$  or  $\widetilde{H}_2^0$ , need not coincide with the type of Higgs expectation value which induces the fermion mass. In contrast, for a tree-level Yukawa coupling, only the Higgsino of the same type appears.

In order to characterize Higgsino couplings to fermions, it is useful to define their ratio to the effective mass Yukawa coupling, in analogy with the Higgs coupling ratio (10). Dropping momentum dependences, this ratio is:

$$\widetilde{r}_{f_{L,R}} \equiv \frac{\widetilde{h}_{f_{L,R}}}{m_f / |\langle H_\alpha \rangle|}. \quad (25)$$

The general expression for these ratios is complicated and can be extracted from (21), (23), and (A25). When superpartner masses are all of the same order, however, the parametric dependence of  $\widetilde{r}_{f_{L,R}}$  is readily determined from the above discussion. For quarks that obtain a radiative mass from soft flavor breaking,  $\widetilde{r}_{f_L}$  is of  $\mathcal{O}(\alpha_2/\alpha_s)$  and  $\widetilde{r}_{f_R}$  of  $\mathcal{O}(\alpha'/\alpha_s)$ , whereas

for leptons,  $\tilde{r}_{f_L}$  is of  $\mathcal{O}(\alpha_2/\alpha')$  and  $\tilde{r}_{f_R}$  of  $\mathcal{O}(1)$ . This is to be compared with a tree-level Yukawa coupling for which  $\tilde{r}_{f_{L,R}} = 1$  at the lowest order.

The large differences between the Higgsino and Higgs or mass Yukawa couplings are a concrete example of apparent hard supersymmetry breaking from the low-energy point of view. The large splittings arise at the leading order and are not small corrections to a supersymmetric relation. In contrast, the equality of tree-level Yukawa couplings in the supersymmetric limit is only slightly modified by higher-order corrections when supersymmetry is broken. With radiative fermion masses, no symmetry exists in the high-energy theory to enforce equality of the radiatively generated low-energy Higgs and Higgsino couplings since these couplings vanish in the supersymmetric limit. Large splittings for the Higgsino–fermion–scalar couplings therefore represent a “smoking gun” for radiatively generated fermion masses from soft chiral flavor breaking. As discussed in section VIII, however, the Higgsino couplings are likely to be difficult to measure experimentally.

### III. PHENOMENOLOGICAL RADIATIVE MODELS

The magnitude of fermion masses which arise from soft chiral flavor violation depends on the soft supersymmetry-breaking parameters  $m_\lambda$ ,  $m_{\tilde{f}_i}$  and  $A$  or  $A'$ , as detailed in section II A. With the radiative mass given in eq. (3), a given quark or lepton mass can be estimated from the magnitude of the ratio  $Am_\lambda/\tilde{m}^2$  or  $A'm_\lambda/\tilde{m}^2$

$$\begin{aligned}
\text{Lepton : } \frac{m_l}{30-100 \text{ MeV}} &\sim \left\{ \sqrt{2} \cos \beta \frac{Am_{\tilde{B}}}{\tilde{m}^2}, \sqrt{2} \sin \beta \frac{A'm_{\tilde{B}}}{\tilde{m}^2} \right\} \\
\text{Down-type quark : } \frac{m_q}{1-3 \text{ GeV}} &\sim \left\{ \sqrt{2} \cos \beta \frac{Am_{\tilde{g}}}{\tilde{m}^2}, \sqrt{2} \sin \beta \frac{A'm_{\tilde{g}}}{\tilde{m}^2} \right\} \\
\text{Up-type quark : } \frac{m_q}{1-3 \text{ GeV}} &\sim \left\{ \sqrt{2} \sin \beta \frac{Am_{\tilde{g}}}{\tilde{m}^2}, \sqrt{2} \cos \beta \frac{A'm_{\tilde{g}}}{\tilde{m}^2} \right\}
\end{aligned} \tag{26}$$

where the first (second) terms in the curly brackets correspond to holomorphic (non-holomorphic) soft flavor breaking,  $m_{\tilde{B}}$  and  $m_{\tilde{g}}$  are the Bino and gluino mass, respectively, and  $\tilde{m} = \max(m_{\tilde{f}_1}, m_{\tilde{f}_2}, m_\lambda)$ . For leptons, the radiative mass is assumed to be dominated by Bino exchange, which is the case in the mostly gaugino or Higgsino region of parameter space. For the numerical estimates (26) the loop function  $\tilde{m}^2 I(m_{\tilde{f}_1}^2, m_{\tilde{f}_2}^2, m_\lambda^2)$  is assumed to be in the range  $\frac{1}{3}-1$ , and  $\langle H_\alpha \rangle \simeq 175 \cos \beta (\sin \beta) \text{ GeV}$  for  $\alpha = 1$  (2).

The radiative masses are maximized if the scalar partner and gaugino masses are of the same order,  $m_\lambda \sim m_{\tilde{f}}$ . Stability of the charge- and color-preserving vacuum, with vanishing squark and slepton expectation values, places an upper limit on the scalar tri-linear  $A$ - or  $A'$ -parameters. The specific bounds are model-dependent and are detailed in section IV. In general  $A/\tilde{m}$  or  $A'/\tilde{m} \lesssim \text{few}$ , is required for stability of the charge- and color-preserving vacuum, where  $\tilde{m}$  is a scalar mass. This constraint implies that the ratios  $Am_\lambda/\tilde{m}^2$  and  $A'm_\lambda/\tilde{m}^2$  cannot be much larger than a few. With this upper limit and the numerical

TABLE I. Magnitude of soft chiral flavor breaking  $A$ - or  $A'$ -terms required for soft radiative fermion masses. For down-type quarks and leptons the first term in brackets corresponds to holomorphic  $A$ -terms, the second to non-holomorphic  $A'$ -terms, and vice versa for up-type quarks. Approximate masses are specified at the electroweak scale.

Fermion	$m_f$ (MeV)	$Am_\lambda/\tilde{m}^2$ or $A'm_\lambda/\tilde{m}^2$ $\times \left\{ \sqrt{2} \cos \beta, \sqrt{2} \sin \beta \right\}$
$e$	0.5	$(0.5\text{--}1.5) \times 10^{-3}$
$u$	1	$(0.3\text{--}1) \times 10^{-3}$
$d$	5	$(2\text{--}5) \times 10^{-3}$
$\mu$	100	1–3
$c$	700	0.2–0.7
$s$	100	0.03–0.1
$b$	3000	1–3

values (26), it is clear that radiative fermion masses for the first generation can be easily accommodated. Second-generation masses can also be accommodated, depending on the size of the ratios  $Am_\lambda/\tilde{m}^2$  or  $A'm_\lambda/\tilde{m}^2$ . For the third generation, it is (not surprisingly) extremely unlikely that the  $\tau$ -lepton or top quark obtain masses from soft chiral flavor violation, because of the very large tri-linear terms required. Avoiding the stability constraints discussed in section IV would require in these cases an extreme tuning of the potential or loss of perturbativity in the scalar sector at a very low scale. However, it is possible in the third generation to obtain a radiative  $b$ -quark mass by this mechanism. The magnitude of the  $A$ - or  $A'$ -terms required for soft radiative masses are listed in table I. (For a recent review of numerical values for running fermion masses, see [15].)

The magnitude of soft radiative masses depends on the ratio of Higgs doublet expectation values,  $\tan\beta$ , as given in table I. For holomorphic chiral flavor breaking in  $A$ -terms, radiative fermion masses arise from the same Higgs doublet as for tree-level Yukawa couplings. However for non-holomorphic breaking in  $A'$ -terms, radiative fermion masses arise from the “wrong Higgs” doublet, and therefore have the “wrong” dependence on  $\tan\beta$ . Soft radiative muon or  $b$ -quark masses require relatively large scalar tri-linear terms, proportional to  $\cos\beta$  in the holomorphic case and  $\sin\beta$  in the non-holomorphic case. So if either of these fermions gain a mass from holomorphic soft chiral flavor breaking in  $A$ -terms, the upper limit on the tri-linear terms from stability of the potential,  $A/\tilde{m} \lesssim \text{few}$ , discussed in section IV, strongly disfavors large values of  $\tan\beta$ . This is simply because the effective Yukawa coupling required for a given muon or  $b$ -quark mass increases with  $\tan\beta$ . Alternatively, large values of  $\tan\beta$  can be accommodated with radiative masses for either the muon or  $b$ -quark from non-holomorphic flavor breaking in  $A'$ -terms. If the charm quark mass, as well as either the muon or  $b$ -quark mass, arise from solely holomorphic or solely non-holomorphic chiral flavor violation, larger values of  $\tan\beta$  are disfavored so that none of the required tri-linear terms is too large. Note that if all standard model fermions obtained mass radiatively from chiral flavor violation in purely non-holomorphic  $A'$ -terms, the role of  $H_1$  and  $H_2$  in the radiative Yukawa couplings would be precisely the reverse of what it is in the minimal case with tree-level masses. In this case, there would be no observational signature of “wrong Higgs”

couplings, because the physical observables in the bosonic sector of the theory are invariant under  $\tan\beta \leftrightarrow \cot\beta$ . However, as noted above, vacuum stability and the absence of fine tuning are not compatible with purely radiative top-quark and  $\tau$ -lepton masses. Therefore in practice with radiative mass arising from  $A'$ -terms, observable differences from minimal models are expected, as will be discussed in section VIII.

A corollary of a radiative soft fermion mass from chiral flavor breaking is an enhanced left–right mixing for the associated scalars,  $m_{LR}^2 = A\langle H_\alpha \rangle$  or  $A'\langle H_\alpha \rangle$ . In a theory with tree-level Yukawa couplings, the mixing scales as the product of fermion and scalar partner masses  $m_{LR}^2 \sim m_f m_{\tilde{f}}$ . However with a soft radiative mass the mixing is effectively a loop factor larger,  $m_{LR}^2 \sim (4\pi/\alpha)m_f \tilde{m}^2/m_\lambda$ , where  $\alpha = \alpha_s$  or  $\alpha'$  for quarks or leptons. In the case of radiative second-generation masses, especially for the muon or charm quark, or radiative  $b$ -quark mass, the mixing can be near maximal because of the required large tri-linear term. This has potentially directly observable consequences for scalar partner production and decay, as discussed in section VIII.

In the quark sector, the CKM mixing matrix is given by  $V_{CKM} = V_u^\dagger V_d$ , where  $V_u$  and  $V_d$  are the unitary matrices that diagonalize the left-handed up- and down-type quarks respectively. If some of the quark masses arise radiatively, then the form of  $V_u$  and/or  $V_d$  follows in part from that of the scalar tri-linear terms. In particular, if any quark receives a mass predominantly from chiral flavor breaking, the source of CP violation in the CKM matrix and QCD vacuum angle are functions of the relative phases between the tree-level Yukawa couplings and tri-linear terms. (The somewhat related idea that tree-level Yukawa couplings could be purely real with all CP violation arising from  $A$ -terms was recently discussed in ref. [16].)

The pattern of tree-level and radiative quark masses can in principle arise in any number of ways. We do not address specific soft and hard textures in this paper, but comment on some interesting possibilities. As discussed above, the down-type quark masses could be purely radiative. If this is the case, and all up-type quark masses are tree-level, then of course  $V_d$  follows entirely from the scalar tri-linear terms, while  $V_u$  follows from the superpotential up-type Yukawa couplings. In this scenario the breaking of down-type right-handed quark symmetries solely in soft tri-linear terms can be naturally implemented by continuous  $U(1)_R$  or discrete  $R$ -symmetries. An accidental  $U(1)_R$  symmetry of this type would arise automatically if, for example, down-type quark symmetries are only broken through auxiliary expectation values, either spontaneously or explicitly in the supersymmetry-breaking sector, while being respected in the supersymmetric sector of the theory. Alternatively, if some of the up-type quark masses are radiative, or only some of the down-type quark masses are radiative, with the remainder tree-level, then  $V_u$  and/or  $V_d$  are block diagonal. Non-trivial three-generation mixing requires that  $V_u$  and  $V_d$  be not simultaneously block diagonal. This type of texture may be enforced by symmetries. It is also possible that in the absence of any specific horizontal  $R$ -symmetries, all fermions receive mass both radiatively from soft breaking, and at tree level from a Yukawa coupling. This would arise in a Froggatt–Nielsen mechanism in which flavor symmetries are broken in both scalar and auxiliary directions. However, for the radiative contribution to be significant in this scheme, the breaking in the auxiliary directions must be stronger than in the scalar directions, so that they overcome the loop factor. However, we concentrate on the cases of purely radiative or dominantly

tree-level masses for a given fermion.

Radiative generation of fermion masses can lead to new sources of flavor violation. In the electroweak scale theory, these amount to misalignments in flavor space between the effective Yukawa couplings, which determine both the fermion mass eigenstates and Higgs sector couplings, and the  $A$ - or  $A'$ -terms and/or left- and right-handed scalar mass-squared matrices, which determine the squark and slepton eigenstates. Misalignment between these terms in general leads to flavor-changing gaugino couplings, which link the fermion and scalar partner sectors, and in Higgs boson and longitudinal gauge couplings to fermions. The magnitudes of induced flavor violations are model-dependent functions of the specific flavor textures and superpartner mass spectrum, and are outside the scope of this work. However, it is worth while to discuss some general features and scenarios in which the new sources of flavor violation associated with radiative masses are suppressed or eliminated.

Dangerous flavor-changing neutral currents in fermionic couplings to Higgs bosons and longitudinal gauge bosons potentially can be produced by misalignment in flavor space between the fermionic couplings to the Higgs doublet expectation values, which give rise to the fermion mass matrix, and the fermionic couplings to the physical Higgs bosons. However, this source of flavor violation is automatically avoided, with no misalignment of the physical Higgs couplings, if the Glashow–Weinberg [17] criterion of coupling all up-type quarks to a single Higgs doublet, all down-type quarks to a single Higgs doublet, and all leptons to a single Higgs doublet, is satisfied. Since the top-quark and  $\tau$ -lepton masses must be at tree level, this condition requires, with a minimal Higgs sector, that any radiative up-type quark or lepton mass arises from holomorphic chiral flavor breaking, and likewise if only some of the down-type quark masses arise radiatively. This potential source of flavor violation is also avoided if all down-type quark masses arise solely from non-holomorphic tri-linear terms. With any of these conditions, the charged Higgs couplings to fermions are also proportional to the charged current CKM mixing matrix, and thus generally safe.

Flavor violation in the superpartner sector is not as readily eliminated. Misalignment between the full fermion Yukawa couplings and  $A$ - or  $A'$ -terms in general arises if a fermion receives mass both radiatively and from a tree-level Yukawa, since the flavor structure of these contributions need not coincide. This misalignment between the hard and soft components of effective Yukawa couplings is eliminated if all fermions receive mass solely from either soft or hard flavor breaking, but not from both. For the quark sector, in which the top quark Yukawa must be at tree level, this source of misalignment is avoided, for example, in the scenario discussed above, in which all down-type chiral flavor symmetries are broken in the supersymmetry-breaking sector, while up-type chiral flavor symmetries are broken by tree-level Yukawa couplings. In the lepton sector, in which the  $\tau$ -lepton Yukawa must be at tree level, the above misalignment is analogously eliminated if the muon and electron chiral flavor symmetries are only broken by auxiliary components in the supersymmetry-breaking sector.

Even if every fermion receives mass solely from either hard or soft flavor breaking, precise alignment between the effective Yukawa couplings and tri-linear  $A$ - or  $A'$ -terms is not guaranteed, if the scalar partner mass matrices have a non-trivial flavor structure. One possible sufficient condition, which guarantees complete alignment, is for all the left- and right-handed

scalar superpartners in each sector to be degenerate, with masses squared of  $m_{LL}^2$  and  $m_{RR}^2$  respectively. The radiative Yukawa couplings are then proportional to the tri-linear  $A$ - or  $A'$ -terms. Consider, for example, the scenario mentioned above in which up-type quark chiral flavor symmetries are broken only by tree-level superpotential Yukawa couplings, while down-type quark symmetries are broken only in the soft tri-linear terms. Then the down-type effective Yukawa couplings with degenerate squarks are  $h_{d,ij} = A_{d,ij} f(m_{d_1}^2, m_{d_2}^2, m_\lambda^2)$ , where  $i, j$  refer to flavor, and  $f$  is a flavor-independent loop function, which may be obtained from (3). The proportionality implies that the fermion and scalar mass matrices are simultaneously diagonalized, with the result that neutralino couplings are flavor-conserving. Chargino couplings are also proportional to the charged current CKM mixing matrix. Precise alignment in this case may also be understood by promoting the flavor symmetries to background symmetries and treat the down-type quark tri-linear terms and up-type quark Yukawa couplings as spurions that spontaneously break the symmetries. Invariance with respect to the background symmetries then implies that any chirality-violating amplitude between external quarks is exactly proportional to a single power of either of these spurions, and therefore has precisely the same flavor structure as the quark mass matrices. This particular alignment is of course in general spoiled by non-degeneracy among the scalar partners. Also, the required degeneracy does not follow *a priori* from any symmetry since the flavor symmetries are broken in the tri-linear terms or Yukawa couplings. Near degeneracy might arise dynamically, however, if there is a relatively large flavor neutral contribution to the soft scalar masses.

There are other scenarios that avoid dangerous levels of quark-sector flavor violation associated with soft radiative masses. If all down-type quarks receive mass from soft flavor breaking as outlined above, but the individual down-type quark number is conserved, the down-type squark mass-squared matrices and  $A$ - or  $A'$ -terms are diagonal (though not necessarily degenerate), as are the down-type effective Yukawa couplings. In this case  $V_{CKM} = V_u^\dagger$ , and all quark mixing and CP violation in the CKM matrix arise from tree-level Yukawa couplings in the up sector. In addition, the chargino couplings are proportional to the charged current CKM mixing matrix. Then all supersymmetric flavor violation occurs in the up-type quark sector, from possible mismatch between the quark and squark mass matrices. At present, experimental probes in this sector are not very sensitive to such flavor violation. An analogous scenario may also be extended to the leptons, with individual lepton number conserved [18].

A very general scenario in which low-energy flavor violations arising from supersymmetric effects are suppressed results if some of the superpartners are much heavier than the electroweak scale. Requiring that two-loop quadratically divergent gauge contributions to the Higgs potential from heavy scalars lead to not excessive tuning of electroweak symmetry breaking implies that first- and second-generation scalar partners and the gluino are lighter than  $\mathcal{O}(20 \text{ TeV})$  [19]. The analogous naturalness requirement from one-loop quadratically divergent contributions from heavy electroweak gauginos implies that these gauginos are lighter than  $\mathcal{O}(2 \text{ TeV})$ . Finally, for the third generation, a similar naturalness requirement from one-loop quadratically divergent contribution through the tree-level top Yukawa implies that the left- and right-handed top squarks, and the left-handed  $b$ -squark are lighter than  $\mathcal{O}(1 \text{ TeV})$ . In the scenario for radiative fermion masses, consider the case where the

first-generation scalars are as heavy as the naturalness bounds allow. If all gauginos have masses at the electroweak scale, the hierarchy  $m_\lambda \ll m_{\tilde{f}}$  provides an attractive explanation for the smallness of first-generation radiative masses. As discussed above, radiative masses for second-generation quarks and the  $b$ -quark require  $m_\lambda \sim m_{\tilde{f}}$ . In this case, the associated scalars cannot be as heavy as allowed by the naturalness bounds unless the gluino is also very heavy. Even if only the first-generation scalars are heavy, flavor violation involving first-generation fermions arising from scalar partner mixing is suppressed by the large mass splitting between first- and second-generation scalars.

#### IV. STABILITY ANALYSIS OF THE SCALAR POTENTIAL

Radiatively generated fermion masses arising from soft chiral flavor violation require sizeable scalar tri-linear couplings, in particular  $A \gg hm_{\tilde{f}}$ , where  $h$  is the effective Yukawa coupling, and  $m_{\tilde{f}}$  represents the scalar masses. For second-generation and  $b$ -quark radiative masses,  $A \sim m_{\tilde{f}}$  are required, as discussed in the previous section and shown in table I. Such large tri-linear terms give negative contributions to the scalar potential along certain directions in field space. If large enough, these can lead to color- and/or charge-breaking minima with non-vanishing squark or slepton expectation values. The possible existence of these vacua gives an upper limit on the magnitude of the tri-linear couplings, and consequently on the radiatively induced fermion mass.

In the vacuum with electroweak symmetry broken by Higgs field expectation values, the scalar tri-linear terms (1) and (2) contribute a left–right mixing term to the squark or slepton mass-squared matrices,  $m_{LR}^2 = A\langle H_\alpha \rangle$  or  $A'\langle H_\alpha^* \rangle$ , which induces the radiative fermion masses. These mixings cause a level repulsion between the scalar mass eigenvalues. Stable electroweak symmetry breaking without color or charge breaking requires that the lightest squark or slepton eigenstate does not become tachyonic. This puts an upper limit on the  $A$ -parameters of  $|A\langle H_\alpha \rangle| < m_{LL}m_{RR}$  or  $|A'\langle H_\alpha \rangle| < m_{LL}m_{RR}$ . For second-generation and  $b$ -quark radiative masses, for which  $A \gtrsim m_{LL,RR}$ , then  $m_{LL,RR} \gtrsim \langle H_\alpha \rangle$  is required in order to achieve stable electroweak symmetry breaking. This is easily satisfied in the scenarios discussed in section III with sufficiently massive squark or sleptons.

The negative contribution of the tri-linear terms to the total potential is maximized in a direction along which all scalar fields that appear in the tri-linear term have equal expectation values:

$$|H_\alpha| = |\phi_L| = |\phi_R| = \frac{1}{\sqrt{6}}\phi, \quad (27)$$

where gauge indices and an over-all phase have been suppressed, and  $\phi$  is a real valued collective coordinate [20,21]. Even if the constraint given above for locally stable electroweak symmetry breaking is satisfied, color- and/or charge-breaking vacua can appear along this direction at larger field values. With the normalization (27),  $\phi$  is a canonically normalized real scalar field with general renormalizable tree-level potential

$$V(\phi) = \frac{1}{2}\tilde{m}^2\phi^2 - \frac{1}{3\sqrt{6}}A\phi^3 + \frac{1}{36}\lambda^2\phi^4, \quad (28)$$

where  $\tilde{m}^2 \equiv \frac{1}{3} (m_{LL}^2 + m_{RR}^2 + m_{H_\alpha}^2)$ . The Higgs mass term  $m_{H_\alpha}^2$  receives a contribution from the Higgs Dirac mass in the superpotential  $W \supset \mu H_1 H_2$ . Hence,  $\tilde{m}^2 \gg m_{LL,RR}^2$  is possible in principle with a large Dirac mass,  $\mu^2 \gg m_{LL,RR}^2$ . However, minimal tuning of electroweak symmetry breaking usually implies  $|m_{H_\alpha}^2| \sim m_Z^2 \lesssim m_{LL,RR}^2$ . In what follows  $\tilde{m} \sim m_{LL,RR}$  is implicitly assumed. The quartic coupling  $(1/36)\lambda^2\phi^4$  is crucial for global stability and can arise in a number of ways, as discussed below.

The potential (28) in general has a local charge- and/or color-breaking minimum at non-vanishing  $\phi$ , in addition to the charge and color preserving minimum  $\phi = 0$ . A sufficient condition to avoid color or charge breaking is to require that the deepest minimum along (27) is at the origin. The global minimum of the theory then conserves color and charge and is absolutely stable. For the potential (28) this stability constraint gives an upper limit  $A/\tilde{m} < \sqrt{3}\lambda$  [20,21], and is plotted in fig. 7.

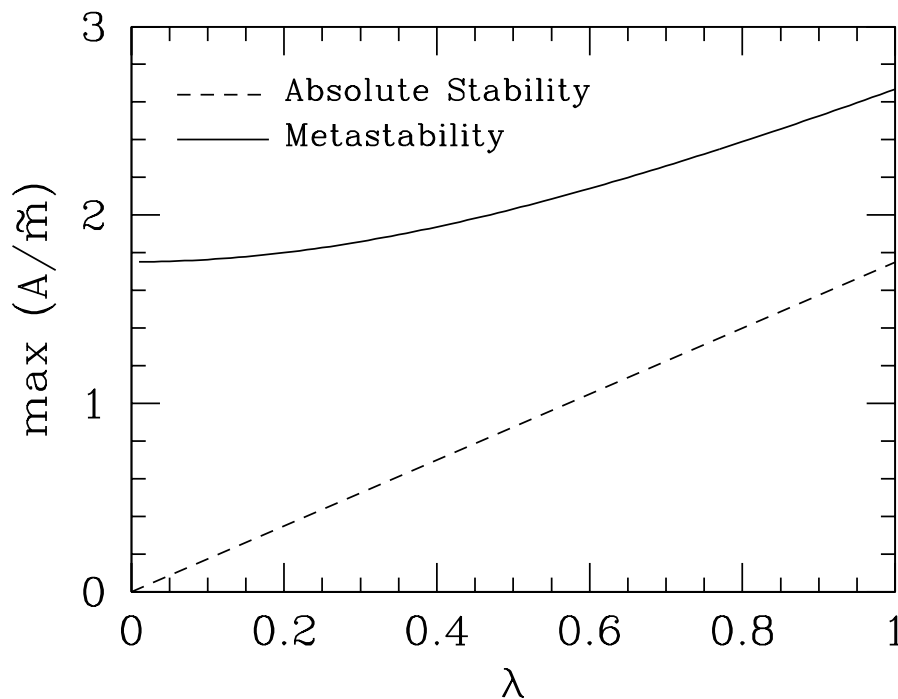


FIG. 7. Maximal value of  $A/\tilde{m}$  for absolute stability and metastability of tree-level scalar potential as a function of the quartic coupling  $\lambda$ , where  $\tilde{m}^2 \equiv \frac{1}{3} (m_{LL}^2 + m_{RR}^2 + m_{H_\alpha}^2)$ . Absolute stability refers to the absence of global charge-breaking minima, while metastability refers to a lifetime of the charge preserving vacuum greater than the age of the Universe, corresponding to a bounce action  $S > 400$ .

If the absolute stability constraint is not satisfied, and the color- and charge-breaking vacuum is the global minimum, a weaker necessary condition is that the time to tunnel from the color and charge preserving metastable vacuum be greater than the present age of the Universe. Cosmological selection of the color and charge preserving vacuum at the origin is natural, since this is a point of enhanced symmetry and always a local minimum of the free energy at high enough temperature. For the potential (28) with electroweak scale mass  $\tilde{m}$ ,



a lifetime greater than the present age of the Universe corresponds to a bounce action out of the metastable vacuum along the direction (27) of  $S \gtrsim 400$  [22]. The bounce action for the potential (28) may be calculated numerically [22,23]. The action interpolates between the thin-wall limit,  $\lambda^2 \widetilde{m}^2/A^2 \rightarrow 1/3^-$ , in which the two vacua are nearly degenerate [24]:

$$S_{\text{thin}} \simeq \frac{9\pi^2}{2} \left( \frac{\widetilde{m}^2}{A^2} \right) \left( 1 - 3\lambda^2 \frac{\widetilde{m}^2}{A^2} \right)^{-3},$$

and the thick-wall limit,  $|\lambda^2 \widetilde{m}^2/A^2| \ll 1$ , in which the quartic term is unimportant [25]

$$S_{\text{thick}} \simeq 1225 \left( \frac{\widetilde{m}^2}{A^2} \right).$$

The maximum value of  $A/\widetilde{m}$  for which  $S > 400$  is shown in fig. 7 as a function of the quartic coupling coefficient  $\lambda$ . This figure employs the empirical fit to the numerically calculated bounce action given in ref. [23]. The maximum allowed  $A/\widetilde{m}$  continues as a smooth monotonically decreasing function for  $\lambda^2 < 0$ , even though the renormalizable potential is unbounded from below in this case. For  $|\lambda^2| \ll 1$  the weak requirement of metastability on a cosmological time scale is met for  $A/\widetilde{m} \lesssim 1.75$ .

The magnitude of the quartic coupling for the direction (27) is clearly crucial for determining the maximum allowed value of  $A/\widetilde{m}$  implied by the absolute or metastability constraints given above. This in turn determines the maximum allowed radiatively induced fermion masses. Quartic couplings can arise from the  $D$ -term gauge potential or tree-level Yukawa coupling  $F$ -terms with standard model fields or mirror matter. These contributions distinguish between different classes of models.

- *Minimal holomorphic models*

A minimal class of models with soft radiative fermion masses are those with the holomorphic tri-linear terms  $AH_\alpha\phi_L\phi_R$ , and no additional significant tree-level Yukawa couplings to the associated fermions. With holomorphic tri-linear terms, gauge invariance implies that the  $D$ -term gauge potential vanishes along the direction (27). This is guaranteed since holomorphic directions are invariant with respect to complexified gauge transformations and are therefore  $D$ -flat. Without additional superpotential couplings, the quartic coupling along the direction (27) vanishes and the tree-level potential (28) is then unbounded from below. This persists at one loop, where a small negative quartic coupling is generated:  $\lambda^2 \simeq -(A/\widetilde{m})^4/96\pi^2$ . Radiative fermion masses in this class of models therefore have a metastable vacuum, and absolute stability of the charge and color preserving vacuum is not possible. In this case, however, the cosmological metastability bound is easily satisfied for first-generation masses for which  $A/\widetilde{m} \sim 10^{-3}$  is required. Second-generation masses for charm and strange quarks, which require  $A/\widetilde{m} \sim 10^{-1}-1$ , can also be accommodated, while for the muon and  $b$ -quark  $A/\widetilde{m} \sim 1-3$  is very close to the maximum value allowed by metastability of  $A/\widetilde{m} \lesssim 1.75$ .

- *Minimal non-holomorphic models*

A non-holomorphic tri-linear term  $A'H_\alpha^*\phi_L\phi_R$  can also give rise to radiative fermion masses. In this case the operator does not correspond to a holomorphic direction and is

not necessarily  $D$ -flat. The  $SU(3)_C$  and  $SU(2)_L$   $D$ -term gauge potentials do in fact vanish along the direction (27), but the  $U(1)_Y$  gauge potential does not. The  $D$ -term potential in this case is then

$$V_D = \frac{g'^2}{2} \left| \text{Tr} \frac{Y_i}{2} \phi_i^* \phi_i \right|^2 = \frac{g'^2}{288} (\text{Tr} Y_i)^2 \phi^4, \quad (29)$$

where the trace is over all fields along the collective direction. For either the quark or lepton non-holomorphic tri-linear terms, this trace is  $|\text{Tr} Y_i| = 2$ . The  $U(1)_Y$   $D$ -term contribution to the quartic coupling along these directions is then  $\lambda = g'/\sqrt{2} \simeq 0.25$ .

With this tree-level quartic coupling, global stability of the charge and color preserving vacuum is easily achieved for first-generation radiative masses. In addition, second-generation strange and charm quark and muon radiative masses do not necessarily lead to a deeper charge- and color-obreaking minimum. A radiative  $b$ -quark mass does lead to a metastable vacuum in this class of models. From fig. 7 it is apparent that the value of the quartic coupling arising from the  $U(1)_Y$  gauge potential is not large enough to significantly modify the metastability constraints with respect to the case of vanishing quartic coupling.

- *Tree-level top Yukawa*

Quartic couplings for the direction (27) can also arise from superpotential  $F$ -terms. Without additional matter, this requires that some of the standard model fermions have tree-level superpotential Yukawa couplings. In the case of a tree-level top quark Yukawa coupling,  $W = h_t H_2 Q U$ , an effective quartic coupling is generated for the direction (27) relevant to a radiative  $b$ -quark mass from a non-holomorphic  $A'_b$  term:

$$V_F = \left| \frac{\partial W}{\partial U} \right|^2 = h_t^2 |H_2 Q|^2 = \frac{1}{36} \lambda^2 \phi^4. \quad (30)$$

The tree-level top Yukawa contribution to the quartic coupling along this direction is then  $\lambda = h_t$ . With such a large quartic coupling, both the metastability and absolute stability bounds on  $A'/\tilde{m}$  are increased and a radiative  $b$ -quark mass can be obtained with  $A'_b/\tilde{m} \sim 1$ –2.5, while preserving the absolute stability of the color and charge preserving global minimum. In a hybrid model with non-holomorphic tri-linear scalar terms, and a tree-level top Yukawa, it is therefore possible to obtain all fermion masses radiatively, aside from the top quark and  $\tau$ -lepton, while preserving the global charge and color preserving minimum.

- *Models with mirror matter*

Effective quartic scalar couplings can also arise from tree-level superpotential couplings between standard model and non-standard model mirror matter. Vector-like Dirac pairs of mirror matter with the same gauge quantum numbers as some standard model fields exist in many extensions of the standard model. Mirror matter may however transform differently from standard model matter under flavor or discrete  $R$ -symmetries. It is therefore possible that such symmetries, which forbid or highly suppress Yukawa couplings for standard model fields, allow large couplings to mirror matter. For example, with massive mirror matter  $\Psi$  and  $\bar{\Psi}$ , mixing with quark or lepton fields can arise from the superpotential coupling

$$W = hH_\alpha\Phi\Psi + M_\Psi\Psi\bar{\Psi}, \quad (31)$$

where  $\Phi$  represents  $\Phi_L$  or  $\Phi_R$  standard model fields. Integrating out the mirror matter with supersymmetry-breaking soft mass potential

$$V = m_\Psi^2 (\Psi^*\Psi + \bar{\Psi}^*\bar{\Psi}) \quad (32)$$

gives the quartic potential  $V \supset \lambda^2 |H_\alpha\Phi|^2$ , with

$$\lambda^2 = h^2 \left( \frac{m_\Psi^2}{M_\Psi^2 + m_\Psi^2} \right). \quad (33)$$

In the supersymmetric limit,  $m_\Psi \rightarrow 0$ , the quartic coupling vanishes as required by supersymmetric decoupling and exactness of the superpotential. Obtaining a sizeable effective scalar quartic coupling for the standard model fields therefore requires both a large mirror matter Yukawa coupling,  $h$ , and that the mirror matter soft supersymmetry-breaking mass,  $m_\Psi$ , be of the order of the supersymmetric Dirac mass,  $M_\Psi$ . The quartic couplings in this case therefore represent an apparent large violation of supersymmetry in the low-energy theory with the mirror matter integrated out. Mirror matter mixing with the Higgs fields can also give rise to analogous effective quartic couplings.

Mirror matter with the properties discussed above arises in many extensions of the standard model. In a grand unified theory, for example, a **27** of  $E_6$  contains, in addition to an entire generation, Dirac pairs of lepton doublets and down-type right-handed quarks. Entire massive pairs of generations and antigerations also often occur in string compactifications. With Yukawa couplings to standard model fields, and electroweak scale Dirac and supersymmetry-breaking masses, these fields yield effective quartic scalar couplings. As another example, theories of gauge mediated supersymmetry breaking often have messenger matter, which has identical gauge quantum numbers as some of the standard model fields. If allowed by flavor or discrete symmetries, the messengers can therefore mix with standard model fields through superpotential Yukawa couplings [26]. In addition, for one-scale theories, the Dirac mass messenger scale and supersymmetry-breaking scale are roughly equal,  $\mathcal{O}(10\text{--}100)$  TeV, as required to obtain a large effective quartic coupling, as discussed above. Finally, theories with additional compact dimensions also often contain mirror matter. For example, massive  $N = 2$  hypermultiplet excitations, which exist in the bulk of the compact space, may mix with standard model matter. If the scale of supersymmetry breaking is related to the size of the compact manifold, for example by twisted boundary conditions [27], both the supersymmetry-breaking, and supersymmetry-preserving  $N = 2$  masses can be of the same order, thereby leading to a large effective quartic coupling. For any type of mirror matter, effective quartic couplings can arise from mixing with either quark or lepton fields, or the Higgs fields.

With large effective quartic couplings arising from mirror matter mixing, the upper limits on soft chiral flavor breaking implied by both metastability and absolute stability can be increased to  $A/\tilde{m} \lesssim \text{few}$ . This could in principle allow all fermions except the top quark and  $\tau$ -lepton to obtain masses radiatively from holomorphic soft chiral flavor breaking, while

TABLE II. The quartic coupling,  $\lambda^2$ , along the equal field direction for different classes of models. For the tree-level top Yukawa models  $\tan\beta > 1$  is assumed for the stability limits.

Model	$\lambda^2$	Absolute stability limits	Metastability limits	Comments
Minimal holomorphic	$\sim \frac{-1}{96\pi^2} \left(\frac{A}{m}\right)^4$	$\frac{A}{m} \ll 1$	$\frac{A}{m} \lesssim 1.75$	Metastable vacuum
Minimal non-holomorphic	$\frac{q'^2}{2}$	$\frac{A'}{m} \lesssim 0.4$	$\frac{A'}{m} \lesssim 1.8$	
Tree-level top Yukawa	$h_t^2$	$\frac{A'_b}{m} \lesssim 1.7 - 2.5$	$\frac{A'_b}{m} \lesssim 2.7 - 3.2$	Relevant to $b$
Mirror matter	$\frac{h^2 m_\Psi^2}{(M_\Psi^2 + m_\Psi^2)}$	$\frac{A}{m} \lesssim \text{few}$	$\frac{A}{m} \lesssim \text{few}$	

keeping the charge and color preserving vacuum as the global minimum. By appropriate choice of the representation, mirror matter can also stabilize non-holomorphic  $A'$  terms.

The different classes of models for the origin of the effective scalar quartic couplings along with the associated absolute or metastability constraints are summarized in table II.

## V. CLASSIFICATION OF OPERATORS

Soft chiral flavor breaking in the scalar tri-linear operators  $AH_\alpha\phi_L\phi_R$  and  $A'H_\alpha^*\phi_L\phi_R$ , along with gluino or neutralino masses, are sufficient to generate radiative fermion masses and Higgs and Higgsino couplings at one loop. Both these operators are gauge-invariant and may be included in the most general low-energy soft supersymmetry-breaking scalar potential [12]. It is instructive to consider the effective operators that couple the visible and supersymmetry-breaking sectors and give rise to these soft terms.

Supersymmetry-breaking is associated with non-zero auxiliary-component expectation values in the supersymmetry-breaking sector. Soft supersymmetry-breaking terms in the visible sector originate in operators that couple these auxiliary components to visible sector fields. Below the messenger scale for transmitting supersymmetry breaking, these give rise to effective operators suppressed by appropriate powers of the messenger scale. The lowest-order operator, which produces holomorphic tri-linear soft terms, is a superpotential term of the form

$$\frac{1}{M} \int d^2\theta \mathcal{Z} H_\alpha \Phi_L \Phi_R, \quad (34)$$

where, as throughout,  $M$  represents the messenger scale, the explicit flavor structure is suppressed, and  $\mathcal{Z} = \mathcal{A} + \theta^2 \mathcal{F}$  represent chiral superfields in the supersymmetry-breaking sector. A non-vanishing auxiliary component gives rise to holomorphic soft tri-linear terms,  $AH_\alpha\phi_L\phi_R$ , with  $A \sim \mathcal{F}/M$ . The scale of soft supersymmetry breaking in the visible sector, in particular the scale for the superpartner and gaugino masses, is  $\tilde{m} \sim \mathcal{F}/M$ . The holomorphic  $A$ -parameters are then parametrically of the same order (up to model-dependent couplings and flavor suppressions),  $A \sim \tilde{m}$ , independent of the messenger scale. In high-scale gravity

mediated supersymmetry breaking, the messenger scale is the Planck scale,  $M \sim M_P$ , and  $\widetilde{m} \sim m_{3/2} \sim \mathcal{F}/M_P$ .

The existence of the coupling (34) requires non-trivial flavor interactions at the messenger scale, or equivalently that the supersymmetry-breaking sector field(s)  $\mathcal{Z}$  transform non-trivially under flavor. Flavor must therefore be intimately linked to the transmission and/or breaking of supersymmetry. Specifically, the flavor symmetries (for fermions with soft radiative masses) are either broken explicitly by the messenger sector interactions and/or spontaneously in the supersymmetry-breaking sector. As discussed in section III, second- and third-generation radiative masses require  $A \sim \widetilde{m}$ . So in this case the flavor scale cannot be greater than the messenger scale. Alternatively, for first-generation radiative masses, which require somewhat smaller tri-linear  $A$ -terms, there could be a small hierarchy between the messenger and flavor scales, so that the operators (34) possess an additional suppression  $M/M_{flav}$  in this case, where  $M_{flav}$  is the flavor scale.

In addition to the soft tri-linear couplings arising from (34), with auxiliary expectation values  $\mathcal{F}$ , superpotential Yukawa couplings in general arise with scalar expectation values  $\mathcal{A}$ . The latter case of scalar expectation values, or spurions in the low-energy theory, which give rise to Yukawa couplings, is nothing but the well-known Froggatt–Nielsen mechanism [1], with the hierarchies in the Yukawa coupling matrix arising from the ratio  $\mathcal{A}/M$ . The soft breaking of chiral flavor symmetries considered here may therefore be thought of as a version of the Froggatt–Nielsen mechanism in which auxiliary spurions break chiral flavor symmetries rather than scalar spurions. In order for the induced Yukawa couplings to be unimportant the scalar expectation values must be insignificant,  $\mathcal{A} \ll M$ , or vanish. This is the case if all scalar expectation values in the supersymmetry-breaking sector are small respect to the messenger scale. This could occur, for example, in a renormalizable hidden sector with high-scale mediation for which  $\mathcal{A}/M \sim m_{3/2}/\sqrt{\mathcal{F}} \ll 1$ .

Since the breaking of chiral flavor symmetries must be linked with the messenger and/or supersymmetry-breaking sectors, there are additional operators beyond (34) which have non-trivial flavor transformation properties in the low-energy theory. In particular, no symmetry can forbid operators of the form

$$\frac{1}{M^2} \int d^2\theta d^2\bar{\theta} \mathcal{Z}^\dagger \mathcal{Z} \Phi^\dagger \Phi, \quad (35)$$

where  $\Phi = \Phi_L$  or  $\Phi_R$ . With auxiliary expectation values, these operators give rise to soft scalar masses in the visible sector,  $\widetilde{m}^2 \phi^* \phi$ , where  $\widetilde{m} \sim \mathcal{F}/M$ . Arbitrary breaking of flavor symmetries in the scalar masses of course leads in general to unacceptable flavor-changing neutral currents. The specific magnitude of the flavor breaking depends on the precise flavor structure of the operators (35) and/or on how the flavor symmetries are broken by the auxiliary expectation values, and may be minimized in particular models. In addition, the problem of excessive flavor-changing can be largely ameliorated if the scalar partners of the first generation, and to a lesser extent those of the second generation, are much heavier than the electroweak scale [19], as discussed in section III.

The form of the coupling (34) between the visible and supersymmetry-breaking sectors, and the subsequent absence of tree-level superpotential Yukawa coupling, can be enforced by discrete or continuous flavor or  $R$ -symmetries. For example, a  $Z_2$   $R$ -symmetry [28]

under which  $\mathcal{Z} \rightarrow -\mathcal{Z}$  and  $H_\alpha \Phi_L \Phi_R \rightarrow -H_\alpha \Phi_L \Phi_R$  allows the coupling (34) but forbids a superpotential Yukawa coupling. This is easily extended to continuous  $U(1)_R$  symmetries, or specific flavor symmetries under which  $\mathcal{Z}$  transforms.

Non-holomorphic tri-linear soft terms can only arise from Kähler potential terms rather than from the superpotential. The lowest-order operator that gives rise to such terms is of the form

$$\frac{1}{M^3} \int d^2\theta d^2\bar{\theta} \mathcal{Z} \mathcal{Z}^\dagger H_\alpha^\dagger \Phi_L \Phi_R. \quad (36)$$

Non-vanishing auxiliary terms give rise to soft tri-linear terms,  $A' H_\alpha^* \phi_L \phi_R$ , with  $A' \sim \mathcal{F}^2/M^3 \sim \tilde{m}^2/M$ . Because of the dimensionality of the Kähler potential, these non-holomorphic tri-linear terms are suppressed for a messenger scale well above the supersymmetry breaking by  $\mathcal{O}(\tilde{m}/M)$ . This non-holomorphic source of chiral flavor breaking can therefore be relevant only with a low scale for both flavor and supersymmetry breaking. In this case the small ratio  $A/\tilde{m} \sim 10^{-3}$  required for first-generation radiative masses could arise wholly or in part from the ratio of the electroweak to messenger/ flavor scale(s),  $\tilde{m}/M$ .

## VI. ANOMALOUS MAGNETIC MOMENTS

With soft chiral flavor breaking, radiative fermion masses arise from effective operators generated at the superpartner mass scale. The same virtual processes which give rise to the fermion mass also generate other chirality violating operators below the superpartner scale. The experimentally most important of these operators is the fermion anomalous magnetic moment. As shown in fig. 8, the anomalous magnetic moment arises from the same one-loop diagram which gives rise to the fermion mass shown in fig. 1, with an external photon coupling to the virtual scalar partner. Since the mass and magnetic moment both arise at

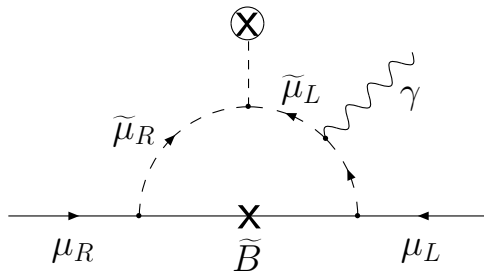


FIG. 8. One-loop radiative contribution to the muon anomalous magnetic moment from soft chiral flavor violation and Bino mass.

one loop with the same chiral structure, the supersymmetric contribution to the dimension-six operator, which gives a fermion anomalous magnetic moment,  $a_f \equiv \frac{1}{2}(g-2)$ , is given parametrically by  $a_f^{\text{SUSY}} \sim m_f^2/\tilde{m}^2$ , where  $\tilde{m} = \max(m_{\tilde{f}_1}, m_{\tilde{f}_2}, m_\lambda)$ . Notice that this is *not* suppressed by a loop factor even though it arises perturbatively. Anomalous magnetic moments suppressed by the relevant heavy mass scale without a loop factor suppression

are a generic feature of any theory of radiative fermion masses [29]. The relatively large supersymmetric contribution to the magnetic moments is in analogy to the relatively large Higgs Yukawa radii discussed in section II B, which also are effectively not suppressed by a loop factor. In fact, in the present scenario for radiative fermion masses, any chirality-violating operator generated at the superpartner mass scale is effectively a loop factor larger than with tree-level Yukawa couplings.

The best measured fermion magnetic moment in relation to its mass squared is by far that of the muon. If the muon mass arises radiatively from soft chiral flavor violation, the loop function for the anomalous magnetic moment can be related to that for the radiative mass

$$a_\mu^{\text{SUSY}} = +2m_\mu^2 \frac{\sum_j K_\mu^j m_{\tilde{\chi}_j^0} I_{g-2}(m_{\tilde{\mu}_1}^2, m_{\tilde{\mu}_2}^2, m_{\tilde{\chi}_j^0}^2)}{\sum_j K_\mu^j m_{\tilde{\chi}_j^0} I(m_{\tilde{\mu}_1}^2, m_{\tilde{\mu}_2}^2, m_{\tilde{\chi}_j^0}^2)}. \quad (37)$$

The loop function  $I_{g-2}(m_{\tilde{\mu}_1}^2, m_{\tilde{\mu}_2}^2, m_{\tilde{\chi}_j^0}^2)$  and details of the calculation are given in appendix B. From the general expressions given in the appendix, one has

$$\frac{I_{g-2}(m_{\tilde{\mu}_1}^2, m_{\tilde{\mu}_2}^2, m_{\tilde{\chi}_j^0}^2)}{I(m_{\tilde{\mu}_1}^2, m_{\tilde{\mu}_2}^2, m_{\tilde{\chi}_j^0}^2)} \sim \frac{1}{6\tilde{m}^2}; \quad \tilde{m} = \max(m_{\tilde{f}_1}, m_{\tilde{f}_2}, m_\lambda), \quad (38)$$

where the prefactor  $1/6$  arises for degenerate superpartners. The supersymmetric contribution to the muon anomalous moment is then  $a_\mu^{\text{SUSY}} \sim m_\mu^2/(3\tilde{m}^2)$ . This result differs in a number of ways from the supersymmetric contribution with tree-level Yukawa couplings, which is dominated by chargino exchange over much of the parameter space and is  $a_\mu^{\text{SUSY}} \sim (g^2/16\pi^2)(m_\mu^2 m_Z \tan\beta/\tilde{m}^3)$  [30]. Besides not being suppressed by a loop factor, the anomalous magnetic moment obtained in the radiative mass scenario is dominated by Bino exchange. Because of the absence of a chargino contribution, which vanishes without a tree-level Yukawa, it is largely independent of  $\tan\beta$ . Finally, it is *necessarily* positive. The positivity may be understood from the real space form of the radiative magnetic moment amplitude. The external low frequency photon field couples to the scalar partner virtual cloud, which necessarily has the same charge as the fermion, and in real space necessarily has positive extent. In addition, the radiative mass and contribution to the magnetic moment have the same fermionic chiral structure as that arising from the virtual neutralino. It then follows that the supersymmetric contribution to the magnetic moment has the same sign as the minimal Dirac term. The positivity of the supersymmetric contribution to the anomalous magnetic moment is an interesting feature and a definite prediction of radiative fermion masses from soft chiral flavor breaking. With a tree-level Yukawa coupling, the supersymmetric contribution is correlated with  $\text{sgn}(\mu)$  over much of the parameter space, and can have either sign [30].

The anomalous magnetic moment (37) is plotted in fig. 9 as a function of the fractional smuon mass-squared splitting,  $\phi_\mu$ , for various values of the ratio  $\rho_\mu^B$  in the pure gaugino limit. Note that the dependence on the  $A$ - or  $A'$ -parameter, or equivalently the smuon left-right mixing angle, is implicitly contained in the muon mass  $m_\mu$ , so that  $a_\mu^{\text{SUSY}}$  is only a function of the superpartner mass spectrum through the loop functions. The current experimental

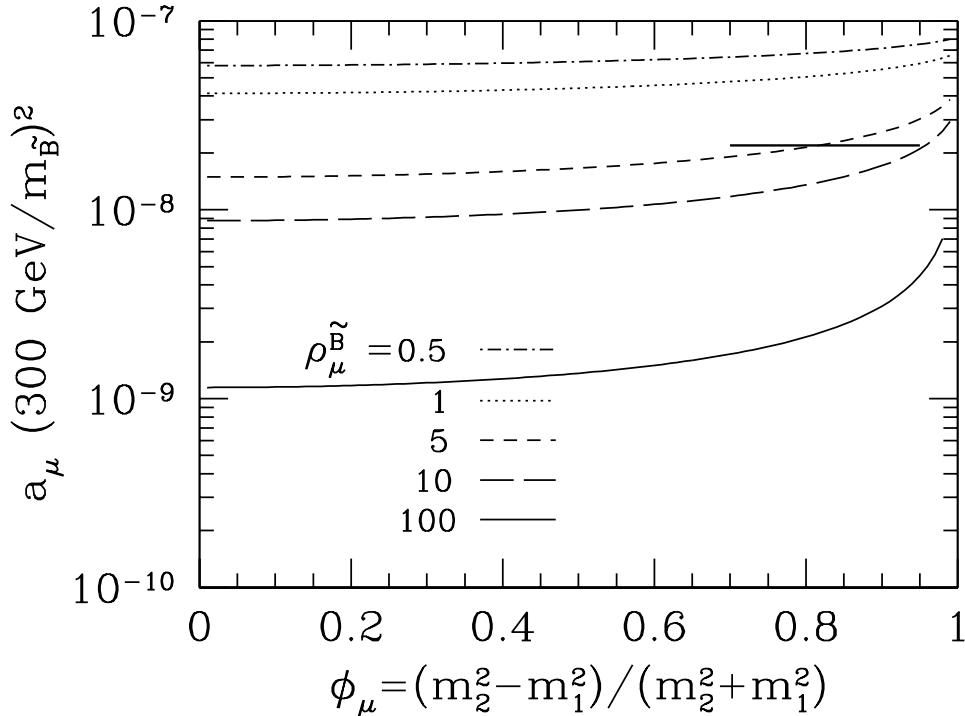


FIG. 9. Supersymmetric contribution to the muon anomalous magnetic moment,  $a_\mu \equiv (g_\mu - 2)/2$ , for a radiative muon mass, as a function of the fractional smuon mass splitting  $\phi_\mu$ . The anomalous moment is given in units of  $(m_{\tilde{B}}/300 \text{ GeV})^{-2}$  for various values of the ratio  $\rho_\mu^{\tilde{B}}$ , neglecting neutralino mixing effects. The current experimental bound of  $a_\mu^{\text{new}} < 220 \times 10^{-10}$  is indicated for comparison, and already constrains the parameter space for low values of  $m_{\tilde{B}}$  and  $\rho_\mu$ .

measurement of  $a_\mu^{\text{exp}}$  [31] is in good agreement with the theoretical calculations, which include  $\mathcal{O}(\alpha^5)$  QED corrections and hadronic vacuum polarization to  $\mathcal{O}(\alpha^3)$  [32]. This agreement allows to put a bound on positive, non-standard model contributions of  $a_\mu^{\text{new}} < 220 \times 10^{-10}$  at the 95% CL [31,32], which is indicated in fig. 9 for comparison. If the muon mass arises radiatively, the current bound already rules out  $m_{\tilde{\mu}_{1,2}} \lesssim 400 \text{ GeV}$  for  $m_{\tilde{B}} \lesssim m_{\tilde{\mu}_{1,2}}$ . The Brookhaven E821 muon  $g - 2$  experiment is expected to reach a level of sensitivity of  $\delta a_\mu^{\text{exp}} \sim 4 \times 10^{-10}$  [33]. If all the standard model contributions can be calculated to this precision, smuon masses up to  $m_{\tilde{\mu}_{1,2}} \sim 3 \text{ TeV}$  can be probed for  $m_{\tilde{B}} \lesssim m_{\tilde{\mu}_{1,2}}$  if the muon mass is radiative. The muon anomalous magnetic moment is by far the best experimental probe of a radiative muon mass arising from soft chiral flavor violation.

If the muon mass does arise radiatively, the indirect constraints on the superpartner masses from the experimental bound on  $a_\mu^{\text{new}}$  discussed above may be used to give an upper limit on the enhancement of the effective Higgs Yukawa coupling over the mass Yukawa,  $r_\mu = \bar{h}_f \langle H_\alpha \rangle / m_\mu$ .

For fixed  $\phi_\mu$  and  $\rho_\mu^{\tilde{B}}$  this bound,  $m_{\tilde{\mu}_{1,2}} \gtrsim 400 \text{ GeV}$  for  $m_{\tilde{B}} \lesssim m_{\tilde{\mu}_{1,2}}$ , may be translated into a lower limit on the combination  $m_{\tilde{B}}^3 \rho_\mu^{\tilde{B}} I(m_{\tilde{\mu}_1}^2, m_{\tilde{\mu}_2}^2, m_{\tilde{B}}^2)$ , which is related to the radiative



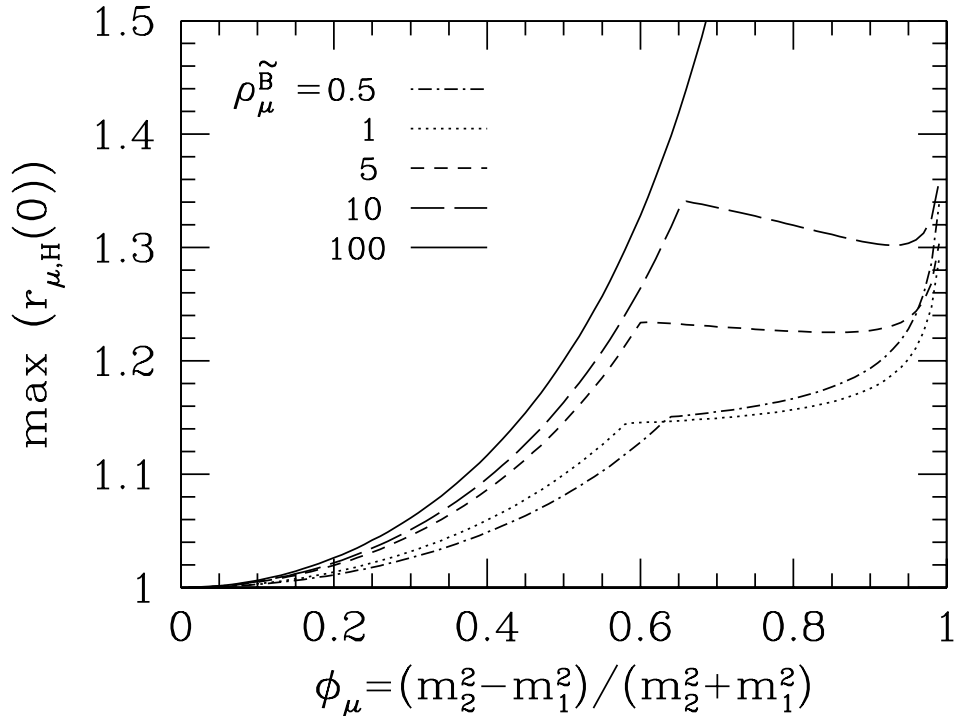


FIG. 10. Upper limit on the Higgs–Yukawa enhancement parameter  $r_{\mu,H}(0)$  at zero momentum transfer for a radiative muon mass as a function of the smuon mass squared splitting  $\phi_\mu$ , for various values of the ratio  $\rho_\mu^{\tilde{B}}$ . The upper limit follows indirectly from the current experimental constraint on non-standard model contributions to the muon anomalous magnetic moment of  $a_\mu^{\text{new}} < 220 \times 10^{-10}$ .

muon mass (6). Given the known muon mass, this may then be used to place an upper limit on the smuon mixing angle  $\sin 2\theta_\mu$  using (6). Finally, these bounds may all be put together to bound the  $q^2 = 0$  effective Higgs Yukawa coupling ratio  $r_{\mu,H}(0)$ , using (9) and (10). This upper limit on  $r_{\mu,H}(0)$  from the current experimental bound on  $a_\mu^{\text{new}}$  is given in fig. 10. For  $\phi_\mu \lesssim 0.6\text{--}0.7$ , the current experimental bound on  $a_\mu^{\text{new}}$  provides no limit on  $\sin 2\theta_\mu$ , and the maximum value of  $r_{\mu,H}(0)$  just follows from (9) and (10) with  $\sin 2\theta_\mu = 1$  (compare fig. 4). This is because, in this region of fractional smuon mass squared splitting  $\phi_\mu$ , the correct value of the muon mass is obtained only with relatively massive superpartners, which are not bounded by  $a_\mu^{\text{new}}$ . However, for  $\phi_\mu \gtrsim 0.6\text{--}0.7$  the current bound on  $a_\mu^{\text{new}}$  does provide a non-trivial limit on  $\sin 2\theta_\mu$ . This is reflected in the maximum value of  $r_{\mu,H}(0)$  shown in fig. 10. As discussed in detail in section VIII, the ratios  $r_{\mu,H}(m_h^2)$  and  $r_{\mu,H}(m_H^2)$  could also be probed at a  $\mu^+\mu^-$  collider by direct measurement of the Higgs–muon coupling. This would give additional sensitivity to possible momentum dependence of the Higgs–muon couplings. However, the Brookhaven E821 muon  $g-2$  experiment will in general be much more sensitive to a radiative muon mass.

The limits on Higgs coupling enhancements for a radiative muon mass implied by the current experimental bound on the muon anomalous magnetic moment may be extended to other fermions with radiative masses, if assumptions about relations within the superpartner

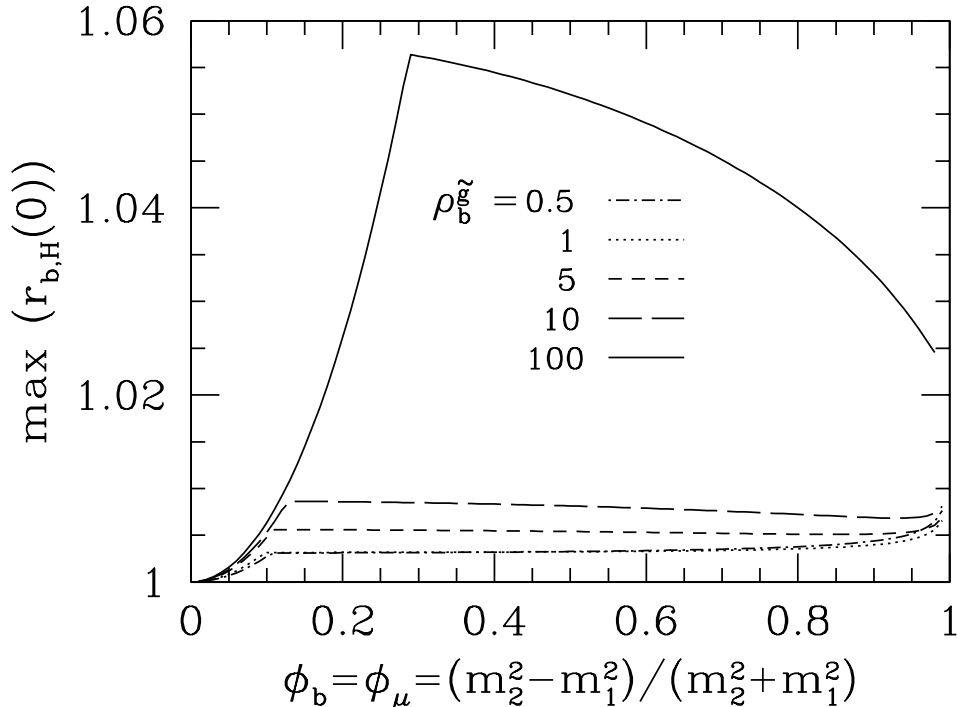


FIG. 11. Upper limit on the Higgs–Yukawa enhancement parameter  $r_{b,H}(0)$  at zero momentum transfer for a radiative  $b$ -quark mass as a function of the sbottom mass splitting  $\phi_b$ , for various values of the ratio  $\rho_b^{\tilde{g}} = \rho_\mu^{\tilde{B}}$ , and assuming  $\phi_b = \phi_\mu$ . The upper limit follows indirectly from the current experimental constraint on non-standard model contributions to the muon anomalous magnetic moment of  $a_\mu^{\text{new}} < 220 \times 10^{-10}$  under the assumption of gaugino unification mass relations. The bound is only obtained if *both* the muon and  $b$ -quark obtain mass radiatively from soft chiral flavor breaking.

mass spectrum are postulated. The Higgs– $b$ -quark coupling may be well measured at future colliders, as detailed in section VIII. If *both* the muon and  $b$ -quark masses arise radiatively, an upper limit on  $r_{b,H}(0)$  can be obtained indirectly from the  $a_\mu^{\text{new}}$  experimental bound. For example, assuming *i*) that there is a gaugino unification relation between the Bino and gluino masses, ( $m_{\tilde{g}} = \frac{3}{5}(\alpha_s/\alpha')m_{\tilde{B}} \simeq 6 m_{\tilde{B}}$ ), *ii*) that  $\rho_\mu^{\tilde{B}} = \rho_b^{\tilde{g}}$ , *iii*) that fractional smuon and sbottom mass squared splittings are the same ( $\phi_\mu = \phi_b$ ), *iv*) that the  $b$ -quark mass has the known value, the bound on  $a_\mu^{\text{new}}$  may be translated into the analogous indirect bound on  $r_{b,H}(0)$  given in fig. 11. The constraint implied on the Higgs– $b$ -quark coupling is more severe than that for the Higgs–muon coupling simply because, under the assumption of gaugino unification, the strongly interacting superpartners, which radiatively generate the  $b$ -quark mass, are somewhat heavier than the weakly interacting superpartners, which generate the muon mass; and  $r_{f,H}(0) \rightarrow 1$  in the superpartner decoupling limit. Other assumptions for the relations between the  $b$ -squark and smuon masses and the gaugino masses would yield different bounds on  $r_{b,H}(0)$ . If the muon mass is tree-level, or if no relations are assumed, then of course no indirect bound on the Higgs– $b$ -quark coupling for a radiative  $b$ -quark mass can be gleaned from the muon anomalous magnetic moment.

It is also possible, in general, for flavor-changing electromagnetic- and chromo-dipole operators to be generated, depending on the precise textures that appear in the scalar partner mass matrices. Within any specific model for the soft and hard textures in the Yukawa couplings, such flavor-changing dipole operators may give the most interesting low-energy probe of supersymmetric flavor violation. These are, however, very model-dependent and outside the scope of this work. In the scenario discussed in section III, in which all the down-type quarks gain a mass radiatively, in the limit of degenerate squarks in each sector, all the transition quark dipole moments vanish. In the same scenario, but with non-degenerate squarks and down-type quark number conserved, all supersymmetric contributions to the flavor-changing down-type dipoles associated directly with the radiative masses also vanish, and likewise for the analogous scenario with radiative electron and/or muon masses.

## VII. CP VIOLATION

In generic supersymmetric theories, virtual contributions to low-energy CP-violating operators, such as electric dipole moments (EDMs) and CP-odd Higgs–fermion couplings, appear due to the presence of intrinsic supersymmetric CP-violating phases. The flavor-conserving phases reside in the complex Lagrangian parameters:  $A$ - or  $A'$ -terms, the gaugino masses,  $m_\lambda$ , the Higgsino mass term  $\mu$ , and the scalar Higgs mass coupling  $m_{12}^2$ . In the case of hard tree-level Yukawa couplings, contributions to the EDMs of the neutron and atoms are generated at one loop. For superpartners at the electroweak scale, these contributions are relatively large with respect to current experimental bounds. The apparent requisite smallness of the intrinsic phases, typically  $10^{-2}$ – $10^{-3}$  [29,34,35], is generally referred to as the SUSY CP problem.

With radiative fermion masses arising from soft chiral flavor breaking, the masses and possible CP-violating operators both arise at the one-loop level. At first sight, the lack of suppression of the CP-violating operators by a relative loop factor would appear to result in an even worse SUSY CP problem with the scenario for radiative masses presented here. In this scenario, however, the phases of chirality-violating operators can be aligned to a very high precision with the phase of the relevant fermion mass. This occurs because the radiative fermion mass and chirality-violating operators arise from very similar diagrams with similar phase structure, as shown in fig. 3 for the Higgs couplings, and fig. 8 for the electromagnetic dipole moment. The natural alignment can significantly suppress the magnitude of such CP-violating operators and may in fact provide an effective solution to the SUSY CP problem within the context of radiatively generated fermion masses. If the light-quark masses arise radiatively, the neutron EDM is highly suppressed, as detailed below, and is compatible with the current experimental bounds [36]. The electron EDM is in general not as strongly suppressed. However, as described below, if the electron mass arises radiatively, there are interesting regions of superpartner parameter space in which it is also sufficiently suppressed.

A CP-odd observable associated with a chirality and CP-violating effective operator such as an EDM is proportional in a general basis to the sine of the relative phase between the mass  $m$  and the coefficient of the chirality-violating operator  $d$ :

$$\sin(\text{Arg}(dm^*)).$$

In terms of field redefinitions, this implies that, the CP-odd observable is proportional to the imaginary part of the coefficient of the effective operator in a basis in which the fermion mass is taken to be real. In the absence of tree-level Yukawa couplings, gauge invariance implies that only the neutralinos, and for quarks the gluino, contribute to the radiative mass at one loop, as noted in section II. The same is true of radiative contributions to the chirality-violating dipole moments and Higgs–fermion couplings. The full one-loop contributions to the (in general complex) mass  $m$  and to the dipole coefficient or Higgs–fermion coupling  $d$  then are:

$$m = \sum_j m_j, \quad d = \sum_j d_j, \quad (39)$$

where the sums are over the individual contributions of each neutralino, and gluino in the case of quarks. In general, the phases of each individual contribution are not related,  $\text{Arg}(m_i m_j^*) \neq 0$  and  $\text{Arg}(d_i d_j^*) \neq 0$ . However, the one-loop contribution of any given neutralino or gluino to the mass does have *exactly* the same phase as the corresponding contribution to the dipole coefficient or Higgs–fermion coupling,

$$\text{Arg}(d_j m_j^*) = 0. \quad (40)$$

This is because the individual one-loop contributions to the mass and dipole moment only differ diagrammatically by the coupling to an external electromagnetic field, so that they necessarily have the same over-all phase up to a possible sign. Neglecting any scalar–pseudoscalar Higgs mixing induced by CP violation in the Higgs potential (which vanishes at tree-level in the MSSM), the same is true of the Higgs–fermion couplings. For the dipole coefficient, this can be seen explicitly by comparing eqs. (3) and (B4) and for the Higgs–fermion coupling directly from eq. (7). The arguments and results given in section VI for the positivity of the anomalous magnetic moment further imply that the contribution of any given neutralino or gluino to the mass and electromagnetic dipole are in fact aligned rather than anti-aligned with opposite sign.

The automatic alignment of the individual one-loop contributions (40) has some interesting consequences in the case that a single neutralino or gluino dominates the total radiative effects. This is in fact expected to be the case for radiative quark masses, and in certain regions of parameter space for radiative lepton masses, as described in detail below. If the  $i$ -th contribution dominates the sums (39), so that  $|m_j/m_i| \ll 1$  and  $|d_j/d_i| \ll 1$  for  $j \neq i$ , the physical CP-violating phase of the effective operator is approximately

$$\sin(\text{Arg}(dm^*)) \simeq \sum_{j \neq i} \left( \left| \frac{d_j}{d_i} \right| - \left| \frac{m_j}{m_i} \right| \right) \sin(\text{Arg}(m_j m_i^*)), \quad (41)$$

where (40) has been used. The leading contribution alone does not give rise to a physical phase because of the automatic alignment of individual contributions noted above in (40). A non-zero physical phase only arises from *interference* between the leading and subdominant contributions. This leads to the suppression factor in parenthesis, multiplying the intrinsic phase contributions to the physical phase. From expression (41) it is apparent that the physical CP-violating phase may be suppressed by any of the following conditions:

1. The subdominant contributions are much smaller than that of the leading diagram:  $|m_j/m_i| \ll 1$  and  $|d_j/d_i| \ll 1$ .
2. The *relative* magnitudes of the subdominant contributions to both the mass and dipole moment operator are nearly equal:  $|m_j/m_i| \simeq |d_j/d_i|$ .
3. The phase of the dominant and subdominant contributions are nearly equal:  $\sin(\text{Arg}(m_j m_i^*)) \ll 1$ .

As detailed below, the first effect significantly suppresses both CP-violating Higgs–quark couplings and quark EDMs; the second effect strongly suppresses CP-violating Higgs–fermion couplings and EDMs in some regions of parameter space; and the third effect further suppresses CP-violating Higgs–quark couplings and quark EDMs under the assumption of strict gaugino mass unification.

Consider first the possible CP-violating couplings of the Higgs bosons to fermions. The CP-conserving and -violating couplings of the lightest Higgs boson to fermions, through scalar and pseudoscalar fermion bilinears respectively, are

$$\mathcal{L} \supset |\lambda_{h^0}| \cos(\text{Arg}(m_f^* h_{f,H})) \bar{f} f h^0 + |\lambda_{h^0}| \sin(\text{Arg}(m_f^* h_{f,H})) \bar{f} i \gamma_5 f h^0, \quad (42)$$

where the magnitude of the Higgs coupling is  $|\lambda_{h^0}| = \Theta\{\cos\beta, \sin\beta\} |h_{f,H}|/\sqrt{2}$ , where the first (second) term in brackets is for  $\alpha = 1$  (2), and  $\Theta$  is the  $h^0$  mixing coefficient given in section VIII. Couplings to other Higgs bosons have similar forms, with scalar and pseudoscalar fermion bilinears exchanged for the pseudoscalar Higgs  $A^0$ . The full expression for the (in general complex) radiatively generated Yukawa coupling,  $h_{f,H}$ , is a sum over the neutralino contributions, and for quarks, the gluino contribution. Neglecting  $\tilde{B}$ – $\tilde{W}_3$  mixing, only the Bino, and for quarks the gluino, contributes at one loop. For a radiative quark mass, in this limit the ratio of Bino contribution to the quark mass,  $m_q^{\tilde{B}}$ , to that of the gluino  $m_q^{\tilde{g}}$ , from the general expression for a radiative fermion mass (3) is

$$\left| \frac{m_q^{\tilde{B}}}{m_q^{\tilde{g}}} \right| = \frac{3\alpha'}{16\alpha_s} \left| \frac{m_{\tilde{B}}}{m_{\tilde{g}}} \right| Y_{qL} Y_{qR} \frac{I(m_{\tilde{q}_1}, m_{\tilde{q}_2}, m_{\tilde{B}})}{I(m_{\tilde{q}_1}, m_{\tilde{q}_2}, m_{\tilde{g}})}, \quad (43)$$

where  $m_{\tilde{B}}$  and  $m_{\tilde{g}}$  are in general complex, but throughout the masses appearing in the loop functions are understood to be the real positive mass eigenvalues. For up- and down-type quarks the product of hypercharges are  $Y_{uL} Y_{uR} = \frac{4}{9}$  and  $Y_{dL} Y_{dR} = -\frac{2}{9}$  respectively. The Bino contribution to the radiative mass is naturally suppressed for a number of reasons. The individual contributions are proportional to the gauge couplings squared times the chirality-violating gaugino mass. Under the assumption of gaugino-mass unification for the magnitudes of the gaugino masses,  $|m_{\tilde{B}}/m_{\tilde{g}}| = \frac{5}{3}\alpha'/\alpha_s$ , this results in a suppression of  $m_{\tilde{B}}\alpha'/(m_{\tilde{g}}\alpha_s) = \frac{5}{3}\alpha'^2/\alpha_s^2 \sim 10^{-2}$ . The ratio of loop functions is not particularly small in this limit:  $I(m_{\tilde{q}_1}, m_{\tilde{q}_2}, m_{\tilde{B}})/I(m_{\tilde{q}_1}, m_{\tilde{q}_2}, m_{\tilde{g}}) \sim 2$ , and equals 2 for  $m_{\tilde{q}_1} = m_{\tilde{q}_2} = m_{\tilde{g}} \gg m_{\tilde{B}}$ . In addition, the color factor and the product of hypercharges give a suppression  $\frac{3}{16} Y_{qL} Y_{qR} \sim 10^{-1}$ . Numerically, then,  $|m_q^{\tilde{B}}/m_q^{\tilde{g}}| \lesssim 10^{-3}$ , so the situation discussed above in which a single contribution dominates is achieved.

The ratio of Bino to gluino contributions to the Higgs–quark coupling (7) is very similar to the ratio for the radiative mass (43), modified only by the ratios of Higgs to mass effective Yukawa couplings defined in (10). Altogether then, the coefficient of the CP-violating Higgs–quark couplings in (42) in the approximation (41) is

$$\begin{aligned} \sin\left(\text{Arg}(m_q^* h_{q,H})\right) &\simeq \frac{3\alpha'}{16\alpha_s} \left| \frac{m_{\tilde{B}}}{m_{\tilde{g}}} \right| Y_{qL} Y_{qR} \left( 1 - \frac{r_{q,H}^{\tilde{B}}(m_{h^0}^2)}{r_{q,H}^{\tilde{g}}(m_{h^0}^2)} \right) \frac{I(m_{\tilde{q}_1}, m_{\tilde{q}_2}, m_{\tilde{B}})}{I(m_{\tilde{q}_1}, m_{\tilde{q}_2}, m_{\tilde{g}})} \\ &\times \sin\left(\text{Arg}(m_{\tilde{B}} m_{\tilde{g}}^*)\right), \end{aligned} \quad (44)$$

where  $r_{q,H}^{\tilde{B}}(m_{h^0}^2)$  and  $r_{q,H}^{\tilde{g}}(m_{h^0}^2)$  are the ratios of Higgs Yukawa coupling at  $q^2 = m_{h^0}^2$  to mass Yukawa coupling for the Bino and gluino contributions respectively. The physical CP-violating phase arises from the interference between the Bino and gluino contributions. It is proportional to the relative phase between the Bino and gluino masses, and is suppressed because of the small magnitude of the subdominant Bino contribution. In addition, the factor  $(1 - r_{q,H}^{\tilde{B}}(m_{h^0}^2)/r_{q,H}^{\tilde{g}}(m_{h^0}^2))$  reflects the second of the general suppressions mentioned above, leading to the alignment of the phases when the *relative contributions* of the Bino to both the mass and Higgs couplings are similar to those of the gluino. Since the loop functions for the mass and Higgs couplings are so similar, this is generally a non-trivial suppression, especially if the superpartners are much heavier than the Higgs boson, for which  $r_{f,H}(m_{h^0}^2) \rightarrow 1$ . As discussed in section VI, if both a quark mass and the muon mass arise radiatively, the current limit on the muon anomalous magnetic moment can be used to bound  $r_{q,H}(0)$  if certain relations are assumed within the superpartner mass spectrum. For  $m_{\tilde{q}_i} \sim m_{\tilde{g}}$  the bounds on  $r_{q,H}^{\tilde{g}}(0)$  shown in fig. 11, obtained under the assumption of gaugino unification for the magnitude of the gaugino masses, also approximately apply to  $r_{q,H}^{\tilde{B}}(0)$ . In this case the  $q^2 = m_{h^0}^2$  corrections should be quite small. With all these assumptions, this additional suppression from the bounds in fig. 11, is conservatively  $(1 - r_{q,H}^{\tilde{B}}(m_{h^0}^2)/r_{q,H}^{\tilde{g}}(m_{h^0}^2)) \lesssim 10^{-1}$ . Taken together all these suppressions imply that the CP-violating Higgs–quark couplings for a quark with a radiative mass are naturally small, i.e.  $\sin(\text{Arg}(m_q^* h_{q,H})) \lesssim 10^{-(3-4)} \sin(\text{Arg}(m_{\tilde{B}} m_{\tilde{g}}^*))$ . In addition, under the assumption of strict gaugino unification,  $m_{\tilde{g}} = m_{\tilde{W}} = m_{\tilde{B}}$  at the unification scale, the phases of the gaugino masses are also correlated. This is the final source of possible suppressions of the physical phases mentioned above. In this case  $\text{Arg}(m_{\tilde{B}} m_{\tilde{g}}^*) = 0$  at lowest order, and the CP-violating Higgs–quarks couplings vanish at one loop in the pure Bino limit. The only contributions at this order arise from gaugino-Higgsino mixing effects.

For radiative lepton masses, in the pure gaugino limit, the  $\tilde{B}$ – $\tilde{W}_3$  mixing vanishes, so only the Bino contributes at one loop to both the radiative mass and Higgs Yukawa couplings of leptons. The phases are then precisely aligned at one loop and the CP-violating Higgs couplings vanish in this limit. Neutralino mixing through electroweak symmetry breaking can however introduce non-trivial phases. In the mostly gaugino or Higgsino region of parameter space, the dominant radiative contributions come from the mostly Bino state, denoted  $\tilde{\chi}_1^0 \simeq \tilde{B}$ , as discussed in section II. Thus the approximation (41) for the CP-violating Higgs–lepton couplings may be employed. Summing over the neutralino contributions to the radiative fermion mass (3) and to the effective Higgs Yukawa coupling parametrized by the

ratios (10), yields:

$$\begin{aligned} \sin(\text{Arg}(m_l^* h_{l,H})) &\simeq \sum_{j=2}^4 \left| \frac{K_l^j m_{\tilde{\chi}_j^0}}{K_l^1 m_{\tilde{\chi}_1^0}} \right| \left( 1 - \frac{r_{l,H}^{\tilde{\chi}_j^0}(m_{h^0}^2)}{r_{l,H}^{\tilde{\chi}_1^0}(m_{h^0}^2)} \right) \frac{I(m_{\tilde{l}_1}, m_{\tilde{l}_2}, m_{\tilde{\chi}_j^0})}{I(m_{\tilde{l}_1}, m_{\tilde{l}_2}, m_{\tilde{\chi}_1^0})} \\ &\times \sin(\text{Arg}(K_l^j m_{\tilde{\chi}_j^0} K_l^{1*} m_{\tilde{\chi}_1^{0*}})), \end{aligned} \quad (45)$$

where  $K_l^j$  are the neutralino coupling coefficients defined in eq. (4). In the mostly gaugino or Higgsino region of parameter space, the neutralino mixing may be treated perturbatively. To first order in mixing, the product of neutralino eigenvectors in (4) is unmodified,  $K_l^j = \frac{1}{2}\delta_{j1}$ , and the physical phase vanishes at this order. To second order, however, a non-trivial phase dependence in the interference terms is introduced by mixing. At this order the Bino mixes with the Higgsino states, giving a small coupling  $K_l^j \sim \mathcal{O}(m_Z^2/\tilde{m}^2)$  for  $j$  the mostly Higgsino states, where  $\tilde{m} = \max(m_{\tilde{B}}, \mu)$ . The physical phase then arises as an interference between the mostly Bino and Higgsino states. The intrinsic phase that appears on the right-hand side of (45) is therefore the phase between the masses of the mostly Bino and Higgsino states,  $\text{Arg}(m_{\tilde{B}}\mu(m_{12}^2)^*)$ , where  $V \supset -m_{12}^2 H_1 H_2 + \text{h.c.}$  determines the phase of the Higgs condensate in a general basis.

In the mostly gaugino or Higgsino region of parameter space, the contribution of the intrinsic phase to the physical CP-violating phase is further suppressed beyond the small  $K_l^j$  couplings of the mostly Higgsino states. The ratio of the loop functions in (45) can be small. For  $m_{\tilde{B}}, \mu \ll m_{\tilde{l}}$  this ratio is of  $\mathcal{O}(1)$ . It is, however, small for  $m_{\tilde{B}} \lesssim m_{\tilde{l}} \ll \mu$ , i.e.  $I(m_{\tilde{l}_1}, m_{\tilde{l}_2}, m_{\tilde{\chi}_j^0})/I(m_{\tilde{l}_1}, m_{\tilde{l}_2}, m_{\tilde{\chi}_1^0}) \sim m_{\tilde{l}}^2/\mu^2$ . In addition, the relative contribution of the mostly Higgsino states to the mass and Higgs-lepton couplings can be very similar, causing the factor  $(1 - r_{l,H}^{\tilde{\chi}_j^0}(m_{h^0}^2)/r_{l,H}^{\tilde{\chi}_1^0}(m_{h^0}^2))$  to give a significant suppression. This relative suppression is dominated by the largest individual deviation from unity of the ratios  $r_{l,H}^{\tilde{\chi}_i^0}$ ,  $i = 1, \dots, 4$ . From the discussion in section II B, the  $D$ -term and finite-momentum contributions to  $r^{\tilde{\chi}_j^0}$  decouple most slowly. For  $m_{h^0}^2 \sim m_Z^2$ , these are both parametrically  $r_{l,H}^{\tilde{\chi}_i^0} \sim 1 + \mathcal{O}(m_Z^2/\tilde{m}'^2)$ , where  $\tilde{m}' = \max(m_{\tilde{\chi}_i^0}, \tilde{m}_l)$ . This suppression, due to the relative similarity of the mostly Higgsino contributions to both the mass and Higgs couplings, can be understood in terms of the effective operator discussion of the Yukawa couplings given in section II B. At the renormalizable level a single operator, namely the effective Yukawa coupling, contributes to both the mass and Higgs couplings. This operator has a definite phase, even if more than one neutralino contributes. The deviations  $(1 - r_{l,H}^{\tilde{\chi}_j^0}(m_{h^0}^2)/r_{l,H}^{\tilde{\chi}_1^0}(m_{h^0}^2))$  represent non-renormalizable operators, which give different contributions to the mass and Higgs effective Yukawa couplings. Thus, it is only the interference between the renormalizable Yukawa coupling, and the non-renormalizable operators that gives rise to a physical phase.

The total suppression of the CP-violating Higgs-lepton coupling can be substantial in the mostly gaugino or Higgsino region of parameter space. Altogether, the following parametric suppression of the physical phase is obtained:

$$\sin(\text{Arg}(m_l^* h_{l,H})) \sim \mathcal{O}(m_Z^4/(\mu m_{\tilde{B}} m_{\tilde{l}}^2)) \sin(\text{Arg}(m_{\tilde{B}}\mu(m_{12}^2)^*)),$$

for  $m_{\tilde{B}} \lesssim \mu \ll m_{\tilde{t}}$ , and

$$\sin(\text{Arg}(m_l^* h_{l,H})) \sim \mathcal{O}(m_Z^4 m_{\tilde{B}} / (\mu^3 m_{\tilde{t}}^2)) \sin(\text{Arg}(m_{\tilde{B}} \mu (m_{12}^2)^*)),$$

for  $m_{\tilde{B}} \lesssim m_{\tilde{t}} \ll \mu$ . If the superpartners are somewhat heavier than the  $Z$  boson, the suppression can be significant, yielding very small CP-violating Higgs–lepton couplings.

Now consider the EDM of the neutron and electron in the case where the light-quark and electron masses are radiative. The discussion parallels that of the Higgs Yukawa couplings in many respects. For the neutron EDM, the dominance of the gluino contribution to light-quark radiative masses turns out to be sufficient, on its own, to render the supersymmetric contribution compatible with current experimental bounds. For the electron EDM, the suppression depends sensitively on the neutralino masses and mixings as described below.

From the definitions in appendix B, a fermion EDM,  $d_f^e$ , is related to the complex coefficient of the electromagnetic dipole operator,  $d_f$ , by eq. (B2)

$$d_f^e = |d_f| \sin(\text{Arg}(d_f m_f^*)).$$

For a radiative quark mass, neglecting  $\tilde{B}$ – $\tilde{W}_3$  mixing, only the gluino and Bino contribute to chirality-violating operators at one loop. The gluino contribution is likely to dominate the Bino contribution, as illustrated in (43) and discussed above. Given the dominance of a single contribution, the approximation (41) may be employed for the relative phase of the mass and dipole-moment coefficient. The magnitude of the Bino and gluino contributions to the dipole-moment coefficient may be obtained from eqs. (B4) and (B9) respectively. With this, the leading contribution to the EDM of a quark with radiative mass is

$$\begin{aligned} d_q^e \simeq & \frac{3\alpha'}{8\alpha_s} \left| \frac{m_{\tilde{B}}}{m_{\tilde{g}}} \right| e Q_q Y_{qL} Y_{qR} m_q \frac{I_{g-2}(m_{\tilde{q}_1}, m_{\tilde{q}_2}, m_{\tilde{g}})}{I(m_{\tilde{q}_1}, m_{\tilde{q}_2}, m_{\tilde{g}})} \sin(\text{Arg}(m_{\tilde{B}} m_{\tilde{g}}^*)) \\ & \times \left( \frac{I_{g-2}(m_{\tilde{q}_1}, m_{\tilde{q}_2}, m_{\tilde{B}})}{I_{g-2}(m_{\tilde{q}_1}, m_{\tilde{q}_2}, m_{\tilde{g}})} - \frac{I(m_{\tilde{q}_1}, m_{\tilde{q}_2}, m_{\tilde{B}})}{I(m_{\tilde{q}_1}, m_{\tilde{q}_2}, m_{\tilde{g}})} \right). \end{aligned} \quad (46)$$

The EDM arises from the interference between the subdominant Bino contribution and leading gluino contribution, and is proportional to the relative phase between the gluino and Bino masses. It is suppressed not by a relative loop factor, but by the small magnitude of the Bino coupling, in analogy to the suppression of the CP-violating Higgs–quark couplings. Under the assumption of unification of gaugino masses,  $|m_{\tilde{B}}/m_{\tilde{g}}| = \frac{5}{3}\alpha'/\alpha_s$ , the factor  $m_{\tilde{B}}\alpha'/(m_{\tilde{g}}\alpha_s) = \frac{5}{3}\alpha'^2/\alpha_s^2$  results in a suppression  $\sim 10^{-2}$ . In addition, the product of color factor and gauge couplings gives a further suppression  $\frac{3}{8}Q_q Y_{qL} Y_{qR} \sim 10^{-1}$ . The difference of the ratio of loop functions in the parenthesis in (46) need not be particularly small, since the mass and dipole loop functions are very different. In the limit  $m_{\tilde{g}} = m_{\tilde{q}_1} = m_{\tilde{q}_2} = \tilde{m} \gg m_{\tilde{B}}$ , the difference approaches  $(\dots) \rightarrow 4$ . So unlike the case of the Higgs–quark CP-violating couplings, there is generally no suppression coming from a relative similarity of Bino contributions to the mass and dipole moment. From the general expressions in appendices A 2 and B, the over-all ratio of loop functions appearing in (46) is  $I_{g-2}(m_{\tilde{q}_1}, m_{\tilde{q}_2}, m_{\tilde{g}})/I(m_{\tilde{q}_1}, m_{\tilde{q}_2}, m_{\tilde{g}}) \sim 1/(6\tilde{m}^2)$ , where the prefactor arises for  $m_{\tilde{g}} = m_{\tilde{q}_1} =$



$m_{\tilde{q}_2} = \tilde{m}$ . The heaviest particle in the gluino loop contribution sets the scale for the EDM operator. Explicitly, for an up-type quark with radiative mass and  $m_{\tilde{B}} \ll m_{\tilde{q}} \lesssim m_{\tilde{g}}$ , the up-quark EDM is  $d_u^e \sim e(2/27)(\alpha'/\alpha_s)(m_u|m_{\tilde{B}}|/|m_{\tilde{g}}|^3) \sin(\text{Arg}(m_{\tilde{B}}m_{\tilde{g}}^*))$ , where the specific prefactor arises for  $m_{\tilde{q}} = m_{\tilde{g}} \gg m_{\tilde{B}}$ .

If the first-generation-quark masses arise radiatively, the up- and down-quark EDMs (46) may be used to estimate the neutron EDM. In this case, the EDMs are related by  $d_d^e = \frac{1}{4}(m_d/m_u)d_u^e$ . The valence approximation for the neutron EDM in the  $SU(2)$  limit is  $d_n^e = \frac{4}{3}d_d^e - \frac{1}{3}d_u^e$ . The resulting neutron EDM from the first-generation quark EDMs is plotted

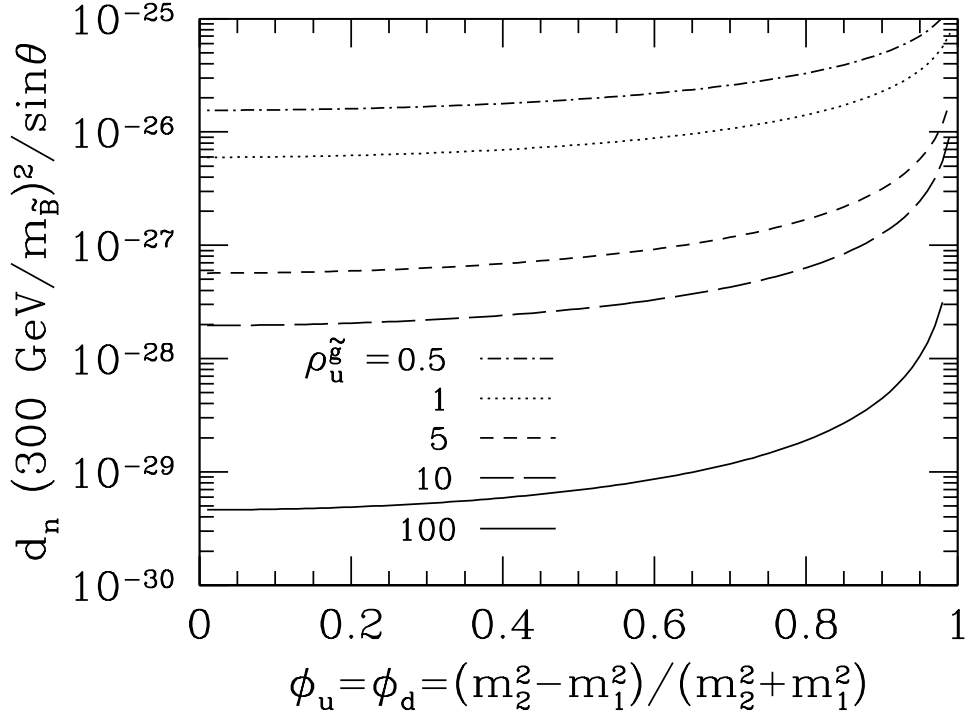


FIG. 12. Leading supersymmetric contribution to the neutron electric dipole moment in units of  $e \cdot \text{cm}$  with radiative masses for the first-generation quarks as a function of the fractional squark mass splitting,  $\phi_u = \phi_d$ . The  $SU(2)$  valence quark approximation and equal up- and down-squark mass eigenvalues are assumed. The modulus of the Bino and gluino masses are assumed to be related by gaugino mass unification, and the electroweak scale masses for the valence quarks are taken to be  $m_u = 1 \text{ MeV}$  and  $m_d = 5 \text{ MeV}$ . The intrinsic CP-violating phase is the relative phase between the Bino and gluino masses,  $\sin \theta \equiv \sin(\text{Arg}(m_{\tilde{B}}m_{\tilde{g}}^*))$ .

in fig. 12 as a function of the fractional mass splitting between squarks. Gaugino mass unification is assumed for the ratio of the Bino and the gluino mass,  $|m_{\tilde{B}}/m_{\tilde{g}}| = \frac{5}{3}\alpha'/\alpha_s$ , and the electroweak scale masses for the quarks are taken to be  $m_u = 1 \text{ MeV}$  and  $m_d = 5 \text{ MeV}$ . Renormalization group running to the QCD scale would increase  $d_n^e$  slightly.

If the first-generation quark masses do in fact arise radiatively, the leading contribution to the neutron EDM in the valence approximation given in fig. 12 is easily compatible with the current experimental bound of  $|d_n^e| < 1.0 \times 10^{-25} e \cdot \text{cm}$ , at the 90% CL [37]. Light-

quark chromo-electric dipole moments (CDMs) can also contribute to the neutron EDM [38]. However, the phases of the chromo-dipole coefficients are also naturally nearly aligned with that of the mass, just as for the EDMs, resulting in a suppression very similar to that of the light-quark EDMs given in (46) and discussed above. With this, estimates of the light-quark CDM contribution to the neutron EDM [38] are very similar to that of the light-quark EDMs. The strange sea content of the neutron may also allow comparable contributions to the neutron EDM from the strange quark EDM and CDM [39]. If the strange quark mass arises radiatively, however, these moments are also significantly suppressed. So if the three lightest quark masses arise radiatively from soft chiral flavor breaking, the present SUSY CP problem for the neutron EDM is essentially eliminated by the natural phase alignment. But, depending on the superpartner mass spectrum and relative phase of the gluino and Bino masses,  $\text{Arg}(m_{\tilde{B}}m_{\tilde{g}}^*)$ , the neutron EDM could be not too far below the current experimental bound.

Of course, if strict gaugino mass unification holds, in which the phases of the gaugino masses are correlated so that  $\text{Arg}(m_{\tilde{B}}m_{\tilde{g}}^*) = 0$  at lowest order, the leading light-quark contributions to the neutron EDM given above vanish, just as for the Higgs–quark CP-violating couplings. In this case the neutron EDM receives contributions from light-quarks with radiative masses mainly from neutralino mixing effects, which can be much smaller than the leading contribution discussed above. There are also potentially small contributions from pure glue operators arising from integrating out heavy quarks [40,41].

For radiative lepton masses, only the neutralinos contribute at one loop to both the dipole moment and mass. Since both the electric and magnetic dipole moments are related to the coefficient of the electromagnetic dipole operator by eqs. (B2) and (B3), it is convenient in this case to relate the EDM to the supersymmetric contribution to the anomalous magnetic moment and intrinsic CP-violating phases. For the lepton EDM, the full one-loop EDM with a radiative mass, using the general expression for a radiative fermion mass (3) and electromagnetic dipole moment (B4), may be written

$$d_l^e = \frac{e a_l^{\text{SUSY}}}{2m_l} \tan \left[ \text{Arg} \left( \frac{\sum_j K_l^j m_{\tilde{\chi}_j^0} I_{g-2}(m_{\tilde{l}_1}, m_{\tilde{l}_2}, m_{\tilde{\chi}_j^0})}{\sum_j K_l^j m_{\tilde{\chi}_j^0} I(m_{\tilde{l}_1}, m_{\tilde{l}_2}, m_{\tilde{\chi}_j^0})} \right) \right] \quad (47)$$

where  $a_l^{\text{SUSY}}$  is the supersymmetric contribution to the lepton anomalous magnetic moment, given in eq. (37). In the pure gaugino limit, only the Bino contributes to both the mass and dipole moment coefficient. The phases appearing in (47) are then aligned, and the one-loop lepton EDMs vanish. In general, however, gaugino–Higgsino mixing through electroweak symmetry breaking introduces non-vanishing phases.

In a region of neutralino parameter space in which there is strong mixing between gaugino and Higgsino states, the phases that appear in (47) are generally not suppressed, potentially leading to a sizeable lepton EDM. For example, if both the electron and muon masses arise radiatively, the anomalous magnetic moments are related by  $a_e^{\text{SUSY}} = (m_e^2/m_\mu^2)a_\mu^{\text{SUSY}}$ , assuming  $m_{\tilde{e}_L} = m_{\tilde{\mu}_L}$  and  $m_{\tilde{e}_R} = m_{\tilde{\mu}_R}$ . In this case the current experimental upper limit on the muon anomalous magnetic moment of  $a_\mu^{\text{new}} < 220 \times 10^{-10}$  [31,32] gives an upper limit on the prefactor in (47) for the electron EDM of  $a_e^{\text{SUSY}} e/(2m_e) < 10^{-23} e \cdot \text{cm}$ . This is to be compared with the current experimental bound on the electron EDM of roughly

$|d_e^e| < 3 \times 10^{-27} e \cdot \text{cm}$  [42]. Therefore in the well-mixed region of neutralino parameter space, compatibility of the electron EDM with the current bound would require either small relative intrinsic phases or a much smaller value of  $a_e^{\text{SUSY}}$  than implied by the current bound on  $a_\mu^{\text{new}}$ . The latter would in fact occur with very heavy selectrons.

In the mostly gaugino or Higgsino region of neutralino parameter space, however, the physical CP-violating phase appearing in a lepton EDM can be significantly suppressed by phase alignment. In this case the mostly Bino state dominates the contribution to both the mass and dipole moment coefficient. The general expression for the physical phase (41) is therefore applicable. The lepton EDM (47) in this limit then reduces to

$$d_l^e \simeq \frac{e a_l^{\text{SUSY}}}{2m_l} \sum_{j=2}^4 \left| \frac{K_l^j m_{\tilde{\chi}_j^0}}{K_l^1 m_{\tilde{\chi}_1^0}} \right| \left( \frac{I_{g-2}(m_{\tilde{l}_1}, m_{\tilde{l}_2}, m_{\tilde{\chi}_j^0})}{I_{g-2}(m_{\tilde{l}_1}, m_{\tilde{l}_2}, m_{\tilde{\chi}_1^0})} - \frac{I(m_{\tilde{l}_1}, m_{\tilde{l}_2}, m_{\tilde{\chi}_j^0})}{I(m_{\tilde{l}_1}, m_{\tilde{l}_2}, m_{\tilde{\chi}_1^0})} \right) \times \sin \left( \text{Arg}(K_l^j m_{\tilde{\chi}_j^0} K_l^{1*} m_{\tilde{\chi}_1^0}^*) \right). \quad (48)$$

Just as in the case of the Higgs-lepton couplings, neutralino mixing induced through electroweak symmetry breaking may be treated perturbatively in this limit, with the coupling coefficients  $K_l^j$  unmodified at first order. At second order in the mixing, a non-trivial phase dependence is introduced by the mixing between the Bino and Higgsino states, with a small coupling  $K_l^j \sim \mathcal{O}(m_Z^2/\tilde{m}^2)$  for  $j$  the mostly Higgsino states, where  $\tilde{m} = \max(m_{\tilde{B}}, \mu)$ . The leading intrinsic phase that appears on the right-hand side of (48) is then the phase between the masses of the mostly Bino and Higgsino states,  $\text{Arg}(m_{\tilde{B}}\mu(m_{12}^2)^*)$ . The suppression for the relative similarity of the mostly Higgsino contributions to the mass and dipole coefficient, contained in the difference of ratios of loop functions in the parenthesis in (48), although not necessarily so, can be significant in certain regions of parameter space. For example, in the limit  $m_{\tilde{B}} \lesssim m_{\tilde{l}} \ll \mu$  the difference factor  $(\dots)$  in (48) is dominated by the ratio of mass loop functions since the non-renormalizable dipole operator decouples more quickly than the renormalizable effective Yukawa coupling. The relative contribution of the mostly Higgsino state to the dipole coefficient is therefore insignificant, and the phase misalignment comes mainly from the mostly Bino and Higgsino contributions to the radiative mass. Parametrically, in this case, the term in parenthesis in (48) is  $(\dots) \sim \mathcal{O}(m_{\tilde{l}}^2/\mu^2)$ . Altogether then, in this limit the lepton EDM is

$$d_l^e \sim \frac{e a_l^{\text{SUSY}}}{2m_l} \mathcal{O}(m_Z^2 m_{\tilde{l}}^2 / (\mu^3 m_{\tilde{B}})) \sin \left( \text{Arg}(m_{\tilde{B}}\mu(m_{12}^2)^*) \right).$$

As another example, in the limit  $m_{\tilde{B}} \lesssim \mu \ll m_{\tilde{l}}$ , the slepton masses set the scale for all the loop functions, and the ratios of loop functions approach unity. The difference of loop functions in (48) may be obtained from the results of appendices A 2 and B. Parametrically, in this case,  $(\dots) \sim \mathcal{O}(\mu^2/m_{\tilde{l}}^2)$ . The lepton EDM in this limit is then

$$d_l^e \sim \frac{e a_l^{\text{SUSY}}}{2m_l} \mathcal{O}(m_Z^2 \mu / (m_{\tilde{B}} m_{\tilde{l}}^2)) \sin \left( \text{Arg}(m_{\tilde{B}}\mu(m_{12}^2)^*) \right).$$

Note in addition that  $a_l^{\text{SUSY}}$  is itself also suppressed in this limit,  $a_l^{\text{SUSY}} \simeq m_l^2/m_{\tilde{l}}^2$ , for  $m_{\tilde{l}_L} = m_{\tilde{l}_R} = m_{\tilde{l}} \gg m_{\tilde{B}}$ . Obtaining a radiative mass for the electron is in fact possible

with very heavy selectrons, since the effective renormalizable Yukawa coupling need not vanish in the superpartner decoupling limit. As discussed in section III, very heavy first-generation scalar partners could partially or fully account for the smallness of the first-generation fermion masses. Depending on the specific superpartner masses and mixings, it is possible for the physical phase appearing in the electron EDM to be suppressed sufficiently to be compatible with the current experimental bound in the radiative electron mass scenario.

In summary, if the light-quark masses arise radiatively from soft chiral flavor breaking, the supersymmetric contribution to the neutron EDM is significantly suppressed because of the natural near-alignment of the phases of the dipole operators and fermion masses. This suppression is numerically significant even though the EDM is not suppressed by a relative loop factor. The leading contribution is proportional to the intrinsic CP-violating phase  $\sin(\text{Arg}(m_{\tilde{B}}m_{\tilde{g}}^*))$ , and is easily compatible with the current experimental bound. Depending on the superpartner mass spectrum and  $\text{Arg}(m_{\tilde{B}}m_{\tilde{g}}^*)$ , the neutron EDM could be not too far below the current experimental bound. However, with strict gaugino mass unification,  $\text{Arg}(m_{\tilde{B}}m_{\tilde{g}}^*) = 0$ , and the neutron EDM is likely to be well beyond the reach of currently anticipated experiments. The electron EDM is also suppressed in the mostly gaugino or Higgsino region of neutralino parameter space, where the leading contribution is proportional to the intrinsic phase  $\sin(\text{Arg}(m_{\tilde{B}}\mu(m_{12}^2)^*))$ . Unlike the neutron EDM, the magnitude of the electron EDM in terms of this intrinsic phase is a very model-dependent function of the neutralino mixings and superpartner masses. In plausible regions of neutralino and scalar partner parameter space it can be consistent with current experimental limits. CP-violating Higgs–fermion couplings are negligible with radiative masses.

## VIII. PROBING THE STIFFNESS OF YUKAWA COUPLINGS

Radiative fermion masses generated at the superpartner mass scale require a relatively large breaking of chiral flavor symmetries in scalar tri-linear terms, and imply that the effective Yukawa couplings are soft, as discussed in section II. This leads to various distinctive effects, which can in principle be probed directly in high energy experiments, including:

1. Form factor effects for the effective Higgs Yukawa couplings, summarized in the ratios  $r_{f,H}(q^2)$  and  $r_{f,A}(q^2)$ .
2. “Wrong Higgs” couplings for radiative masses arising from non-holomorphic  $A'$  operators.
3. Large left–right mixing for second-generation scalar partners.
4. Apparent, hard supersymmetry-breaking effects in Higgsino–matter couplings.

In this section the possibilities for detecting and measuring these effects are outlined. As discussed below, one of the most useful tools would be the proposed  $\mu^+\mu^-$  collider, which can produce the neutral Higgs bosons as  $s$ -channel resonances and make precision measurements of Higgs–fermion couplings [43].

TABLE III. The neutral Higgs boson mixing coefficients  $\Theta$  appearing in the effective Higgs–fermion Yukawa coupling. The coefficient for a particular fermion depends on whether the fermion mass originates from a holomorphic  $A$ -term, non-holomorphic  $A'$ -term, or tree-level superpotential Yukawa coupling.

Higgs boson	Radiative up-type $\propto A$	Radiative up-type $\propto A'$
	Radiative down-type/lepton $\propto A'$	Radiative down-type/lepton $\propto A$
	Tree-level up-type	Tree-level down-type/lepton
$h^0$	$\cos \alpha / \sin \beta$	$-\sin \alpha / \cos \beta$
$H^0$	$\sin \alpha / \sin \beta$	$\cos \alpha / \cos \beta$
$A^0$	$i \cot \beta$	$i \tan \beta$

The most obvious arena for direct experimental probes of radiatively generated effective Yukawa couplings are precision measurements of the physical Higgs–fermion couplings. These couplings are given by  $\lambda_{h^0, H^0} = \Theta \{\cos \beta, \sin \beta\} \bar{h}_{f, H} / \sqrt{2}$  with  $H = h^0, H^0$ , and  $\lambda_{A^0} = \Theta \{\cos \beta, \sin \beta\} \bar{h}_{f, A} / \sqrt{2}$ , where the first (second) terms in curly brackets corresponds to  $\alpha = 1$  (2), and  $\Theta$  represents the Higgs mixing matrix between physical and interaction eigenstates [44,45] relevant to the fermion in question. The mixing coefficients  $\Theta$  are given in table III, where  $\alpha$  is the  $h^0$ – $H^0$  mixing angle, and  $\tan \beta = \langle H_2 \rangle / \langle H_1 \rangle$ . From (10) and (17),  $\bar{h}_{f, H} = r_{f, H} h_{f, m}$ , and  $\bar{h}_{f, A} = r_{f, A} h_{f, m}$ , where  $r_{f, H}$ ,  $r_{f, A}$  are the magnitude of the effective Yukawa couplings relative to a tree-level coupling. The form factor effect is contained in the magnitude and momentum dependence of the ratios  $r_{f, H}$ ,  $r_{f, A}$ . For  $m_f^2, m_\lambda^2 \sim m_H^2$  the ratio  $r_f(q^2)$  has a non-trivial momentum dependence in addition to the logarithmic momentum dependence from renormalization group evolution. The logarithmic dependence may be subsumed in the definition  $m_f = m_f(q^2)$  or  $h_{f, m} = h_{f, m}(q^2)$  above. For  $m_f^2, m_\lambda^2 \gtrsim m_H^2$ , the scalar Higgs–fermion radiative coupling ratios are greater than unity,  $r_{f, H}(m_{h^0}^2), r_{f, H}(m_{H^0}^2) \geq 1$ , from intrinsic coupling effects in the one-loop diagram, as described in section II B. Thus, even if the momentum dependence cannot be determined experimentally, the over-all magnitude of the effective Yukawa coupling can differ from the minimal case with tree-level masses. In contrast, the pseudoscalar Higgs–fermion radiative coupling ratios deviate from unity only from neutralino mixing in the one-loop diagram, and through non-trivial momentum dependence. Comparison of scalar and pseudoscalar Higgs couplings, as discussed below, might then in principle allow the momentum dependence of the Yukawa couplings, or equivalently of the finite Yukawa mass radii, to be disentangled from intrinsic coupling effects.

The Higgs mixing effects in the Higgs–fermion couplings, contained in  $\Theta$ , depend on the projection of the physical Higgs bosons onto the Higgs doublet, which gives rise to the fermion mass. In any supersymmetric theory with tree-level fermion masses and a single pair of Higgs doublets,  $H_1$  with  $U(1)_Y$  hypercharge  $Y = -1$ , and  $H_2$  with  $Y = +1$ , gauge invariance and holomorphy of the superpotential guarantee that, at tree level, up-type quarks receive mass from  $H_2$  while down-type quarks and leptons receive mass from  $H_1$ . The coupling coefficients of the physical scalar Higgs bosons  $h^0$  and  $H^0$ , and physical pseudoscalar  $A^0$ , are then fixed to be those given in table III. For radiative masses arising from holomorphic chiral flavor breaking, the fermions receive mass from the same type

of Higgs doublets, and the coupling coefficients are the same as with tree-level masses. In this case the Higgs–fermion couplings differ from those in the minimal case with tree-level masses only through the magnitude of the momentum-dependent form factors  $r_{f,H}(q^2)$ ,  $r_{f,A}(q^2)$ . However, with non-holomorphic chiral flavor breaking, radiative up-type quark masses arise from  $H_1$ , while radiative down-type quark and lepton masses arise from  $H_2$ . The resulting “wrong Higgs” coupling coefficients to physical Higgs bosons in this case are given in table III. Depending on  $\alpha$  and  $\beta$ , these coupling coefficients can drastically differ from those in the minimal case with tree-level masses or those obtained with holomorphic chiral flavour breaking. The “wrong Higgs” modifications of the couplings persist in the strict superpartner decoupling limit of  $m_{\tilde{f}}^2, m_{\tilde{\lambda}}^2 \gg m_H^2$ , even though  $r_{f,H}, r_{f,A} \rightarrow 1$  in this limit.

Because the Higgs coupling coefficients depend on two mixing parameters, even in the minimal model, multiple measurements are necessary in order to discern any radiative contribution to a fermion mass. Fortunately, it is very unlikely that the top quark or  $\tau$ -lepton masses arise radiatively, as discussed in section III. The couplings of these fermions to various Higgs bosons can be used as “standard candles” by which to compare other fermion couplings. For the lightest Higgs boson,  $h^0$ , the theoretical upper bound in supersymmetric theories on the Higgs mass and the measured top-quark mass imply  $m_{h^0} < m_t$ . The channel  $h^0 \rightarrow tt$  is therefore closed, so  $h^0 \rightarrow \tau\tau$  must be used as a “standard candle”. In a minimal theory with tree-level masses, all the down-type quarks and leptons gain mass from a single Higgs doublet,  $H_1$ . For  $h^0$  couplings, the most useful quantity to consider is therefore the ratio of branching ratios for a down-type quark or lepton to that of the  $\tau$ -lepton

$$\frac{m_\tau^2}{N_c m_f^2} \frac{\text{Br}(h^0 \rightarrow ff)}{\text{Br}(h^0 \rightarrow \tau\tau)} = r_{f,H}^2(m_{h^0}^2) \left\{ 1, \cot^2 \alpha \cot^2 \beta \right\}, \quad (49)$$

where  $N_c$  is a color factor,  $N_c = 3$  for quarks and  $N_c = 1$  for leptons. Throughout this section the first term in curly brackets refers to tree-level masses or radiative masses from holomorphic A-terms; the second term to “wrong Higgs” couplings for radiative masses from non-holomorphic A'-terms. Finite fermion mass effects in the final-state phase space are ignored throughout, except for the top quark. Analogous relations hold for the heavy Higgs scalar  $H^0$ :

$$\frac{m_\tau^2}{N_c m_f^2} \frac{\text{Br}(H^0 \rightarrow ff)}{\text{Br}(H^0 \rightarrow \tau\tau)} = r_{f,H}^2(m_{H^0}^2) \left\{ 1, \tan^2 \alpha \cot^2 \beta \right\}, \quad (50)$$

and for the pseudoscalar  $A^0$ :

$$\frac{m_\tau^2}{N_c m_f^2} \frac{\text{Br}(A^0 \rightarrow ff)}{\text{Br}(A^0 \rightarrow \tau\tau)} = r_{f,A}^2(m_{A^0}^2) \left\{ 1, \cot^4 \beta \right\}, \quad (51)$$

where  $f$  is a down-type quark or lepton. In the Higgs decoupling limit of  $m_{A^0}^2 \gg m_Z^2$ , the light-Higgs projection onto the Higgs doublets aligns with the expectation values and the  $h^0$  couplings become standard-model-like, giving  $\cot^2 \alpha \rightarrow \tan^2 \beta$ . This occurs even for radiative Yukawa couplings, and implies that all  $h^0$  branching ratios approach standard-model values in the Higgs decoupling limit, up to possible form-factor effects. Thus in this

limit, independently of whether the fermion masses are tree-level or radiative from either holomorphic or non-holomorphic chiral flavor breaking, the ratio (49) for  $h^0$  just depends on the form factor. However, in the case of non-holomorphic breaking, the ratios (50) and (51) for  $H^0$  and  $A^0$  can differ drastically from unity because of the “wrong Higgs” coupling. In particular, in the “wrong Higgs” case, it holds:

$$\text{Br}(A^0 \rightarrow \tau\tau) > \text{Br}(A^0 \rightarrow bb) \text{ for } \tan\beta > \sqrt{\sqrt{3}m_b/m_\tau} \simeq 1.7.$$

The momentum dependence of the effective Higgs Yukawa coupling can in principle be probed by comparing  $r_{f,H}(m_{h^0}^2)$  with  $r_{f,H}(m_{H^0}^2)$  or  $r_{f,A}(m_{A^0}^2)$  for a given final state.

It is important to emphasize that any supersymmetric theory with tree-level Yukawa couplings and only a pair of Higgs doublets is guaranteed by holomorphy of the superpotential to give a ratio of unity for (49)–(51) up to small and calculable quantum corrections, as described above. Deviations of the lowest-order ratios would therefore be an indication of either additional Higgs doublets or, with only a single pair of doublets, radiative contributions to the masses – through form-factor effects and/or non-holomorphic “wrong Higgs” couplings.

For the heavy-Higgs pseudoscalar, if kinematically open,  $A^0 \rightarrow tt$  can compete with  $A^0 \rightarrow bb$  depending on the value of  $\tan\beta$ . For reference, with a tree-level or radiative mass for the  $b$ -quark with holomorphic chiral flavor breaking, the  $A^0 tt$  coupling is larger than the  $A^0 bb$  coupling for  $\tan\beta < \sqrt{m_t/m_b} \simeq 7.5$ . In this case the (tree-level) top quark coupling can be used as a “standard candle” with which to compare the charm quark coupling through the ratio

$$\frac{m_t^2 \text{Br}(A^0 \rightarrow cc) \sqrt{1 - 4m_t^2/m_{A^0}^2}}{m_c^2 \text{Br}(A^0 \rightarrow tt)} = r_{c,A}^2(m_{A^0}^2) \{1, \tan^4\beta\}, \quad (52)$$

where  $\sqrt{1 - 4m_t^2/m_{A^0}^2}$  is a kinematic correction for the  $S$ -wave decay of a pseudoscalar. In a theory with tree-level Yukawa couplings, or radiative masses with holomorphic flavor breaking, if  $A^0 \rightarrow tt$  is open,  $\text{Br}(A^0 \rightarrow cc)$  is unobservably small. However, from (52), if the charm quark gains a mass from the “wrong Higgs” through non-holomorphic flavor breaking,  $\text{Br}(A^0 \rightarrow cc)$  can be non-negligible, and even dominate  $\text{Br}(A^0 \rightarrow tt)$  if  $\tan\beta \gtrsim \sqrt{m_t/m_c} \simeq 16$ . In this case  $\text{Br}(A^0 \rightarrow cc)$  can be small or large, depending on the origin of the  $b$ -quark mass. If the  $b$ -quark mass is tree-level or radiative through a holomorphic  $A$ -term,  $\text{Br}(A^0 \rightarrow cc) \leq m_c^2/(m_b^2 + m_c^2) \simeq 0.05$  (neglecting the form factors). However, if the  $b$ -quark mass arises radiatively from a non-holomorphic  $A'$ -term,  $\text{Br}(A^0 \rightarrow cc) \simeq 1$  in the large  $\tan\beta$  limit, even if  $A^0 \rightarrow tt$  is open. An analogous relation to (52) holds for the heavy Higgs scalar  $H^0$  with  $P$ -wave kinematic correction and with  $\tan^4\beta$  replaced by  $\cot^2\alpha \tan^2\beta$ . With  $\tan\beta \gg 1$ ,  $\text{Br}(H^0, A^0 \rightarrow cc)$  are therefore very sensitive to possible “wrong Higgs” couplings arising from a radiative charm quark mass. This is in contrast to  $\text{Br}(h^0 \rightarrow cc)$ , which, in the Higgs decoupling limit, approaches the standard model value up to form factor effects, as discussed above.

Measurements of the above ratios of branching ratios requires flavor identification of the final states. With adequate  $\tau$ - and  $b$ -tagging at future lepton and possibly hadron colliders,

the ratios (49)–(51) can be used to probe a radiative  $b$ -quark mass. The ratio (52) also requires  $c$ -tagging and top identification to probe a radiative charm-quark mass. Extension to other fermions is problematic since in most scenarios the branching ratios will be small. However, the proposed  $\mu^+\mu^-$  collider, which can produce the Higgs bosons as  $s$ -channel resonances, provides the possibility of measuring the muon–Higgs couplings [43]. For  $h^0$ , with width less than the beam width,  $\Gamma_{h^0}^{\text{tot}} \lesssim \Gamma_{\text{beam}}$ , the total cross section  $\sigma(\mu^+\mu^- \rightarrow h^0 \rightarrow X)$  gives a measure of  $\Gamma(h^0 \rightarrow \mu\mu)\text{Br}(h^0 \rightarrow X)$ . Independent measurements of  $\text{Br}(h^0 \rightarrow X)$  can then give  $\Gamma(h^0 \rightarrow \mu\mu)$  to a few percent precision [46]. A measurement of  $\Gamma_{h^0}^{\text{tot}}$  from scanning around the  $h^0$  resonance, with a beam energy resolution better than the beam width  $\delta\sqrt{s} \ll \Gamma_{\text{beam}}$ , then yields  $\text{Br}(h^0 \rightarrow \mu\mu) = \Gamma(h^0 \rightarrow \mu\mu)/\Gamma_{h^0}^{\text{tot}}$  [43]. For  $H^0$  and  $A^0$  with  $\Gamma_{H^0, A^0}^{\text{tot}} \gtrsim \Gamma_{\text{beam}}$ , the peak cross sections  $\sigma(\mu^+\mu^- \rightarrow H^0, A^0 \rightarrow X)$  at the center of the resonances give a direct measure of  $\text{Br}(H^0, A^0 \rightarrow \mu\mu)\text{Br}(H^0, A^0 \rightarrow X)$ . Thus, a measurement of these ratios can also test whether the muon mass is generated radiatively. Note, however, that  $r_{\mu, H}(0)$  is already bounded by muon magnetic moment measurements, and will be very well bounded or determined by such measurements by the time the  $\mu^+\mu^-$  collider is in operation. In this case, the ratios (49)–(51) for the muon will provide a test for possible “wrong Higgs” couplings.

In addition to the branching ratios, a  $\mu^+\mu^-$  collider also allows the possibility of determining absolute widths, as described above. The absolute magnitude of the Higgs–muon coupling obtained from  $\Gamma(h^0 \rightarrow \mu\mu)$  cannot in general be interpreted directly because of Higgs mixing effects and the  $\tan\beta$  dependence of the  $h^0\mu\mu$  coupling. In the Higgs decoupling limit of  $m_{A^0}^2 \gg m_Z^2$ , however, the light Higgs couplings for either tree-level or radiative fermion masses become standard-model-like, up to the form-factor ratios, as discussed above. So in the Higgs decoupling limit

$$\left. \frac{\Gamma(h^0 \rightarrow ff)}{\Gamma(\phi^0 \rightarrow ff)} \right|_{m_{A^0}^2 \rightarrow \infty} = r_{f, H}^2(m_{h^0}^2), \quad (53)$$

where  $\Gamma(\phi^0 \rightarrow ff)$  is the width for the decay of the standard model Higgs boson,  $\phi^0$ , which is calculable in terms of the fermion mass. However, away from the decoupling limit, deviations of the  $h^0$ –fermion couplings only vanish like  $\mathcal{O}(m_Z^2/m_{A^0}^2)$ , and can be significant for finite  $m_{A^0}$ . Therefore, the ratio (53) of absolute to standard-model widths is not as useful as ratios of physical Higgs boson branching ratios for disentangling the effects of the form factor and possible “wrong Higgs” coupling from Higgs mixing effects.

The absolute widths for  $\Gamma(H^0, A^0 \rightarrow ff)$  can also be determined at a  $\mu^+\mu^-$  collider. Given measurements of  $\text{Br}(H^0, A^0 \rightarrow ff)$ , either independently or as described above, measurements of  $\Gamma_{H^0, A^0}^{\text{tot}}$  by precision scans of the line shapes yield the widths  $\Gamma(H^0, A^0 \rightarrow ff) = \text{Br}(H^0, A^0 \rightarrow ff)\Gamma_{H^0, A^0}^{\text{tot}}$ . Again, the absolute magnitude of the  $H^0$ –fermion couplings suffer from mixing effects. The pseudoscalar couplings are independent of  $h^0$ – $H^0$  mixing, but do depend on  $\tan\beta$  as shown in table III. The normalized  $A^0$  partial widths for down-type quarks or leptons are

$$\frac{\Gamma(A^0 \rightarrow ff)}{\Gamma(\phi^0 \rightarrow ff)} = r_{f, A}^2(m_{A^0}^2) \{ \tan^2\beta, \cot^2\beta \}. \quad (54)$$



Making use of these ratios requires an independent measurement of  $\tan\beta$ . Alternatively, if perturbativity of the top-quark Yukawa coupling up to a large scale is imposed, implying  $\tan\beta \gtrsim 1.8$ , a value of the normalized widths  $\leq 3.2$  could be taken as evidence of form-factor effects or “wrong Higgs” couplings.

At a  $\mu^+\mu^-$  collider, with the possibility of measuring absolute decay widths, also tests of supersymmetric theories with tree-level Yukawa couplings and a single pair of Higgs doublets can be made. Another way to eliminate Higgs mixing effects in the minimal case is to sum the normalized decay widths of both  $h^0$  and  $H^0$  to a given fermion final state. For down-type quarks or leptons with tree-level or radiative masses from holomorphic flavor breaking, or for up-type quarks with radiative masses from non-holomorphic flavor breaking, this sum gives:

$$\frac{\Gamma(\phi^0 \rightarrow ff)}{\Gamma(h^0 \rightarrow ff)} + \frac{\Gamma(\phi^0 \rightarrow ff)}{\Gamma(H^0 \rightarrow ff)} = \frac{\cos^2\beta}{r_{f,H}^2(m_{h^0}^2)\sin^2\alpha + r_{f,H}^2(m_{H^0}^2)\cos^2\alpha}. \quad (55)$$

For up-type quarks with tree-level or radiative masses from holomorphic  $A$ -terms, or for down-type quarks or leptons with radiative masses from non-holomorphic  $A'$ -terms, (55) holds with the substitutions  $\cos^2\beta \rightarrow \sin^2\beta$  and  $\cos^2\alpha \leftrightarrow \sin^2\alpha$ . With tree-level masses the denominator on the right-hand side of (55) sums to unity, up to quantum corrections. Thus, with a radiative fermion mass, (55) can be sensitive to the momentum dependence of the form factor, if an independent measurement of  $\tan\beta$  is available. Alternatively, with tree-level masses the sum of (55) for a down-type quark or lepton and the analogous relation for an up-type quark is unity. This quantity for  $bb$  and  $cc$  widths or  $\mu\mu$  and  $cc$  widths would provide an interesting test for form-factor effects for these fermions. Making use of the latter sums with holomorphic flavor breaking in general requires that  $H^0 \rightarrow tt$  be closed so that  $\text{Br}(H^0 \rightarrow cc)$  is non-negligible.

Another quantity that eliminates all Higgs mixing effects, including  $\tan\beta$  dependence, is the product of normalized partial widths for  $A^0$  decay to up-type quarks and down-type quarks or leptons. If  $A^0 \rightarrow tt$  is open,

$$\frac{\Gamma(A^0 \rightarrow tt)\Gamma(A^0 \rightarrow ff)(1 - 4m_t^2/m_{A^0}^2)}{\Gamma(\phi^0 \rightarrow tt)\Gamma(\phi^0 \rightarrow ff)} = r_{f,A}^2(m_{A^0}^2) \{1, \cot^4\beta\}, \quad (56)$$

where  $f = b, \tau, \mu$ , and  $(1 - 4m_t^2/m_{A^0}^2)$  is a kinematic correction factor for the  $S$ -wave decay of a pseudoscalar, compared with the  $P$ -wave decay of a scalar. If open,  $\text{Br}(A^0 \rightarrow tt)$  depends on  $\tan\beta$ , as discussed above. If  $\text{Br}(A^0 \rightarrow tt)$  is non-negligible, the product (56) with  $f = \mu$  from measurements at a  $\mu^+\mu^-$  collider provides an interesting test of form factors or “wrong Higgs” couplings to the muon. If  $\text{Br}(A^0 \rightarrow tt)$  and  $\text{Br}(A^0 \rightarrow bb)$  are comparable, the  $b$ -quark coupling can be probed. Note that with  $f = \tau$  the product (56) is unity for a single pair of Higgs doublets with tree-level top quark and  $\tau$ -lepton Yukawa couplings. This may therefore be used as a good test for multiple pairs of Higgs doublets. If  $A^0 \rightarrow tt$  is closed, analogous relations may be applied with  $\Gamma(A^0 \rightarrow cc)$ .

A final interesting quantity for testing  $A^0$  couplings is the sum of normalized decay widths to an up-type quark and a down-type quark or lepton. If  $A^0 \rightarrow tt$  is open,

$$\frac{\Gamma(A^0 \rightarrow ff)}{\Gamma(\phi^0 \rightarrow ff)} + \frac{\Gamma(A^0 \rightarrow tt)(1 - 4m_t^2/m_{A^0}^2)}{\Gamma(\phi^0 \rightarrow tt)} = \left\{ r_{f,A}^2(m_{A^0}^2) \tan^2 \beta + \cot^2 \beta, (r_{f,A}^2(m_{A^0}^2) + 1) \cot^2 \beta \right\}, \quad (57)$$

with  $f = b, \tau, \mu$ . In the minimal case with tree-level masses the sum (57) is strictly  $\geq 2$ , up to calculable quantum corrections. With a radiative mass for  $f$  from holomorphic chiral flavor breaking this bound can be modified by the magnitude of the form factor ratio  $r_{f,A}^2(m_{A^0}^2)$ . The effect is most dramatic when  $f$  obtains a mass radiatively from non-holomorphic breaking, in which case the sum (57) is in principle arbitrary. If perturbativity of the top Yukawa up to a large scale is imposed, implying  $\tan \beta \gtrsim 1.8$ , the sum (57) can be significantly lower than the bound implied by tree-level masses. Again a violation of the lower bound for (57) would be a clear signal in a supersymmetric theory for either more than a single pair of Higgs doublets or, with a single pair, of radiative masses.

The requirement of large tri-linear terms for radiative second-generation masses leads to large left–right mixing for second-generation scalars, as mentioned at the beginning of this section. This may be probed in a number of ways in high-energy experiments. The large tri-linear terms coupling a Higgs doublet to left- and right-handed scalars can lead directly to enhanced decays involving Higgs bosons and second-generation mass eigenstate scalars,  $\tilde{f}_1$  and  $\tilde{f}_2$ . For example, if open,  $\text{Br}(\tilde{f}_2 \rightarrow \tilde{f}_1 h^0)$  or  $\text{Br}(H^0, A^0 \rightarrow \tilde{f}_1 \tilde{f}_2)$  can be non-negligible. In contrast, with tree-level masses, these are expected to be insignificant for second-generation scalars. In addition, left–right mixing can also directly affect production cross sections. For example, the polarized cross sections  $\sigma(e_{L,R}^+ e_{L,R}^- \rightarrow \tilde{f}_i \tilde{f}_i)$  etc., depend sensitively on the gauge couplings of  $\tilde{f}_i$ . In the minimal case, second generation scalar mass eigenstates are expected to be nearly pure gauge eigenstates. But with radiative masses, since the tri-linear terms are so large, the mass eigenstates are very likely to be well-mixed combinations of left- and right-handed scalars.

Finally, with radiative masses from scalar chiral flavor breaking, the radiatively generated Higgsino coupling can differ drastically from the radiative Higgs coupling, with even different parametric dependence on the underlying couplings, as described in section II C. This is a clear prediction of the present scenario for radiative fermion masses. To an electroweak scale observer who assumes tree-level masses, this appears as a hard violation of the supersymmetric relation between the Higgs and Higgsino couplings. Unfortunately, because of complicated gaugino–Higgsino mixing effects, disentangling the Higgsino–matter couplings from couplings of physical neutralinos and charginos in, for example,  $\chi_i^0 \rightarrow \tilde{f} \tilde{f}$  and  $\chi_i^\pm \rightarrow \tilde{f} \tilde{f}'$ , or  $\tilde{f} \rightarrow \chi_i^0 f$  and  $\tilde{f} \rightarrow \chi_i^\pm f'$ , is much more difficult than disentangling Higgs–matter couplings. Unless some of the neutralino and chargino states are very nearly pure Higgsino-like, this would require precision branching-ratio measurements for many final states.

## IX. SOFTLY BROKEN LEPTON NUMBER

In addition to chiral flavor symmetries, it is also possible that other global chiral symmetries such as lepton or baryon number or matter parity [28] are broken in the low-energy

theory predominantly by auxiliary rather than scalar expectation values. Consider the case, for example, of lepton-number violation. Soft lepton-number violation involving the bilinear terms  $\mathcal{L} \supset m^2 LH_2$  was considered in ref. [47]. Here we discuss the consequence of lepton-number violating tri-linear scalar terms analogous to (1) and (2) in the holomorphic operators

$$\mathcal{L} \supset \widehat{A}LQD + \widehat{A}LLE \quad (58)$$

and the non-holomorphic operator

$$\mathcal{L} \supset \widehat{A}'L^*QU \quad (59)$$

where the flavor structure is suppressed. Note that the non-holomorphic operator involves right-handed up-squarks. This differs from the standard tree-level superpotential lepton-number violating Yukawa couplings, which are restricted to be holomorphic. The lepton-number violating operators (58) give rise to a radiatively generated neutrino mass. At one loop a soft lepton-number violating sneutrino–antisneutrino mixing term,  $\mathcal{L} \supset \delta m_{\tilde{\nu}}^2 \tilde{\nu} \tilde{\nu} + \text{h.c.}$ , is generated with

$$\delta m_{\tilde{\nu}}^2 \sim \frac{\langle H_\alpha \rangle^2 A^2 \widehat{A}^2}{16\pi^2 m_{\tilde{f}}^4} \quad (60)$$

and likewise for the non-holomorphic operator (59). Gauge invariance implies that this mixing is proportional to two powers of both lepton-number violating and lepton-number conserving tri-linear scalar terms. The induced sneutrino–antisneutrino mixing in turn gives rise to a neutrino mass at two loops

$$m_\nu \sim \frac{\alpha_2 m_{\tilde{W}} \delta m_{\tilde{\nu}}^2}{4\pi m_{\tilde{\nu}}^2}, \quad (61)$$

through diagrams such as in fig. 13. Since the neutrinos are left-handed, only the  $\widetilde{W}_3$

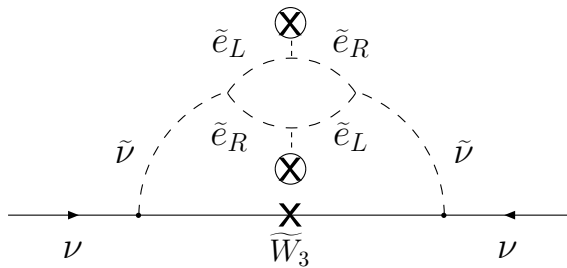


FIG. 13. Two-loop contribution to the neutrino mass from soft lepton-number violation.

chirality-violating mass contributes to the radiatively induced neutrino mass in the pure gaugino limit. The magnitude of the tri-linear scalar terms for a given neutrino mass is numerically, very roughly,  $A\widehat{A}/\widetilde{m}^2 \sim (m_\nu/3 \text{ MeV})^{1/2}(\widetilde{m}/100 \text{ GeV})^{1/2}$ , assuming  $\widetilde{m} \simeq m_{\tilde{W}} \simeq$

$m_{\tilde{\nu}}$ . The specific pattern of neutrino masses and mixings of course depends on the flavor structure of both the lepton-number violating and lepton-number conserving scalar tri-linear terms. Notice that, unlike quark and lepton masses, radiatively induced neutrino masses arise from non-renormalizable operators in the low-energy theory, and therefore vanish in the superpartner decoupling limit in which all soft supersymmetry-breaking parameters are taken simultaneously large.

One generic consequence of this mechanism for soft radiative neutrino masses is the relatively large ratio  $\delta m_{\tilde{\nu}}^2/m_{\tilde{\nu}}^2 \sim (4\pi/\alpha_2)(m_\nu/m_{\tilde{W}})$ . This is to be compared with a standard scenario in which neutrino masses arise directly from tree-level superpotential couplings. In this case, a sneutrino–antisneutrino mixing arises radiatively from the neutrino mass (rather than the other way around) yielding  $\delta m_{\tilde{\nu}}^2/m_{\tilde{\nu}}^2 \sim (\alpha_2/4\pi)(m_\nu m_{\tilde{W}}/m_{\tilde{\nu}}^2)$ . For a massive  $\tau$ -neutrino, the relatively large  $\delta m_{\tilde{\nu}}^2/m_{\tilde{\nu}}^2$  associated with a soft neutrino mass might be probed in  $\tilde{\nu}_\tau$ – $\tilde{\bar{\nu}}_\tau$  oscillation experiments [48]. Lastly, it is interesting to note that the simple assumption of degeneracy among respective tri-linear couplings corresponds to the case of large neutrino mixing angles.

## X. SUMMARY AND DISCUSSION

Supersymmetric theories have the property that the chiral flavor symmetries required for quark and lepton masses may be broken either in hard renormalizable terms, or in soft supersymmetry-breaking terms. This interesting feature arises because the squark and slepton superpartners necessarily carry the same flavor symmetries as the quarks and leptons. In this paper we have investigated the possibility that some of the fermion masses arise predominantly radiatively from chiral flavor violation in soft supersymmetry-breaking terms. The breaking of such symmetries exclusively in soft and not in hard terms is technically natural and may be enforced by horizontal  $R$ -symmetries. In this scenario some of the flavor symmetries are broken either explicitly in the messenger sector or spontaneously in the supersymmetry-breaking sector. In the latter case this amounts to an auxiliary field version of the Froggatt–Nielsen mechanism.

Soft chiral flavor violation can in principle be the source of radiative masses for all the first- and second-generation quarks and leptons and the  $b$ -quark. Since radiative masses are intrinsically suppressed by a loop factor, the smallness of the first generation masses can be due in part to this suppression. The remaining suppression in this radiative scenario can be obtained in part from a hierarchy between the gaugino and scalar superpartner masses, or from a hierarchy between the supersymmetry-breaking and flavor-breaking scales. The loop factor is sufficient to account for essentially all of the suppression of second-generation masses with respect to the electroweak scale.

Radiative fermion masses, especially for the second generation or  $b$ -quark, require significant left–right scalar superpartner mixing from scalar tri-linear terms. Such large mixings introduce potentially dangerous directions in field space, along which charge and/or color are broken. However, metastability of the charge- and color-preserving vacuum on cosmological time scales is possible in many models. In addition, some classes of models with non-holomorphic tri-linear terms or mixing with mirror matter at the supersymmetry-breaking

scale contain stabilizing terms in the potential, which eliminate these dangerous directions and render the charge- and color-preserving vacuum absolutely stable.

Since the dominant source of flavor violation for fermions with soft radiative masses resides in supersymmetry-breaking terms, interesting levels of low-energy flavor violation may arise. These are functions of the specific textures for the scalar masses and tri-linear terms and therefore very model-dependent. The study of such flavor changing associated with soft fermion masses is outside the scope of this work, but should be considered in any future work on specific models of the soft and hard textures. In some classes of models certain relations or symmetries among the soft terms can lead to partial or complete alignment in flavor space of non-renormalizable chirality-violating operators with the effective Yukawa couplings and reduce or eliminate observable flavor breaking. It is noteworthy that when all the soft supersymmetry-violating parameters are taken simultaneously large, radiative Yukawa couplings approach finite limits, whereas flavor violation induced by virtual superpartners in non-renormalizable operators is suppressed. This is particularly relevant in schemes with heavy first- and second-generation scalars.

Radiative fermion masses lead to a number of striking phenomenological consequences. Chief among these is that new contributions to chirality-violating operators are effectively not suppressed by a loop factor compared with the fermion mass, which itself arises at one loop. This is a generic feature of any theory of radiative fermion masses. The most important such operators are anomalous magnetic moments for fermions with soft radiative masses. In this scenario the supersymmetric correction to the anomalous moment only depends on the superpartner mass spectrum, and is necessarily positive. The anomalous magnetic moment of the muon is by far the most sensitive probe of a radiative muon mass. The current experimental bound already constrains part of the supersymmetric parameter space in this scenario. Even if the muon mass is not predominantly radiative, a contribution to the muon anomalous magnetic moment from relatively large chiral flavor violation in the muon tri-linear term might provide an interesting interpretation for a non-vanishing measurement of  $a_\mu^{\text{new}}$ .

CP-violating Higgs–fermion couplings and electric dipole moments are naturally suppressed by the alignment of the phases of radiatively generated chirally violating operators with the phase of a radiatively generated mass. This alignment is naturally very precise in interesting regions of parameter space. Thus, the standard supersymmetric CP problem, is mitigated or eliminated in the scenario of radiative fermion masses studied here.

Other phenomenological consequences of radiative masses are related to the softness of the Yukawa couplings. Most notably, the Higgs–fermion couplings are momentum-dependent with non-trivial form factors. The lowest-order operator, which represents the momentum dependence, may be characterized in terms of a finite Higgs Yukawa radius. This radius, like the anomalous magnetic moment, is not suppressed by a loop factor. Even at zero momentum the Higgs Yukawa coupling can differ from the mass Yukawa coupling. In addition, “wrong Higgs” couplings result if the radiative mass arises from non-holomorphic soft terms. All these Higgs–fermion coupling effects may be tested at future colliders by looking for deviations of various sum rules and relations among Higgs boson decay widths and branching ratios to fermion final states. Many of these sum rules and relations are guaranteed by

holomorphy to be satisfied at lowest order in any supersymmetric theory with a single pair of Higgs doublets and hard fermion masses.

A further signal of the softness of a fermion mass is the associated radiatively generated Higgsino coupling. Large differences between the couplings of Higgs and Higgsinos to matter are expected in this scenario. To a low-energy observer who assumes hard Yukawa couplings, these would manifest themselves as apparent hard violations of supersymmetry in renormalizable interactions. Unfortunately direct measurement of such couplings at future colliders is likely to be very difficult. Finally, the relatively large left–right scalar superpartner mixing associated with second-generation or  $b$ -quark radiative masses can lead to significant modifications of supersymmetric production cross sections and branching ratios from minimal expectations.

The spontaneous breaking of chiral flavor symmetries in the supersymmetry-breaking sector through auxiliary rather than scalar directions can be extended to other global chiral symmetries such as lepton number. Soft lepton number violation gives rise, radiatively, to lepton-violating sneutrino masses which in turn induce radiative neutrino masses. Sneutrino–antisneutrino oscillations are relatively large in this scenario and might be probed if the  $\tau$ -neutrino is not too light.

In summary, the interesting features of radiative fermion masses arising from soft chiral flavor violation include:

- Radiative masses for first- and second-generation quarks and leptons and for the  $b$ -quark can be accommodated while satisfying (meta)stability requirements for the charge- and color-preserving vacuum.
- Higgs Yukawa couplings are momentum-dependent with non-trivial form factors and finite Higgs Yukawa radii.
- “Wrong Higgs” radiative Yukawa couplings arise from non-holomorphic soft chiral flavor breaking.
- Apparent large hard violation of supersymmetry in Higgsino couplings.
- Supersymmetric contributions to anomalous magnetic moments are positive and not suppressed by a loop factor. A radiative muon mass will be very well probed by the Brookhaven muon  $g - 2$  experiment.
- CP-violating electric dipole moments are suppressed by natural phase alignment. Both the neutron and electron EDMs could be not too far below current experimental bounds.
- Left–right scalar superpartner mixing is enhanced.
- Radiative neutrino masses arising from soft lepton number violation imply enhanced sneutrino–antisneutrino oscillations.

Specific models for the hard and soft textures should be developed to further explore this interesting possibility for the origin of some of the fermion masses.

## ACKNOWLEDGMENTS

The authors thank A. Djouadi, C. Greub, H. Haber, U. Nierste, G.J. van Oldenborgh, and D. Wyler for discussions, and M. Dress for comments on the manuscript. F. B. and S. T. acknowledge the hospitality of the high-energy group at Rutgers University and N. P. that of the CERN theory group. F. B., N. P., and S. T. are also grateful to the Aspen Center for Physics, where parts of this work were done. F. B. and G. F. respectively acknowledge the support of the Schweizerischer Nationalfonds and Rutgers University throughout most of this research. This work was supported by the US Department of Energy under grant DE-FG02-96ER40559, the US National Science Foundation under grants PHY-94-23002 and PHY-98-70115, the Alfred P. Sloan Foundation, and Stanford University through a Fredrick E. Terman Fellowship.

## APPENDIX A: DEFINITIONS AND INTEGRALS

### 1. Scalar superpartner mass and mixing

The  $2 \times 2$  squark or slepton mass squared matrix,

$$\mathcal{M}^2 = \begin{pmatrix} m_{LL}^2 & (m_{LR}^2) \\ (m_{LR}^2)^* & m_{RR}^2 \end{pmatrix}, \quad (\text{A1})$$

written here in the basis  $\{\tilde{f}_L, \tilde{f}_R\}$ , is Hermitian  $\mathcal{M}^2 = (\mathcal{M}^2)^\dagger$ , with eigenvalues

$$m_{\tilde{f}_{1,2}}^2 = \frac{1}{2} \left\{ (m_{LL}^2 + m_{RR}^2) \mp \sqrt{(m_{LL}^2 - m_{RR}^2)^2 + 4|m_{LR}^2|^2} \right\}. \quad (\text{A2})$$

Notice that  $\tilde{f}_R$  is here the actual right component of  $\tilde{f}$  and corresponds to the conjugate of the field  $\phi_R$  used in the text.

The eigenvectors  $\tilde{f}_1$  and  $\tilde{f}_2$  corresponding to the eigenvalues in (A2) are obtained from  $\tilde{f}_L, \tilde{f}_R$  through a unitary transformation :

$$\begin{pmatrix} \tilde{f}_1 \\ \tilde{f}_2 \end{pmatrix} = U \begin{pmatrix} \tilde{f}_L \\ \tilde{f}_R \end{pmatrix} \equiv \begin{pmatrix} \cos \theta_f e^{+i\phi} & \sin \theta_f \\ \sin \theta_f & -\cos \theta_f e^{-i\phi} \end{pmatrix} \begin{pmatrix} \tilde{f}_L \\ \tilde{f}_R \end{pmatrix}, \quad (\text{A3})$$

where  $\phi \equiv \text{Arg}(m_{LR}^2) = -\text{Arg}(A\langle H_\alpha \rangle)$  or  $\phi = -\text{Arg}(A'\langle H_\alpha^* \rangle)$ . The mixing angle  $\theta_f$  is defined, up to a two-fold ambiguity by the relations

$$\sin 2\theta_f = -\frac{2|m_{LR}^2|}{m_{\tilde{f}_2}^2 - m_{\tilde{f}_1}^2}; \quad \cos 2\theta_f = \pm \frac{m_{LL}^2 - m_{RR}^2}{m_{\tilde{f}_2}^2 - m_{\tilde{f}_1}^2}. \quad (\text{A4})$$

Note that in the strict superpartner decoupling limit, for which  $m_{LR}^2/m_{LL,RR}^2 \rightarrow 0$ , the mixing angles approach  $\cos \theta_f \rightarrow 0$  and  $\sin \theta_f \rightarrow 1$ .

The fractional splitting of the mass squared eigenvalues used in the text is related to the mass squared matrix by

$$\phi_f \equiv \frac{m_{\tilde{f}_2}^2 - m_{\tilde{f}_1}^2}{m_{\tilde{f}_2}^2 + m_{\tilde{f}_1}^2} = \frac{1}{\text{Tr} \mathcal{M}^2} \sqrt{(\text{Tr} \mathcal{M}^2)^2 - 4 \text{Det} \mathcal{M}^2}. \quad (\text{A5})$$

Note that  $\phi_f \rightarrow 1^-$  for  $\text{Det} \mathcal{M}^2 \rightarrow 0^+$ , corresponding to a vanishing eigenvalue in the scalar mass matrix.

### 2. Fermion mass integral

The two-point function  $I(m_1^2, m_2^2, m_\lambda^2)$ , introduced in section II A, is a completely symmetric function in its three variables



TABLE IV. Limiting behavior of  $I(m^2, m^2, m_\lambda^2)$  and  $I(0, m^2, m_\lambda^2)$  for either fixed gaugino mass  $m_\lambda = \overline{m}_\lambda$  or fixed scalar mass  $m = \overline{m}$ . The limit in the first column reflects the infrared behavior of the loop integral for  $m$  or  $m_\lambda \rightarrow 0$ .

$m_\lambda = \overline{m}_\lambda$ fixed	$m \rightarrow 0$	$m \rightarrow \overline{m}_\lambda$	$m \rightarrow \infty$
$I(m^2, m^2, \overline{m}_\lambda^2)$	$\frac{1}{\overline{m}_\lambda^2} \left( -\ln\left(\frac{m^2}{\overline{m}_\lambda^2}\right) \right) \rightarrow +\infty$	$\frac{1}{\overline{m}_\lambda^2} \cdot \frac{1}{2}$	$\frac{1}{m^2} \rightarrow 0$
$I(0, m^2, \overline{m}_\lambda^2)$	$\frac{1}{\overline{m}_\lambda^2} \left( -\ln\left(\frac{m^2}{\overline{m}_\lambda^2}\right) \right) \rightarrow +\infty$	$\frac{1}{\overline{m}_\lambda^2}$	$\frac{1}{m^2} \left( \ln\left(\frac{m^2}{\overline{m}_\lambda^2}\right) \right) \rightarrow 0$
$m = \overline{m}$ fixed	$m_\lambda \rightarrow 0$	$m_\lambda \rightarrow \overline{m}$	$m_\lambda \rightarrow \infty$
$I(\overline{m}^2, \overline{m}^2, m_\lambda^2)$	$\frac{1}{\overline{m}^2}$		$\frac{1}{m_\lambda^2} \left( \ln\left(\frac{m_\lambda^2}{\overline{m}^2}\right) \right) \rightarrow 0$
$I(0, \overline{m}^2, m_\lambda^2)$	$\frac{1}{\overline{m}^2} \left( -\ln\left(\frac{m_\lambda^2}{\overline{m}^2}\right) \right) \rightarrow +\infty$		$\frac{1}{m_\lambda^2} \left( \ln\left(\frac{m_\lambda^2}{\overline{m}^2}\right) \right) \rightarrow 0$

$$I(m_1^2, m_2^2, m_\lambda^2) = -\frac{m_1^2 m_2^2 \ln(m_1^2/m_2^2) + m_2^2 m_\lambda^2 \ln(m_2^2/m_\lambda^2) + m_\lambda^2 m_1^2 \ln(m_\lambda^2/m_1^2)}{(m_1^2 - m_2^2)(m_2^2 - m_\lambda^2)(m_\lambda^2 - m_1^2)}. \quad (\text{A6})$$

It may be cast in the simpler form:

$$I(m_1^2, m_2^2, m_\lambda^2) = \frac{1}{m_1^2 - m_2^2} \left( \frac{\ln \beta_1}{\beta_1 - 1} - \frac{\ln \beta_2}{\beta_2 - 1} \right), \quad (\text{A7})$$

where  $\beta_i = m_\lambda^2/m_i^2$ ,  $i = 1, 2$ , in which, however, only the symmetry between two of the three variables is manifest. This form is more useful to obtain some interesting limiting cases. In the limit of degenerate scalar-partner masses the loop function (A7) becomes

$$I(m^2, m^2, m_\lambda^2) = \frac{1}{m^2} \frac{1}{(\beta - 1)^2} (1 - \beta + \beta \ln \beta), \quad (\text{A8})$$

whereas in the limit of highly non-degenerate eigenvalues,  $m = m_2 \gg m_1$ ,

$$I(0, m^2, m_\lambda^2) = \frac{1}{m^2} \frac{\ln \beta}{\beta - 1}. \quad (\text{A9})$$

The limiting behavior of these functions for either fixed gaugino mass or fixed scalar mass is shown in table IV. The loop function is typically bounded by  $I(m_1^2, m_2^2, m_\lambda^2) \times \max(m_1^2, m_2^2, m_\lambda^2) \lesssim \mathcal{O}(1)$ , but this can be enhanced in certain limits by a logarithm. Large scalar splittings also slightly enhance the loop integral.

### 3. Higgs vertex function

Except for a sign difference, the convention of the first reference in [49] is followed in the definition of the three-point function employed here:  $C_0(p_1^2, p_2^2, 2p_1 \cdot p_2; m_1^2, m_\lambda^2, m_2^2)$ . Explicitly,

$$\begin{aligned}
& C_0(p_1^2, p_2^2, 2p_1 \cdot p_2; m_1^2, m_\lambda^2, m_2^2) \\
& \equiv \frac{i}{\pi^2} \int d^4k \frac{1}{[k^2 - m_1^2 + i\epsilon][(k + p_1)^2 - m_\lambda^2 + i\epsilon][(k + p_1 + p_2)^2 - m_2^2 + i\epsilon]} \\
& = \int_0^1 dx \int_0^x dy \frac{1}{[ax^2 + by^2 + cxy + dx + ey + f]}, \tag{A10}
\end{aligned}$$

where the  $a, b, c, d, e,$  and  $f$  are

$$a = p_2^2; \quad b = p_1^2; \quad c = 2p_1 \cdot p_2; \quad d = -p_2^2 + m_\lambda^2 - m_2^2; \quad e = -p_1^2 - 2p_1 \cdot p_2 + m_1^2 - m_\lambda^2; \quad f = m_2^2 - i\epsilon. \tag{A11}$$

The general solution is:

$$\begin{aligned}
& C_0(p_1^2, p_2^2, 2p_1 \cdot p_2; m_1^2, m_\lambda^2, m_2^2) \\
& = \frac{1}{(c + 2\alpha b)} \sum_{j=1}^3 (-1)^{j+1} \sum_{k=1,2} \left[ Li_2 \left( \frac{y_j}{y_j - y_{jk}} \right) - Li_2 \left( \frac{y_j - 1}{y_j - y_{jk}} \right) \right], \tag{A12}
\end{aligned}$$

where the  $y_j$  are

$$y_1 = -\frac{(d + e\alpha + 2a + c\alpha)}{c + 2\alpha b}, \quad y_2 = -\frac{(d + e\alpha)}{c + 2\alpha b} \frac{1}{1 - \alpha}, \quad y_3 = \frac{(d + e\alpha)}{c + 2\alpha b} \frac{1}{\alpha}, \tag{A13}$$

and  $\alpha$  is one of the two solutions of the equation  $\alpha^2 b + \alpha c + a = 0$ . Finally, for each  $j = 1, 2, 3$ , the quantities  $y_{j1}$  and  $y_{j2}$  are the roots of the quadratic equations

$$\begin{aligned}
Q_1(y) &= p_1^2 y^2 + (m_1^2 - m_\lambda^2 - p_1^2)y + m_\lambda^2 - i\epsilon \\
Q_2(y) &= (p_1 + p_2)^2 y^2 + (m_1^2 - m_2^2 - (p_1 + p_2)^2)y + m_2^2 - i\epsilon \\
Q_3(y) &= p_2^2 y^2 + (m_\lambda^2 - m_2^2 - p_2^2)y + m_2^2 - i\epsilon. \tag{A14}
\end{aligned}$$

In the case of the decay  $H \rightarrow f\bar{f}$ , or of the resonant production  $f\bar{f} \rightarrow H$ , the momenta are such that  $p = q, p_1 = q_1, q_2 = -p_2$ . All external fields are on-shell, and the approximation  $p_1^2 = p_2^2 = 0$  and  $2p_1 \cdot p_2 = m_H^2$  is appropriate for  $m_f^2 \ll m_H^2$ . Both  $\alpha$ 's also vanish in this limit ( $a = b = 0$ ). An independent integration then yields

$$\begin{aligned}
& C_0(0, 0, m_H^2; m_1^2, m_\lambda^2, m_2^2) \\
& = \frac{1}{m_H^2} \left\{ \sum_{i=1,2} \left[ Li_2 \left( \frac{x_0}{x_0 - x_i} \right) - Li_2 \left( \frac{x_0 - 1}{x_0 - x_i} \right) \right] - \left[ Li_2 \left( \frac{x_0}{x_0 + f/d} \right) - Li_2 \left( \frac{x_0 - 1}{x_0 + f/d} \right) \right] \right\}, \tag{A15}
\end{aligned}$$

where  $x_0$  is the root of the linear equation,  $cx + e = 0$  and  $x_1, x_2$  the roots of the quadratic equation  $cx^2 + (d + e)x + f = 0$ ,

$$x_{1,2} = \frac{m_2^2 - m_1^2 + m_H^2}{2m_H^2} \mp \left[ \left( \frac{m_2^2 - m_1^2 + m_H^2}{2m_H^2} \right)^2 - \left( \frac{m_2^2}{m_H^2} \right)^2 + i\epsilon \right]^{1/2} \quad (\text{A16})$$

and  $d$  and  $f$  follow from (A11) in this limit.

Notice that the arguments of logarithms and dilogarithms in (A12) and (A15) are in general complex. Moreover, depending on the relative size of the masses involved, some arguments of  $Li_2(x)$  in (A12) and (A15) may be such that  $\text{Re}(x) > 1$ . Since  $Li_2(x)$  has a cut on the real axis, starting from 1, the relations

$$\begin{aligned} Li_2(x) &= -Li_2(1-x) + \frac{1}{6}\pi^2 - \ln(x)\ln(1-x) \\ Li_2(x) &= -Li_2\left(\frac{1}{x}\right) - \frac{1}{6}\pi^2 - \frac{1}{2}\ln^2(-x) \end{aligned} \quad (\text{A17})$$

may have to be used.

With general superpartner masses, the limit of vanishing Higgs mass,  $m_H \rightarrow 0$ , reduces (A15) to the mass loop function

$$C_0(0, 0, 0; m_1^2, m_\lambda^2, m_2^2) = I(m_1^2, m_2^2, m_\lambda^2). \quad (\text{A18})$$

If  $m_H \neq 0$ , the two limits of degenerate scalar masses,  $m_1^2 = m_2^2 = m^2$ , and of maximally split ones,  $m_1^2 = 0, m_2^2 = m^2$ , explicitly analysed for the mass loop function, do not yield considerable simplifications for  $C_0(0, 0, m_H^2; m^2, m_\lambda^2, m^2)$  and  $C_0(0, 0, m_H^2; 0, m_\lambda^2, m^2)$  with respect to (A15). For fixed  $m$  scalar mass  $m = \bar{m}$ ,  $C_0(0, 0, m_H^2; \bar{m}^2, m_\lambda^2, \bar{m}^2)$  and  $C_0(0, 0, m_H^2; 0, m_\lambda^2, \bar{m}^2)$  acquire simple analytic expressions in the limit  $m_\lambda \rightarrow \bar{m}$ . In both cases,  $a = b = d = 0$ . In addition, in the first case, it is  $e = -c$  and the three-point function is then

$$C_0(0, 0, m_H^2; \bar{m}^2, \bar{m}^2, \bar{m}^2) = \frac{1}{m_H^2} \left\{ Li_2\left(\frac{1}{x_2}\right) + Li_2\left(\frac{1}{x_1}\right) \right\}. \quad (\text{A19})$$

The roots  $x_{1,2}$  are in this limit

$$x_{1,2} = \frac{1}{2} \left[ 1 \mp \sqrt{1 - 4\frac{\bar{m}^2}{m_H^2} + i\epsilon} \right]. \quad (\text{A20})$$

Using (A17),  $x_1 + x_2 = 1$ , and analytic continuation

$$C_0(0, 0, m_H^2; \bar{m}^2, \bar{m}^2, \bar{m}^2) = \frac{1}{2m_H^2} \begin{cases} - \left[ \ln\left(\frac{1 + \sqrt{1 - 4\bar{m}^2/m_H^2}}{1 - \sqrt{1 - 4\bar{m}^2/m_H^2}}\right) - i\pi \right]^2 & 2\frac{\bar{m}}{m_H} < 1, \\ + 4 \arcsin^2\left(\frac{m_H}{2\bar{m}}\right) & 2\frac{\bar{m}}{m_H} \geq 1. \end{cases} \quad (\text{A21})$$

The imaginary piece for  $2m/m_H < 1$  corresponds to the cut for physical intermediate states.

In the case of maximal splitting, it is

$$\begin{aligned}
& C_0(0, 0, m_H^2; 0, \bar{m}^2, \bar{m}^2) \\
&= \frac{1}{m_H^2} \left\{ Li_2 \left( \frac{1 + \bar{m}^2/m_H^2}{x_2} \right) + Li_2 \left( \frac{1 + \bar{m}^2/m_H^2}{x_1} \right) - Li_2 \left( \frac{\bar{m}^2/m_H^2}{x_2} \right) - Li_2 \left( \frac{\bar{m}^2/m_H^2}{x_1} \right) \right\}, \tag{A22}
\end{aligned}$$

with  $x_{1,2}$  given by:

$$x_{1,2} = \frac{1}{2} \left[ \left( 1 + \frac{\bar{m}^2}{m_H^2} \right) \mp \sqrt{\left( 1 - \frac{\bar{m}^2}{m_H^2} \right)^2 + i\epsilon} \right]. \tag{A23}$$

Using again (A17) and the fact that  $x_1 + x_2 = 1 + \bar{m}^2/m_H^2$ , it can be shown that

$$C_0(0, 0, m_H^2; 0, \bar{m}^2, \bar{m}^2) = \frac{1}{m_H^2} \begin{cases} -\frac{1}{2} \left( \ln \frac{\bar{m}^2}{m_H^2} + i\pi \right)^2 - \frac{\pi^2}{6} - Li_2 \left( \frac{\bar{m}^2}{m_H^2} \right) & \frac{\bar{m}}{m_H} < 1, \\ + Li_2 \left( \frac{m_H^2}{\bar{m}^2} \right) & \frac{\bar{m}}{m_H} \geq 1, \end{cases} \tag{A24}$$

where  $Li_2(x)$  is a real number for  $x < 1$ .

#### 4. Higgsino vertex function

The vertex function  $V_{ijklh}$  appearing in the Higgsino coupling relevant to the decays  $\tilde{f}_h(q_2) \rightarrow \tilde{\chi}_i^0(q) f_{L,R}(q_1)$  is given by

$$\begin{aligned}
V_{ijklh} &= \left[ m_{\tilde{\chi}_j^0} - m_{\tilde{\chi}_i^0} \left( \frac{m_{\tilde{f}_k}^2 - m_{\tilde{\chi}_j^0}^2}{m_{\tilde{f}_h}^2 - m_{\tilde{\chi}_i^0}^2} \right) \right] C_0(q^2, 0, q_2^2; m_{H_l^0}^2, m_{\tilde{\chi}_j^0}^2, m_{\tilde{f}_k}^2) \\
&\quad + \left( \frac{m_{\tilde{\chi}_i^0}}{m_{\tilde{f}_h}^2 - m_{\tilde{\chi}_i^0}^2} \right) \left[ B_0(q^2; m_{\tilde{\chi}_j^0}^2, m_{H_l^0}^2) - B_0(q_2^2; m_{H_l^0}^2, m_{\tilde{f}_k}^2) \right]. \tag{A25}
\end{aligned}$$

The definition of the two-point function  $B_0(q^2; m_1^2, m_2^2)$  follows standard conventions, as for example in [49], except for a minus sign

$$B_0(q^2; m_1^2, m_2^2) = (\mu^2 \pi e^\gamma)^{(4-n)/2} \frac{i}{\pi^2} \int d^n k \frac{1}{[k^2 - m_1^2 + i\epsilon][(k+q)^2 - m_2^2 + i\epsilon]} \tag{A26}$$

where  $\gamma$  is Euler's constant.

## APPENDIX B: ANOMALOUS MAGNETIC AND ELECTRIC DIPOLE MOMENTS

The electromagnetic dipole operator for a Dirac fermion is given by the Lagrangian operator

$$\mathcal{L} \supset -\frac{1}{2}d_f \bar{f}_L \sigma^{\mu\nu} f_R F_{\mu\nu} + \text{h.c.} \quad (\text{B1})$$

where  $d_f$  is the dipole moment coefficient, which is, in general complex and  $f_{L,R} = P_{L,R}f$  are the left- and right-handed chiral components of the Dirac fermion. In a general basis with complex fermion mass  $m_f$ , the electric dipole moment is

$$d_f^e = |d_f| \sin \left( \text{Arg}(d_f m_f^*) \right) \quad (\text{B2})$$

and the anomalous magnetic moment is

$$a_f = \frac{2m_f}{eQ_f} |d_f| \cos \left( \text{Arg}(d_f m_f^*) \right), \quad (\text{B3})$$

where  $Q_f$  is the fermion electric charge.

In the CP-conserving case,  $\text{Arg}(d_f m_f^*) = 0$ , the one-loop chirality-violating contribution of fig. 8 to the muon anomalous magnetic moment is given by

$$\mathcal{L} \supset +\frac{\alpha'}{4\pi} (eQ_\mu) m_{LR}^2 \sum_j K_f^j m_{\tilde{\chi}_j^0} I_{g-2}(m_{\tilde{\mu}_1}^2, m_{\tilde{\mu}_2}^2, m_{\tilde{\chi}_j^0}^2) \mathcal{O}_{g-2}, \quad (\text{B4})$$

where  $Q_\mu = -1$  is the muon electric charge, the operator  $\mathcal{O}_{g-2} \equiv \bar{\mu}(p') \sigma^{\mu\nu} F_{\mu\nu} \mu(p)$ , and the loop function is

$$I_{g-2}(m_1^2, m_2^2, m_\lambda^2) = \frac{1}{m_\lambda^2} \frac{1}{m_2^2 - m_1^2} \left\{ \frac{\beta_1 (\beta_1^2 - 1 - 2\beta_1 \ln \beta_1)}{2(\beta_1 - 1)^3} - (1 \rightarrow 2) \right\}, \quad (\text{B5})$$

with  $\beta_i = m_\lambda^2/m_i^2$ ,  $i = 1, 2$ . For comparison with the mass loop function, the limiting behavior of (B5) for degenerate scalar partners masses is

$$I_{g-2}(m^2, m^2, m_\lambda^2) = \frac{1}{(m^2)^2} \frac{1}{2(\beta - 1)^4} \left( 2\beta(\beta + 2) \ln \beta - 5\beta^2 + 4\beta + 1 \right), \quad (\text{B6})$$

while for large scalar splitting

$$I_{g-2}(0, m^2, m_\lambda^2) = \frac{1}{m^2} \frac{1}{m_\lambda^2} \frac{1}{2(\beta - 1)^3} \left( 2\beta^2 \ln \beta - 3\beta^2 + 4\beta - 1 \right). \quad (\text{B7})$$

The limiting behavior of these functions for either fixed gaugino mass or fixed scalar mass is shown in table (V). Using the expression for the radiatively generated mass (3), the coupling (B4) may be written

TABLE V. Limiting behavior of  $I_{g-2}(m^2, m^2, \overline{m_\lambda^2})$  and  $I_{g-2}(0, m^2, \overline{m_\lambda^2})$  for either fixed gaugino mass  $m_\lambda = \overline{m_\lambda}$ , or fixed scalar mass  $m = \overline{m}$ . The limit in the first column reflects the infrared behavior of the loop integral for  $m$  or  $m_\lambda \rightarrow 0$ .

$m_\lambda = \overline{m_\lambda}$ fixed	$m \rightarrow 0$	$m \rightarrow \overline{m_\lambda}$	$m \rightarrow \infty$
$I_{g-2}(m^2, m^2, \overline{m_\lambda^2})$	$\frac{1}{(\overline{m_\lambda^2})^2} \left( -\ln\left(\frac{m^2}{\overline{m_\lambda^2}}\right) \right) \rightarrow +\infty$	$\frac{1}{(\overline{m_\lambda^2})^2} \cdot \frac{1}{12}$	$\frac{1}{(m^2)^2} \cdot \frac{1}{2} \rightarrow 0$
$I_{g-2}(0, m^2, \overline{m_\lambda^2})$	$\frac{1}{(\overline{m_\lambda^2})^2} \left( -\ln\left(\frac{m^2}{\overline{m_\lambda^2}}\right) \right) \rightarrow +\infty$	$\frac{1}{(\overline{m_\lambda^2})^2} \cdot \frac{1}{3}$	$\frac{1}{m^2} \frac{1}{\overline{m_\lambda^2}} \cdot \frac{1}{2} \rightarrow 0$

$m = \overline{m}$ fixed	$m_\lambda \rightarrow 0$	$m_\lambda \rightarrow \overline{m}$	$m_\lambda \rightarrow \infty$
$I_{g-2}(\overline{m^2}, \overline{m^2}, m_\lambda^2)$	$\frac{1}{(\overline{m^2})^2} \cdot \frac{1}{2}$		$\frac{1}{(m_\lambda^2)^2} \left( \ln\left(\frac{m^2}{\overline{m^2}}\right) \right) \rightarrow 0$
$I_{g-2}(0, \overline{m^2}, m_\lambda^2)$	$\frac{1}{\overline{m^2}} \frac{1}{m_\lambda^2} \cdot \frac{1}{2} \rightarrow +\infty$		$\frac{1}{(m_\lambda^2)^2} \left( \ln\left(\frac{m^2}{\overline{m^2}}\right) \right) \rightarrow 0$

$$\mathcal{L} \supset -\frac{e Q_\mu}{2} m_\mu \frac{\sum_j K_f^j m_{\tilde{\chi}_j^0} I_{g-2}(m_{\tilde{\mu}_1}^2, m_{\tilde{\mu}_2}^2, m_{\tilde{\chi}_j^0}^2)}{\sum_j K_f^j m_{\tilde{\chi}_j^0} I(m_{\tilde{\mu}_1}^2, m_{\tilde{\mu}_2}^2, m_{\tilde{\chi}_j^0}^2)} \mathcal{O}_{g-2} \equiv -a_\mu \frac{e Q_\mu}{4 m_\mu} \mathcal{O}_{g-2}. \quad (\text{B8})$$

The supersymmetric contribution to the muon anomalous magnetic moment,  $a_\mu^{\text{SUSY}}$ , is then explicitly given in eq. (37). For a quark, the dominant gluino contribution to the dipole moment is given by the Lagrangian operator

$$\mathcal{L} \supset \frac{2\alpha_s}{3\pi} (e Q_q) m_{LR}^2 m_{\tilde{g}} I_{g-2}(m_{\tilde{q}_1}^2, m_{\tilde{q}_2}^2, m_{\tilde{g}}^2) \mathcal{O}_{g-2} \quad (\text{B9})$$

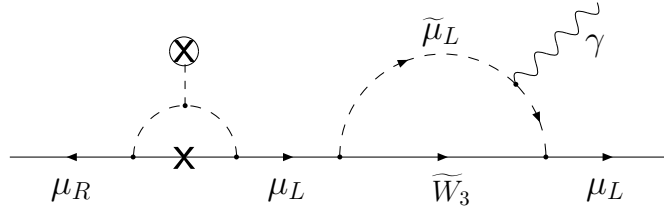


FIG. 14. Two-loop one-particle-reducible contribution to the muon anomalous magnetic moment. The chirality-violating loop corresponds to an external mass insertion through the on-shell equation of motion.

Before concluding, it is worth noting that the result (B4) obtained from the chirality-violating gaugino propagator in fig. 8 is the leading contribution to the anomalous magnetic moment. In models with hard Yukawa couplings, supersymmetric one-loop contributions in general arise also from the chirality-conserving gaugino propagator. The fermion on-shell equation of motion produces an external mass insertion, thereby giving a contribution to the chirality-violating anomalous magnetic moment. With a radiatively generated fermion mass, such contributions are formally two-loop one-particle-reducible since the external mass insertion is one-loop, as shown in fig. 14. These are of the same order as chirality-violating

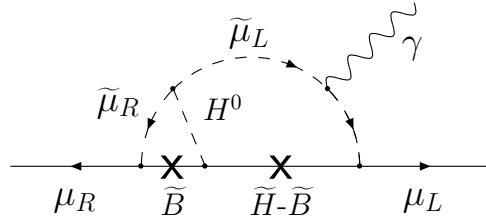


FIG. 15. Two-loop one-particle-irreducible contribution to the muon anomalous magnetic moment. In the heavy Higgs limit the one-loop sub-diagram on the left corresponds to the radiative Higgsino–scalar–fermion coupling of fig. 6. There are additional contributions from chirality conserving gaugino propagators.

two-loop one-particle-irreducible contributions, such as those arising from the effective one-loop Yukawa coupling, as shown in fig. 15. The result (B4) therefore represents the full one-loop supersymmetric contribution to the anomalous magnetic moment of a fermion with a soft radiative mass.

## REFERENCES

- [1] C. Froggatt and H. B. Nielsen, Nucl. Phys. **B147** (1979) 277.
- [2] M. Dine, R. Leigh, and A. Kagan, Phys. Rev. **D48** (1990) 4269;  
 Y. Nir and N. Seiberg, Phys. Lett. **B309** (1993) 337;  
 P. Pouliot and N. Seiberg, Phys. Lett. **B318** (1993) 169;  
 M. Leurer, Y. Nir, and N. Seiberg, Nucl. Phys. **B420** (1994) 468;  
 D. Kaplan and M. Schmaltz, Phys. Rev. **D49** (1994) 3741;  
 L. J. Hall and H. Murayama, Phys. Rev. Lett. **75** (1995) 3985.
- [3] For a review of anomalous Abelian horizontal symmetries, see P. Ramond, hep-ph/9604251 and references therein.
- [4] L.J. Hall, R. Rattazzi, and U. Sarid, Phys. Rev. **D50** (1994) 7048;  
 R. Hempfling, Phys. Rev. **D49** (1994) 6168;  
 M. Carena, M. Olechowski, S. Pokorski, and C.E.M. Wagner, Nucl. Phys. **B426** (1994) 269;  
 B. Wright, hep-ph/9404217;  
 A. Donini, Nucl. Phys. **B467** (1996) 3;  
 D.M. Pierce, J.A. Bagger, K. Matchev, R.-J. Zhang, Nucl. Phys. **B491** (1997) 3.
- [5] F.M. Borzumati, M. Olechowski, and S. Pokorski, Phys. Lett. **B349** (1995) 311;  
 T. Blazek, S. Raby, and S. Pokorski, Phys. Rev. **D52** (1995) 4151;  
 N. Polonsky, Phys. Rev. **D54** (1996) 4537;  
 R. Rattazzi and U. Sarid, hep-ph/9612464;  
 F.M. Borzumati, hep-ph/9702307.
- [6] F. del Aguila, M. Dugan, B. Grinstein, L. Hall, G.G. Ross, and P. West, Nucl. Phys. **B250** (1985) 225.
- [7] T. Banks, Nucl. Phys. **B303** (1988) 172.
- [8] E. Ma, Phys. Rev. **D39** (1989) 1922.
- [9] N.V. Krasnikov, Phys. Lett. **B302** (1993) 59.
- [10] N. Arkani-Hamed, C.-H. Cheng, and L.J. Hall, Phys. Rev. **D54** (1996) 2242 and Nucl. Phys. **B472** (1996) 95.
- [11] F. Borzumati, G. R. Farrar, N. Polonsky and S. Thomas, hep-ph/9712428; hep-ph/9805314.
- [12] L.J. Hall and L. Randall, Phys. Rev. Lett. **65** (1990) 2939.
- [13] M. Carena *et al.* in [4].
- [14] G.J. van Oldenborgh and J.A.M. Vermaseren, Z. Phys. **C46** (1990) 425;  
 G.J. van Oldenborgh, Comput. Phys. Commun. **66** (1991) 1.
- [15] H. Fusaoka and Y. Koide, Phys. Rev. **D57** (1998) 3986.
- [16] S.A. Abel and J.M. Frère, Phys. Rev. **D55** (1997) 1623.
- [17] S. Glashow and S. Weinberg, Phys. Rev. **D15** (1977) 1958.
- [18] E. Ma, D. Ng, and G.-G. Wong, Z. Phys. **C47** (1990) 431.
- [19] S. Dimopoulos and G.F. Giudice, Phys. Lett. **B357** (1995) 573;  
 A. Pomarol and D. Tommasini, Nucl. Phys. **B466** (1996) 3;  
 A.G. Cohen, D.B. Kaplan, and A.E. Nelson, Phys. Lett. **B388** (1996) 588.
- [20] J.F. Gunion, H.E. Haber, and M. Sher, Nucl. Phys **B306** (1988) 1.
- [21] See appendix B in P. Langacker and N. Polonsky, Phys. Rev. **D50** (1994) 2199.



- [22] M. Claudson, L. J. Hall, and I. Hinchliffe, Nucl. Phys. **B228** (1983) 501;  
T. C. Shen, Phys. Rev. **D37** (1988) 3537;  
A. Kusenko, P. Langacker, and G. Segre, Phys. Rev. **D54** (1996) 5824.
- [23] U. Sarid, Phys. Rev. **D58** (1998) 085017.
- [24] S. Coleman, Phys. Rev. **D15** (1977) 2929;  
C. Callan and S. Coleman, Phys. Rev. **D16** (1977) 1762.
- [25] A. D. Linde, Nucl. Phys. **B216** (1983) 421.
- [26] M. Dine, Y. Nir, and Y. Shirman, Phys. Rev. **D55** (1997) 1501;  
T. Han and R.J. Zhang, Phys. Lett. **B428** (1998) 120.
- [27] See, for example, A. Pomarol and M. Quiros, Phys. Lett. B **438** (1998) 255.
- [28] G. Farrar and P. Fayet, Phys. Lett. **B76** (1978) 575.
- [29] J.L. Hewett, T. Takeuchi, and S. Thomas, in *Electroweak Symmetry Breaking and New Physics at the TeV Scale*, ed. by T. Barklow *et al.* (World Scientific, Singapore, 1996), p. 548, hep-ph/9603391.
- [30] P. Fayet, in *Unification of the Fundamental Particle Interactions*, eds. S. Ferrara, J. Ellis and P. van Nieuwenhuizen (Plenum Press, New York, 1980) p. 587;  
J.A. Grifols and A. Mendez, Phys. Rev. **D26** (1982) 1809;  
J. Ellis, J.S. Hagelin, and D.V. Nanopoulos, Phys. Lett. **B116** (1982) 283;  
R. Barbieri and L. Maiani, Phys. Lett. **B117** (1982) 203;  
D.A. Kosower, L.M. Krauss, and N. Sakai, Phys. Lett. **B133** (1983) 305;  
T.C. Yuan, R. Arnowitt, A.H. Chamseddine, and P. Nath, Z. Phys. **C26** (1984) 407;  
J. Lopez, D.V. Nanopoulos, and X. Wang, Phys. Rev. **D49** (1991) 366;  
For recent calculations and estimates of the anomalous muon magnetic moment in typical supersymmetric models see:  
U. Chattopadhyay and P. Nath, Phys. Rev. **D53** (1996) 1648;  
T. Moroi, Phys. Rev. **D53** (1996) 6565, E.: *ibid.* **D56** (1997) 4424;  
M. Carena, G.F. Giudice, and C. E. M. Wagner, Phys. Lett. **B390** (1997) 234.
- [31] J. Bailey *et al.*, Nucl. Phys. **B150** (1979) 1.
- [32] T. Kinoshita and W. Marciano, in *Quantum Electrodynamics*, eds. T. Hasegawa *et al.* (Universal Academy Press, Tokyo, 1992), p. 419;  
A. Czarnecki and W. Marciano, hep-ph/9810512;  
G. Degrandi and G.F. Giudice, Phys. Rev. **D58** (1998) 053007.
- [33] V. Hughes, in *Frontiers of High Energy Physics*, eds. T. Hasagawa *et al.* (Universal Academy Press, Tokyo, 1992), p. 717.
- [34] J. Ellis, S. Ferrara, and D. Nanopoulos, Phys. Lett. B **114** (1982) 231;  
W. Buchmüller and D. Wyler, Phys. Lett. B **121** (1983) 321;  
J. Polchinski and M. Wise, Phys. Lett. B **125** (1983) 393.
- [35] For a discussion of bounds on supersymmetric phases implied by EDM measurements, see W. Fischler, S. Paban, and S. Thomas, Phys. Lett. B **289** (1992) 373.
- [36] E. Ma and D. Ng, Phys. Rev. Lett. **65** (1990) 2499.
- [37] I .S. Altarev *et al.*, Yad. Fiz. **59** (1996) 1204, Phys. Atom. Nucl. **59** (1996) 1152.
- [38] R. Arnowitt, J. Lopez, and D. Nanopoulos, Phys. Rev. D **42** (1990) 2423;  
R. Arnowitt, M. Duff, and K. Stelle, Phys. Rev. D **43** (1991) 3085;  
Y. Kizikuri and N. Oshimo, Phys. Rev. D **45** (1992) 1806.
- [39] A. Zhitnitsky and I. Khriplovich, Yad. Fiz. **34** (1981) 167 [Sov. J. Nucl. Phys. **34** (1981)

- 95];  
V. M. Khatsymovsky, I. Khriplovich, and A. Zhitnitsky, *Z. Phys. C* **36** (1987) 455;  
X.-G. He, B. Mckellar, and S. Pakvasa, *Phys. Lett. B* **254** (1991) 231;  
J. Ellis and R. Flores, *Phys. Lett. B* **377** (1996) 83.
- [40] S. Weinberg, *Phys. Rev. Lett.* **63** (1989) 2333;  
D. Chang, J. Kephart, W.-Y. Keung, and T. C. Yuan, *Phys. Lett. B* **68** (1992) 439.
- [41] A. Morozov, *Yad. Fiz.* **40** (1984) 788 [*Sov. J. Nucl. Phys.* **40** (1984) 505];  
E. Braaten, C. S. Li, and T. C. Yuan, *Phys. Rev. Lett.* **64** (1990) 1709, *Phys. Rev. D* **42** (1990) 276;  
D. Chang, W.-Y. Keung, C. S. Li, and T. C. Yuan, *Phys. Lett. B* **241** (1990) 589.
- [42] E. Commins, S. Ross, D. DeMille, and B. Regan, *Phys. Rev. A* **50** (1994) 2960.
- [43] V. Barger, M.S. Berger, J.F. Gunion, and T. Han, *Phys. Rev. Lett.* **75** (1995) 1462;  
*Phys. Rep.* **286** (1997) 1;  
V. Barger, talk presented at the *4th International Conference on the Physics Potential and Development of  $\mu^+\mu^-$  Colliders*, Dec. 1997, hep-ph/9803480.
- [44] J.F. Gunion and H.E. Haber, *Nucl. Phys.* **B272** (1986) 1; E: *ibid.* **402** (1993) 567 and University of California, Davis preprint, UCD-92-31, 1992, hep-ph/9301205
- [45] J. Gunion, H. Haber, G. Kane, and S. Dawson, *The Higgs Hunter's Guide* (Addison-Wesley, New York, 1990).
- [46] J.F. Gunion, talk presented at the *4th International Conference on the Physics Potential and Development of  $\mu^+\mu^-$  Colliders*, Dec. 1997, hep-ph/9804358.
- [47] I. Lee, *Nucl. Phys.* **B246** (1984) 120.
- [48] M. Hirsch, H.V. Klapdor-Kleingrothaus, and S.G. Kovalenko, *Phys. Lett.* **B398** (1997) 311;  
Y. Grossman and H.E. Haber, *Phys. Rev. Lett.* **78** (1997) 3438.
- [49] U. Nierste, D. Müller, and M. Böhm, *Z. Phys.* **C57** (1993) 605;  
G. 't Hooft and M. Veltman, *Nucl. Phys.* **B153** (1979) 365.